e - ISSN 2586-9396

Current Applied Science and Technology

Vol. 19 No. 3

September - December 2019

KING MONGKUT'S INSTITUTE OF TECHNOLOGY LADKRABANG

Advisory Board

Current Applied Science and Technology or CAST, formerly KMITL Science and Technology Journal, has been established since its inception as KMITL Science Journal published by King Mongkut's Institute of Technology Ladkrabang (KMITL) in 2001. The journal has been dedicated to publishing advanced and applied knowledge in the form of high-quality research and review articles covering the main areas of Biotechnology, Environmental Science, Agricultural Technology and other fields related to Applied Science and Technology. Special issues devoted to important topics in advanced science and technology will occasionally be published.

The journal is an open access peer-reviewed and double blinded journal using Online Journal System (OJS) publishing online academic research and review articles. Previously, articles were published in print on a regular basis (two issues per year) since 2001 and since 2010 onward the articles have been published both in print and electronic forms starting from volume 10. In 2017, the journal title has been changed from *KMITL Science and Technology Journal* to *Current Applied Science and Technology* (CAST) (e-ISSN 2586-9396) to be more identifiable to the international scientific community according to the suggestion of Thai-Journal Citation Index Centre. The journal has been published online only since volume 17(2) (July-December, 2017). In addition, the journal has attracted researchers from other countries more than 22% according to the data. Because of more demands on publication in CAST, the editorial board has decided to publish online original academic research and review articles three issues per year (April, August and December) from 2018 onward.

Furthermore, the advisory board and editorial board comprises honorable and well-known members from around the world in which 50% of editorial board members are from various countries like U.K., Norway, Japan, India, China, Canada, Estonia and Egypt. Only 25% of Thai editorial board members are from the publisher organization and 25% from other publisher organizations. Most of advisory and editorial board members have high H-index according to SCOPUS.

The journal is also committed to maintaining the high level of integrity in the content published and has a Conflict of Interest policy in place. The journal uses plagiarism detection software to screen the submissions. The journal has been working closely with Thai-Journal Citation Index Centre to ensure that the journal complies with international standard of SCOPUS.

Current Applied Science and Technology (CAST)

(formerly KMITL Science and Technology Journal)

Editor

Dusanee Thanaboripat
King Mongkut's Institute of Technology Ladkrabang, Thailand

Editorial Board

CONTENTS

Isolation and Characterization of Poly-γ-glutamic Acid Producing Bacteria from Plant Rhizoplane

Sirirat Siripornvisal* and Teerayuth Suddee

Department of Microbiology, Faculty of Science and Technology
Phranakhon Si Ayutthaya Rajabhat University, Ayutthaya, Thailand

Received: 28 September 2017, Revised: 21 May 2019, Accepted: 4 June 2019

Abstract

The purpose of this study was to isolate and evaluate the diversity of poly-γ-glutamic acid (γ-PGA) producing bacteria from rhizoplane of three Poaceae plants viz. rice (*Oryza sativa* Linn.), maize (*Zea mays* Linn.) and sugarcane (*Saccharum officinarum* Linn.), which are considered the most important agronomic crops of Thailand. A total of 368 isolates of rhizoplane bacteria were obtained from the root samples: 200 isolates from rice roots, 112 isolates from maize roots and 56 isolates from sugarcane roots. All isolates were screened for γ-PGA production consecutively by plate and tube culture assay. There were 186 isolates which exhibited γ-PGA producing capability. The γ-PGA concentrations obtained ranged from 12.62 - 18.46 g/L. Of those 186 isolates, 16 isolates were capable of producing γ-PGA higher than 15 g/l and these isolates were selected as the most efficient γ-PGA producers for further molecular characterization. The molecular genetic study based on 16S rRNA genes analysis revealed that the selected γ-PGA producers were closely related to 9 *Bacillus* species, namely *B. amyloliquefaciens* subsp. *amyloliquefaciens*, *B. atrophaeus*, *B. methylotrophicus*, *B. siamensis*, *B. subtilis* subsp. *inaquosorum*, *B. subtilis* subsp. *subtilis*, *B. tequilensis*, *B. vallismortis* and *B. velesensis*. All of them are belonging to *B. subtilis* and *B. amyloliquefaciens* groups. These results indicate that the rhizoplane of Poaceae plants are an important reservoir of natural isolates of γ-PGA producing bacteria.

Keywords: poly-γ-glutamic acid, γ-PGA, rhizoplane, Poaceae plants, *Bacillus*
DOI 10.14456/cast.2019.17

*Corresponding author: E-mail: sirirat2@yahoo.com

1. Introduction

Biopolymer, γ-polyglutamic acid (γ-PGA), is a natural and multifunctional poly-amino acid which can be produced by a range of bacteria. It is constituted of D- and/or L-glutamic acid units which are polymerized by gamma amide linkages [1]. As a biopolymer material, γ-PGA has several attractive physicochemical and biological properties such as high water solubility, excellent absorb ability, metal-binding capacity, good thickening capacity and biodegradability [2]. This polymer is also edible and non-toxic towards humans and environment [3]. These properties of γ-PGA are attractive for applications in many fields. This polymer can be used as a novel drug delivery material [4, 5], an osteoporosis-preventing factor in medicine [6, 7], an antifreeze agent, a food thickener [8-10] and a flocculent or absorption agent for biotechnological and environmental applications [11, 12].

Bacteria of the genus *Bacillus* are the best known γ-PGA producer [13, 14]. It was widely known that glutamic acid is the stringent precursor for γ-PGA biosynthesis and the γ-PGA-producing bacteria can obtain from two different sources; exogenously acquired from environment or endogenously synthesized by itself. This leads to the classification of the γ-PGA producing bacteria into two groups, i.e. glutamic acid dependence- and independence strains, according to the requirement of exogenous glutamic acid [15]. From the economic viewpoint, industrial production of γ-PGA may be limited by the high cost of glutamic acid and it would be attractive to shift to the utilization of glutamic acid by independent strains instead.

In the past recent years, short lists of glutamic acid-independent strains have been published such as *Bacillus methylotrophicus* [2], *B. subtilis* C10 [15] and *B. amyloliquefaciens* LL3 [16]. These bacteria can self-synthesize a considerable yield of γ-PGA without the addition of glutamic acid. In some glutamic acid-independent strains such as *B. licheniformis* ATCC 9945a, an addition of a small amount of glutamic acid in the media can significantly enhance γ-PGA synthesis [17]. It is clear that the glutamic acid-independent strains have potential to be improved by further comprehensive researches in which metabolic pathways and the enzymes can be related to γ-PGA synthesis under the optimal culture conditions. However, a few number of the glutamic acid-independent strains have been studied. In addition, the native glutamic acid-independent strains that have been reported, were found to synthesize a little amount of γ-PGA, generally lower than 15g/l [2]. Therefore, it remains meaningful to search for glutamic acid-independent strains with high-levels of γ-PGA production, as these strains involve lower costs and simplified processes for industry. The objective of this study was to isolate a number of γ-PGA producing bacteria from rhizoplane of three Poaceae plants viz. rice (*Oryza sativa* Linn.), maize (*Zea mays* Linn.) and sugarcane (*Saccharum officinarum* Linn.) and to reveal the co-occurrence of both glutamic acid-dependence and glutamic acid-independent strains in these habitats.

2. Materials and Methods

2.1 Isolation and screening of γ-PGA producing bacteria

Samples of root of three Poaceae plants *viz*. rice (*Oryza sativa* Linn.), maize (*Zea mays* Linn.) and sugarcane (*Saccharum officinarum* Linn.) were collected from cultivation area in central provinces of Thailand, including Ang Thong, Phra Nakhon Si Ayutthaya and Saraburi.

To isolate rhizoplane bacteria, the root samples were gently washed with sterilized water with the aids of sonication to remove adhered soils. Then the final rinsing water was spread on a minimal medium containing glutamic acid. After incubation period for 24 h at 37°C, single mucoid colonies were selected for secondary screening [18].

Secondary screening was done by streaking each mucoid colony on a differential medium (1 % glucose, 0.5 % yeast extract, 0.5 % L-glutamic acid, 0.05 % KH_2PO_4, 0.05 % K_2HPO_4, 0.01 % $MgSO_4$ $7H_2O$, and 1.5 % agar, pH 7.2±0.1) supplemented with 0.006% (w/v) neutral red as differential indicator. Any colony which interacted with the dye and formed a specific concentric zone after incubation at 37 °C was selected for further analysis as a potent γ-PGA-producing strain [19].

To differentiate whether the selected isolates are glutamic acid-dependent or -independent strains, the isolates were inoculated on a modified Basal medium without the supplement of L-glutamic acid (1% tryptone, 1% beef extract, 1% yeast extract, 1% glucose, 0.5% NaCl and 1.5% agar). Isolates which form observable mucoid colonies on the medium were considered as glutamic acid-independent strains [15].

2.2 Tube culture assay for γ-PGA production

Rapid growing colonies which produced clear concentric zone were selected and inoculated into 50 ml sterile tubes containing 5 ml of fermentation medium (3% glucose, 0.25% yeast extract, 2% L-glutamate, 0.05% KH_2PO_4, 0.05 % K_2HPO_4, 0.01% $MgSO_4 \cdot 7H_2O$, pH7.2±0.1) and incubated in a shaking incubator at 37 °C with shaking at 200 rpm for 48 h.

After incubation, the culture broth was diluted with an appropriate volume of deionized water to reduce the viscosity of the medium. Cells were separated from the medium by centrifugation at 12,000 rpm for 20 min and the supernatant was precipitated with four volumes of ice-cold ethanol. After centrifugation, the sediment was collected and dissolved in an appropriate volume of deionized water. Any insoluble contaminants was removed by centrifugation and the solution was then used for further quantification of γ-PGA. The yield of γ-PGA was determined by measurement absorbance of the sample solution at 216 nm using a UV/VIS spectrophotometer (Lambda 25; PerkinElmer, USA). A standard curve was plotted between the average blank corrected absorbance of each standard at 216 nm and its concentration (20-200 µg/ml). Bacterial isolates which produce considerable quantity of γ-PGA were selected and subjected to the identification and phylogeny study [19].

2.3 Bacterial identification and phylogeny study

Selected bacteria were grown in LB medium with shaking at 37°C overnight. Cells were collected by centrifugation. Genomic DNA was extracted using the Qiagen DNA extraction kit per manufacturer's protocol (Qiagen Inc., Valencia, USA). Almost complete 16S rDNA fragment was amplified by polymerase chain reaction (PCR) in a thermocycler (GeneAmp PCR system 9700, PerkinElmer-Applied Biosystems, USA) with the specific primers, 63f (5′-CAG GCC TAA CAC ATG CAA GTC-3′) and 1387r (5′-GGG CGG WGT GTA CAA GGC-3′) [20]. Purification of the PCR products was performed using a commercial kit per manufacturer's protocol (QIAGEN PCR Purification Kit, Qiagen Inc., Valencia, USA). The purified 16S rDNA fragments were sent to Macrogen Sequencing Service (Macrogen Inc., Seoul, Korea). The obtained sequences of 16S rRNA gene were assembled and manually corrected using the BioEdit program version 7.0 [21]. The primary comparison of the obtained sequences with the sequences available in GenBank was performed using the NCBI BLAST software (http://www.ncbi.nlm.nih.gov/blast). The sequences were aligned with the corresponding sequences of the closest bacterial species using the CLUSTAL_W program incorporated in the MEGA-X software package. Pair-wise evolutionary distances were calculated and a neighbour-joining phylogenetic tree was constructed using the MEGA-X. The stability of phylogenetic tree was assessed by bootstrap analysis with 1000 replicates.

3. Results and Discussion

3.1 Isolation and screening of γ-PGA producing bacteria

The polymer γ-PGA has attracted much attention as an environment-friendly material and many researchers have put efforts on searching for novel bacterial strains with more efficient production of γ-PGA. From previous literatures, there are a growing number of reports related to the isolation and screening for new bacteria with γ-PGA producing capability and almost entirely focused on the bacteria from food sources, particularly from fermented soybean products. Additionally, some of the recent knowledge has suggested that γ-PGA is a polymeric substance found in *Bacillus* biofilm and plays a role in the bacterial colonization on plant surfaces including fruit and root surface [22, 23]. In this study, we hypothesized that γ-PGA producing bacteria may be the common inhabitant of root rhizoplane of higher plants because of its capability to produce adhesive biofilm with γ-PGA as the main component.

The isolation of rhizoplane bacteria with γ-PGA producing capability was conducted with the combination of conventional and newly proposed methods. First, rhizoplane bacteria were isolated from the root samples using a minimal medium containing 0.5 % L-glutamic acid. According to the conventional criteria, single mucoid colonies emerged on the medium were presumed to be γ-PGA producing bacteria and were chosen for further screening using the differential medium proposed by Zeng *et al*. [19]. From the isolation and screening, a total of 368 isolates of probable producer of γ-PGA were obtained, 200 isolates from rice rhizoplane, 112 isolates from maize rhizoplane and the remaining 56 isolates from sugarcane rhizoplane.

In addition, a result of the discrimination of the γ-PGA producing isolates on glutamic acid-free medium revealed 86 isolates as glutamic acid-independent stains, representing about 23 percent of the total isolates obtained, implied that the population of glutamic acid-independent strain was in much less abundance.

3.2 γ-PGA production capability

The tube culture assay was conducted to quantitatively evaluate the capability of the isolated bacteria producing γ-PGA in a formulated glutamate containing medium. The results revealed 186 isolates (approximately 50 % of the total isolates) as potentially efficient γ-PGA producer with γ-PGA yields ranging from 12.62 - 18.46 g/l of culture broth. Among them, there were 16 isolates which produced higher than 15 g/l γ-PGA (Table 1). Thus these isolates were considered as the most efficient strains and were selected for further identification and phylogeny study.

Table 1. γ-PGA content produced by 16 most efficient strains after 48 h cultivation and their type of γ-PGA production.

Isolate	Sources	γ-PGA production (g/l)	Type of γ-PGA production
PGA 005	Rice	15.64	GD*
PGA 006	Rice	16.88	GD
PGA 009	Rice	18.36	GID**
PGA 21	Rice	15.06	GD
PGA 29	Rice	16.56	GD
PGA 52	Rice	17.36	GD
PGA 54	Rice	15.88	GID
PGA 62	Rice	16.92	GD
PGA 69	Rice	18.46	GD
PGA 75	Maize	18.01	GID
PGA 77	Maize	17.42	GD
PGA 84	Maize	17.33	GD
PGA 100	Sugarcane	17.81	GD
PGA 102	Sugarcane	18.01	GD
PGA 103	Sugarcane	15.48	GD
PGA 109	Sugarcane	16.92	GID

*Glutamic acid-dependence
**Glutamic acid-independence

3.3 Bacterial identification and phylogeny study

Based on the preliminary observation on morphology and some physiological properties, all the selected isolates were found to be Gram positive, rod shaped, spore forming and catalase positive bacteria, which are the common features of bacteria of the genus *Bacillus*.

Following the phenotypic characterization, the result from 16S rRNA gene analysis has confirmed that all the 16 isolates are phylogenetically close to *Bacillus* species as shown in Table 2 and in Figure 1. The results are in alignment with the most of previous studies which reported that bacteria of the genus *Bacillus* were the main producer of γ-PGA, including *B. amyloliquefaciens* subsp. *amyloliquefaciens, B. atrophaeus, B. methylotrophicus, B. siamensis, B. subtilis* subsp. *inaquosorum, B. subtilis* subsp. *subtilis, B. tequilensis, B. vallismortis* and *B. velesensis*.

Table 2. Sixteen most efficient strains producing γ-PGA after 48 h cultivation and their related taxa.

Isolate	Sources	Closely related taxa	Strain	Similarity (%)
PGA 005	Rice	*Bacillus amyloliquefaciens* subsp. *amyloliquefaciens*	DSM7$^{(T)}$	99
PGA 006	Rice	*Bacillus vallismortis*	DV1-F-3$^{(T)}$	100
PGA 009	Rice	*Bacillus siamensis*	KCTC 13613$^{(T)}$	98.9
PGA 21	Rice	*Bacillus atrophaeus*	JCM 9070$^{(T)}$	99.9
PGA 29	Rice	*Bacillus siamensis*	KCTC 13613$^{(T)}$	99.9
PGA 52	Rice	*Bacillus siamensis*	KCTC 13613$^{(T)}$	99.9
PGA 54	Rice	*Bacillus methylotrophicus*	XY18$^{(T)}$	99.9
PGA 62	Rice	*Bacillus tequilensis*	KCTC 13622$^{(T)}$	99.9
PGA 69	Rice	*Bacillus tequilensis*	KCTC 13622$^{(T)}$	99.9
PGA 75	Maize	*Bacillus subtilis* subsp. *subtilis*	NCIB 3610$^{(T)}$	99.9
PGA 77	Maize	*Bacillus siamensis*	KCTC 13613$^{(T)}$	99.9
PGA 84	Maize	*Bacillus siamensis*	KCTC 13613$^{(T)}$	99.9
PGA 100	Sugarcane	*Bacillus tequilensis*	KCTC 13622$^{(T)}$	100.0
PGA 102	Sugarcane	*Bacillus tequilensis*	KCTC 13622$^{(T)}$	99.9
PGA 103	Sugarcane	*Bacillus subtilis* subsp. *inaquosorum*	KCTC 13429$^{(T)}$	100.0
PGA 109	Sugarcane	*Bacillus velesensis*	CR-502 $^{(T)}$	99.9

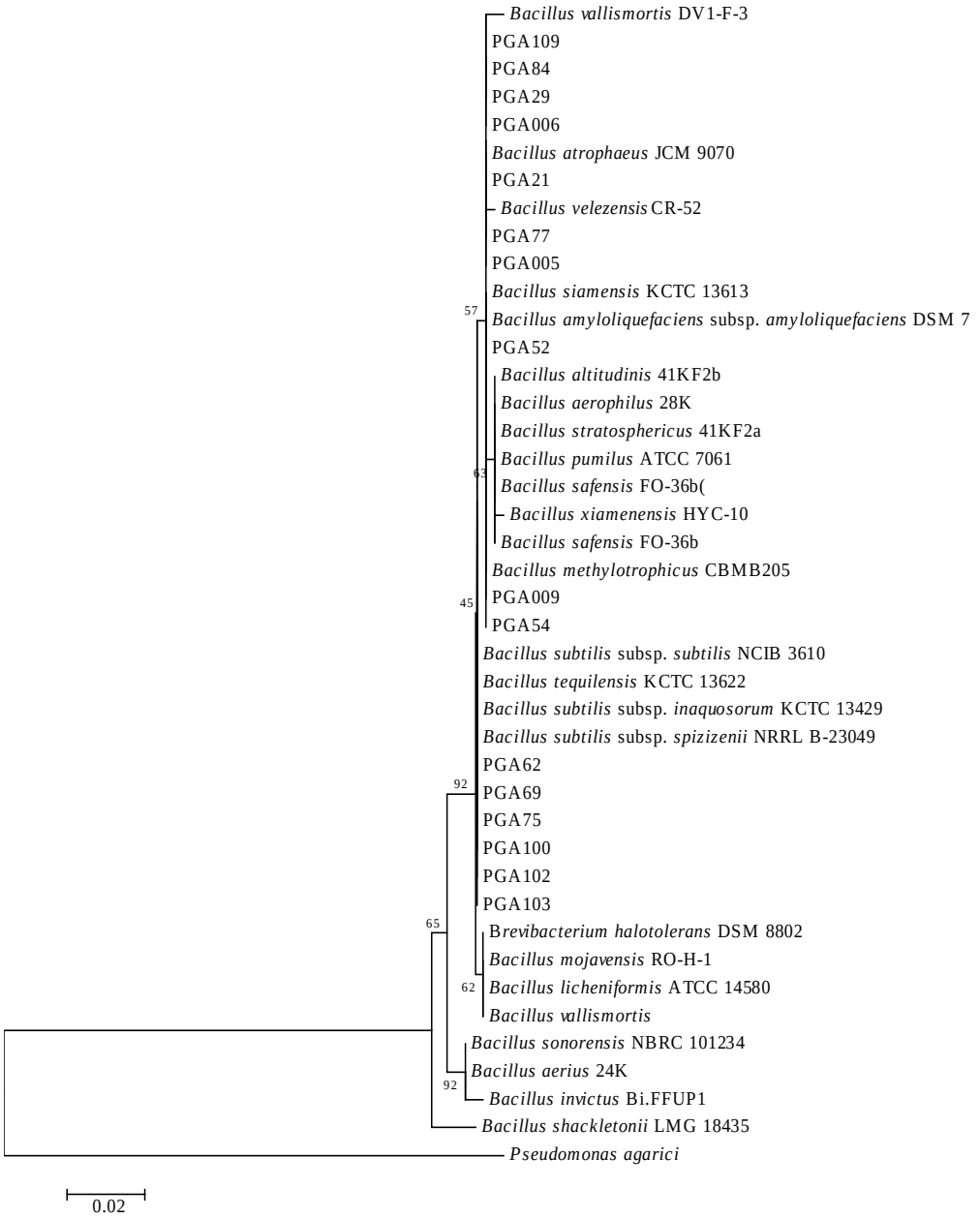

Figure 1. Phylogenetic tree of 16S rDNA sequences of the γ-PGA producing strains isolated from rhizoplane of rice, maize, sugarcane showing the relationship with members of the genus *Bacillus.* The phylogenetic tree was constructed by the neighbor-joining method. The type strain of *Pseudomonas agarici* was used as an outgroup organism. Numerals at nodes indicate bootstrap values (%) derived from 1,000 replications.

4. Conclusions

The results of this study have suggested that rhizoplane of three Poaceae plants, i.e. rice, maize and sugarcane are the natural habitat of γ-PGA producing bacteria, particularly of the genus *Bacillus*. Out of 200 isolates, 16 most efficient strains of the genus *Bacillus* produced γ-PGA between 15.06-18.46 g/l. Furthermore, it might be presumed that natural isolates of γ-PGA producing bacteria may also be prevalent on rhizoplane of other plant families.

5. Acknowledgement

This research work was supported by the National Research Council of Thailand.

References

[1] Ashiuchi, M. and Misono, H., 2002. Biochemistry and molecular genetics of poly-γ-glutamate synthesis. *Applied Microbiology and Biotechnology*, 59, 9-14.

[2] Peng, Y., Jiang, B., Zhang, T., Mu, W., Miao, M. and Hua, Y., 2015. High-level production of poly (γ-glutamic acid) by a newly isolated glutamate-independent strain, *Bacillus methylotrophicus*. *Process Biochemistry*, 50, 329-335.

[3] Tang, D.W., Yu, S.H., Ho, Y.C., Huang, B.Q., Tsai, G.J., Hsieh H.Y., Sung, H.W. and Mi, F.L., 2013. Characterization of tea catechins-loaded nanoparticles prepared from chitosan and an edible polypeptide. *Food Hydrocolloids*, 30(1), 33-41.

[4] Liang, H.F., Chen, C.T, Chen, S.C., Kulkarni, A.R., Chiu, Y.L., Chen, M.C. and Sung, H.W., 2006. Paclitaxel-loaded poly (γ-glutamic acid)-poly(lactide) nanoparticles as a targeted drug delivery system for the treatment of liver cancer. *Biomaterials*, 27, 2051-2059.

[5] Li, C., 2002. Poly (l-glutamic acid)-anticancer drug conjugates. *Advanced Drug Delivery Reviews*, 54, 695-713.

[6] Tanimoto, H., Fox, T., Eagles, J., Satoh, H., Nozawa, H., Okiyama, A., Morinaga, Y. and Fairweather-Tait, S., 2007. Acute effect of poly-γ-glutamic acid on calcium absorption in post-menopausal women. *Journal of the American College of Nutrition*, 26, 645-649.

[7] Yang, L.C., Wu, J.B., Ho, G.H., Yang, S.C., Huang, Y.P. and Lin, W.C., 2008. Effects of poly-γ-glutamic acid on calcium absorption in rats. *Bioscience, Biotechnology and Biochemistry*, 72, 3084-3090.

[8] Shih, I.L., Van, Y.T. and Sau, Y.Y., 2003. Antifreeze activities of poly (gamma-glutamic acid) produced by *Bacillus licheniformis*. *Biotechnology Letters*, 25, 1709-1712.

[9] Bhat, A.R., Irorere, V.U., Bartlett, T., Hill, D., Kedia G., Morris M.R., Charalampopoulos, D. and Radecka, I., 2013. *Bacillus subtilis* natto: a non-toxic source of poly-γ-glutamic acid that could be used as a cryoprotectant for probiotic bacteria. *AMB Express*, 3(1), 36. doi:10.1186/2191-0855-3-36

[10] Lee, C.Y. and Kuo, M.I., 2011. Effect of γ-polyglutamate on the rheological properties and microstructure of tofu. *Food Hydrocolloids*, 25, 1034-1040.

[11] Wang, F., Zhao J., Wei, X., Huo, F., Li, W., Hu, Q. and Liu, H., 2014. Adsorption of rare earths (III) by calcium alginate-poly glutamic acid hybrid gels. *Journal of Chemical Technology and Biotechnology*, 89, 969-977.

[12] Zheng. H., Gao, Z., Yin, J., Tang, X., Ji, X. and Huang, H., 2012. Harvesting of microalgae by flocculation with poly (γ-glutamic acid). *Bioresource Technology*, 112, 212-220.

[13] Shih, I.L. and Van Y.T., 2001. The production of poly-γ-glutamic acid from microorganisms and its various applications. *Bioresource Technology*, 79, 207-225.
[14] Buescher, J.M. and Margaritas, A., 2007. Microbial biosynthesis of polyglutamic acid biopolymer and applications in the biopharmaceutical, biomedical and food industries. *Critical Review in Biotechnology*, 27, 1-19.
[15] Zhang, H., Zhu, J., Zhu, X., Cai, J., Zhang, A., Hong, Y., Huang, J., Huang, L. and Xu, Z., 2012. High-level exogenous glutamic acid-independent production of poly-(gamma-glutamic acid) with organic acid addition in a new isolated *Bacillus subtilis* C10. *Bioresource Technology*, 116, 241-246.
[16] Cao, M., Geng, W., Liu, L., Song, C., Xie, H., Guo, W., Jin, Y. and Wang, S., 2011. Glutamic acid independent production of poly-γ-glutamic acid by *Bacillus amyloliquefaciens* LL3 and cloning of *pgs* BCA genes. *Bioresource Technology*, 102, 4251-4257.
[17] Ko, Y.H. and Gross, R.A., 1997. Effects of glucose and glycerol on γ-poly (glutamic acid) formation by *Bacillus licheniformis* ATCC 9945. *Biotechnology and Bioengineering*, 57, 430-437.
[18] Ueda, Y., Frindte, K., Knief, C., Ashrafuzzaman, M. and Frei, M., 2016. Effects of elevated tropospheric ozone concentration on the bacterial community in the phyllosphere and rhizoplane of rice. *PLoS One* 11, e0163178. https://doi.org/10.1371/journal.pone.0163178
[19] Zeng, W., Lin, Y., Qi, Z., He, Y., Wang, D., Chen, G. and Liang, Z., 2013. An integrated high-throughput strategy for rapid screening of poly (gamma-glutamic acid) -producing bacteria. *Applied Microbiology and Biotechnology*, 97, 2163-2172.
[20] Marchesi, J.R., Sato, T., Weightman, A.J., Martin, T.A., Fry, J.C., Hiom, S.J., Dymock, D. and Wade, W.G., 1998. Design and evaluation of useful bacterium-specific PCR primers that amplify genes coding for bacterial 16S rRNA. *Applied and Environmental Microbiology*, 64, 795-799.
[21] Hall, T.A., 1999. BioEdit: a user-friendly biological sequence alignment editor and analysis program for Windows 95/98/NT. *Nucleic Acids Symposium Series*, 41, 95-98.
[22] Liu, J., He, D., Li, X-Z., Gao, S., Wu, H., Liu, W., Gao, X. and Zhou, T., 2010. γ-Polyglutamic acid (γ-PGA) produced by *Bacillus amyloliquefaciens* C06 promoting its colonization on fruit surface. *International Journal of Food Microbiology*, 142, 190-197.
[23] Yu, Y., Yan, F., Chen, Y., Jin, C., Guo, J.-H. and Chai, Y., 2016. Poly-γ-Glutamic acids contribute to biofilm formation and plant root colonization in selected environmental isolates of *Bacillus subtilis*. *Frontiers in Microbiology*, 7, 1811. doi: 10.3389/fmicb.2016.01811

Developing Stubble Chopper Device Adequate for Small Livestock Barns

Ahmed Shawky El-Sayed[1*], Mohamed Ali Ibrahim Al-Rajhi[2] and Ayman Mousa Abdel-AZeem El-Beba[3]

[1]Department of Biological Engineering, Agriculture Engineering Research Institute (AENRI), Agriculture Research Center (ARC), Dokki, Giza, Egypt
[2]Department of Animal Production Mechanization, Agriculture Engineering Research Institute (AENRI), Agriculture Research Center (ARC), Dokki, Giza, Egypt
[3]Department of Field and Horticultural Crops Mechanization, Agriculture Engineering Research Institute (AENRI), Agriculture Research Center (ARC), Dokki, Giza, Egypt

Received: 20 November 2018, Revised: 25 May 2019, Accepted: 6 June 2019

Abstract

The main objectives of this research are to develop a sustainable feeding unit in the small barns for daily fresh feed production by minimizing the operation cost of feed manufacturing and mixing the good soften cutter feed with nutrient supplements mechanically using an easy operating system. The storage of mixed fodder for a long period can expose its validity into rancidity and oxidation and reduces the nutritional value. Thus, an adequate feeding unit suitable for small barns is developed. Three experiments are conducted to test the developed unit on the variable levels of the cutting speeds (7.540, 9.426 and 11.304m/s), three feeding rates of (0.3, 0.6 and 0.9 ton/h) and three knife interferences of (5, 10 and 15 mm) to measure the performance rates, efficiency and economic evaluation. The results indicated that the maximum percentage in the soften cutting length > 5 cm was 92.82 % at the helical distribution with the maximum speed of 11.304 m/s, feeding rate of 0.9 ton/h and the largest knife interference of 15 mm. Besides, the maximum feed mixing efficiency (95.45 %) was recorded at the highest adaptable settings. Meanwhile, the maximum machine productivity was recorded at 0.85 ton/h at the same variables. Moreover, the maximum power consumption value (6.85 kWh/ton) was obtained at the lowest cutting speed of 7.540 m/s, feeding rate of 0.85 ton/h and knife interference of 5 mm. The maximum operation cost was 121.20 Egyptian pound/ton with the same factors.

Keywords: rancidity, oxidation, validity, cutting, mixing, feeding
DOI 10.14456/cast.2019.18

*Corresponding author: E-mail: a.shawky71@ yahoo.com

1. Introduction

Feed manufacturers usually choose ingredients that are the least cost but still meet the desired nutritive properties for a given species [1] The primary force driving changes in feeding practices has been economic on how to bring food animals up to weight as quickly and cheaply as possible [1]. Feed availability, new feed ingredients and new feeding practices have played important roles in the concentration of animal food production operations [2].

The reviewed researches are branched into five main topics. First topic is focused on the use of agricultural residues in feed ingredients. Rice straw represents an important agricultural residual in Egypt and approximately 3.5 million tons of rice straw is produced every year.

In general, the maximum intake of rice straw by ruminants is about 1.0 to 1.2 kg per 100 kg live weight [3]. Also crops residues (CRs) are roughages that become available as livestock feeds after crops have been harvested [4]. Livestock farmers, especially in the sector of goats, sheep and cattle, are constantly faced with problem of feed shortage during the dry season [5]. However**,** crop residue such as rice straw could be treated with urea or calcium hydroxide or by supplementing rice straw with protein for the enhancement of intake, degradability and milk yield [6-7]. Second topic concerns improving the feed nutrient value. Generally, supplementation of a ration of rice straw with protein, energy and/or minerals may optimize rumen function and also increase intake [1]. Molasses can be a source of quick energy and an excellent source of minerals for farm animals and it is an effective way to increase the palatability of feeds through the use of diluted molasses (with water) by sprinkle its solution over the fodder from 0.1 % and 0.4 % (when a forage-based diet was fed) to 1 % and 3 %, respectively [8]. Third topic emphasizes on the effect of storage on feed validity. Clearly, oxidation is one of the major reasons that feeds deteriorate and is caused by the reaction of fats and oils with molecular oxygen leading to off-flavors that are generally called rancidity [9]. However, oxidative rancidity is of special interest as it leads to the development of unfavorable off-flavors that can be detected early on in the development of rancidity [10]. Also, keeping quality of alimentary animal fats is governed by factors such as storage temperature, permeability of the packaging material to air and moisture [11]. However, nutritional losses and other deteriorative changes in animal fats are concerned with the changes that result from their reaction with atmospheric oxygen [9]. Fourth, the benefits of feed cutting are examined. More clearly, quality of crop residues and roughages are improved by both chemical and physical methods [12]. Physical treatment of residues prior to chemical treatment improves materials acceptance of chemical treatment. Physical treatment includes chopping, shredding, grinding and pelleting [12]. Also, knife mills or choppers work successfully for shredding forages under various crops and machine conditions. Disc mills produce very small particles if input feed is provided by knife mills or hammer mills [13]. The range of cutting crop residues (1-3 cm) is suitable for sheep and goats while the range of 3-5 cm is suitable for large animals [2]. However, using different chopped roughage can solve serious problems of animal feeding shortage in Egypt [14]. Chopping farm residues in pieces less than 3 cm improves its efficiency when used in feeding livestock [14]. Fifth topic concerns the development of feed cutting devices. The results for an improved designed cutting machine for rice straw and maize stalks indicated that the maximum percentages (87.80 and 92%) in cutting length of less than 5 cm were obtained for rice straw and corn stalks residues, respectively, at cutting speed of 10.09 m/s, feeding rate of 0.771 ton/h and knife clearance of 1.5 mm while the energy consumed was 6.36 and 6.17 kWh/ton [15]. However, a developed combined cutting-unit with the harvesting combine machine was designed and about 27% from straw length < 5 cm was recorded at cutting speed 12.65 m/s while rice-straw length between 5-15 cm was about 54% and rice-straw length > 15 cm was about 19% [16]. In addition, the cutting unit in the Japanese combine was modified and tested and it was found that the power consumption increased with increasing forward speed and cutting speeds, while the energy

requirement (kWh/ton) increased with decreasing forward speed and increasing cutting speed with highest percentage value 83% of short pieces < 6 cm was obtained at 0.75m/s [17]. Besides, a suitable developed cutting rice-straw machine was developed for appropriate lengths for the manufacture of animal feed and compost [18]. The productivity of 892 kg/h, power requirement about 5.05 kW, the operation cost of 13.63 Egyptian pound/h at 2015 and specific energy 5.67 kWh/t were obtained [18].

The main objectives of the research are to investigate on the production of fresh daily feed for the small barns and how to minimize the operating cost of manufacturing feed. The good soften cutter feed mixed with nutrient supplements mechanically with easy operating system was also examined.

2. Materials and Methods

2.1 Design of developed unit

The developed unit depended on the cutting disks knives in the rear part for the Japanese rice combine harvesters is designed. Usually, operating combines in Egypt are conducted without using these parts due to its problems from increasing the mechanical loads so it was removed from rice combine harvesters. The utilization of reusing these units to make separate equipment is examined. The modification of the developed unit is to make a propelled equipment suits small barns using small tractors as the power source from tractor power take off (PTO) or using a separate gasoline motor. The general description of the developed equipment is shown in the schematic drawing (Figure 1).

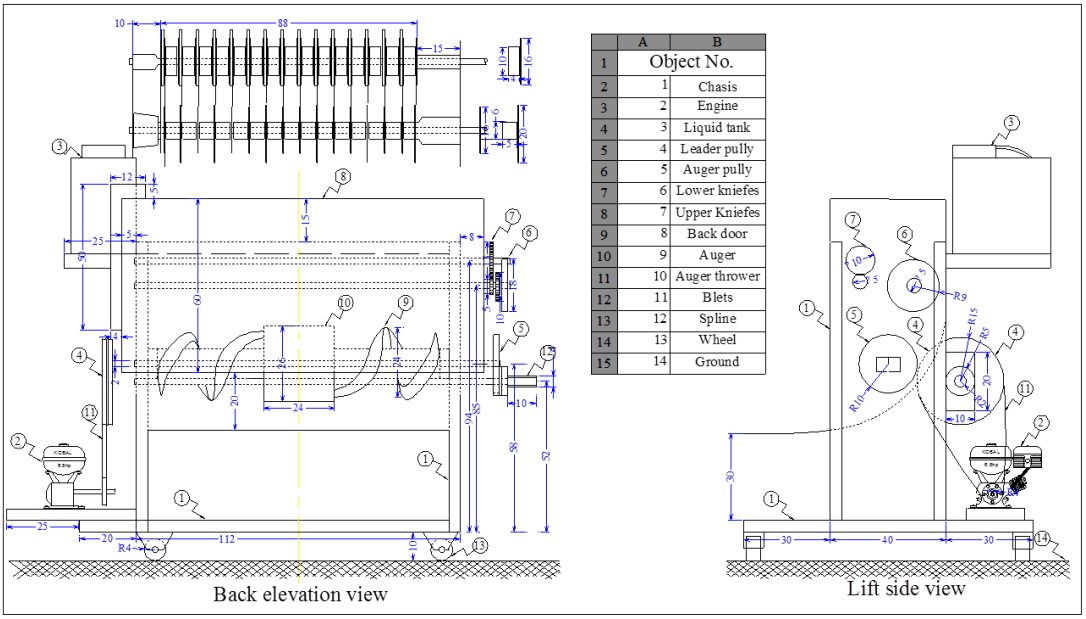

	A	B
1	Object No.	
2	1	Chasis
3	2	Engine
4	3	Liquid tank
5	4	Leader pully
6	5	Auger pully
7	6	Lower kniefes
8	7	Upper Kniefes
9	8	Back door
10	9	Auger
11	10	Auger thrower
12	11	Blets
13	12	Spline
14	13	Wheel
15	14	Ground

Figure 1. Schematic drawing for the developed feeding equipment (dimensions: cm)

The new developed cutting and mixing unit consists of the following parts as follows:

1) Power source: The power source has duel outlets portions. The first one, as shown in Figures 2-5 built from the hexagonal attached shaft which connected to the PTO in the low power tractors (less than 30 hp) which fits the required power consumption that ranges about 6.85 kWh/ton. On the other hand, a separate gasoline motor 6.5 hp is attached to operate the feeding equipment as shown in Figure 3 and its specifications are listed in Table1.

Table 1. The used gasoline motor specifications

Model	**Kobal, made in China**
Certification	EPA
Engine displacement (cc)	212
Horsepower (hp)	6.5
Speed (max) RPM	3800

Figure 2. The developed unit (rear side view)

Figure 3. The developed unit (front side view)

Figure 4. The developed unit (right plane view)

Figure 5. The developed unit (left plane view)

2) Chassis: The chassis is made from iron heavy square pipes (4 cm) which welded and manufactured locally to stand tracking on its own four wheels (12 cm dia.) and trailed by the tractor with two front bearer bars that turns the feeding equipment on pivotal axial coupling. The developed unit has dimensions of 2.5×0.75×1.65 m (length× width× height) as shown in the schematic drawing Figure 1.

3) The cutting unit: As shown in Figures 6-9, two inside different cutter drums have the cutting action for the picked feed to the unit which do the work by organized steps. The mirrored straw was first caught by the top drum. The straw was then pressed between the cutting edges of the top and the lower cutter drums which rotates in reverse to each other. The top drum consists of two kinds of vertical disc knives. One of these knives has tags to catch the straw and prevent it from sliding as shown in Figure 10(a). Fifteen knives which have tags or the caught disks were arranged side by side sixteen cutter knives disks on the hexagonal section shaft.

Figure 6. The cutting and mixing unit initial parts

Figure 7. The electrical sprayer distributor

Figure 8. The cutting unit feeding trays

Figure 9. The outlet cutting rough feed

4) The cutting unit modification: There are three main modifications as follows:

a) The lower cutting rotor as shown in Figures 10-11, the bottom cutting rotor has been modified by adding and distributing an additional cutting blades between collars of the cutting rotor with two distributions arranged as the vertical one and the helical one, along the cutting rotor drum to duplicate the cutting force on the feeding forages to decreases its lengths as required (Figure 9).

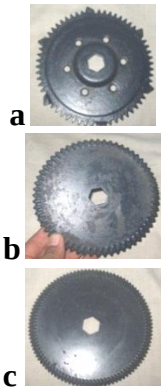

Figure 10. The different disc knives (a and b 16 cm dia.) for the upper rotor and (c) for the lower rotor (16 cm dia.).

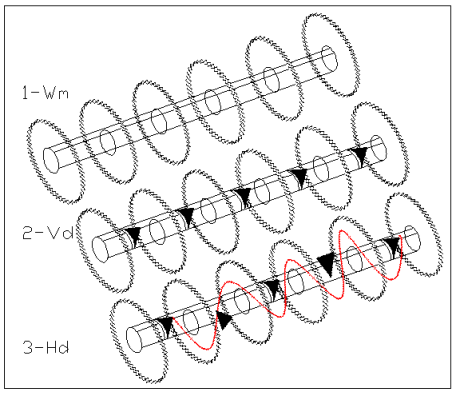

Figure 11. The different attached knives distributions (1-Wm: without modification, 2-Vd: vertical distribution and 3- Hd: helical distribution).

b) The inlet feeding trays: Two main trays on the both sides of the cutting unit are merged to set the feed rate equally between the used straw residual and the dried forage and to balance the feed ingredients (Figure 8). The tray dimension is 120×30 cm.

c) The outlet tray: This part was designed as shown in Figures 5 and 7 to provide the feeding directly to the animals, which falcate the feed process.

5) The mixing unit: As shown in Figures 6 and 12, the right hand of the auger has double sides which conveys each other inversely in the direction to the convey zone that mixes the fallen mixed cutter feed.

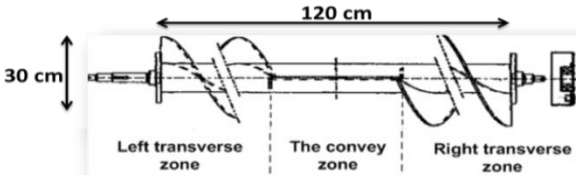

Figure 12. The mixing feed auger

Figure 13. The duel sprayer nozzles

6) The electrical sprayer distributor (for useful supplements liquid): As shown in Figure 7, an adequate garden sprayer is used for spraying liquid through the outlet cutter feed with reviewed ranges of its discharge rate (1 l/10 kg dry rough-feed) from doubled hanged sprayers on the cutting door (as shown in Figure 13). The sprayer has 12 litre tank with rechargeable 12 volt battery and operates with inlet strong pump that provides flow rate up to 1 l/min. In addition, the mass of the discharged supplement was controlled by adapting the nozzles collar to set its cone diameter by rolling it.

7) The transmission unit: The power transmitted (as shown in Figures 2 and 3) from the driving pulley of 7 cm dia. on the gasoline motor shaft to the main idler shaft front pulley (22 cm dia.) to the other left pulley (12 cm dia.) on the same shaft. The power was then branched to the cutting and the mixing unit pulleys, respectively (17 and 20 cm dia.), as shown in Table 2. The different changeable linear speeds are due to controlling the gasoline lever at three different loads as listed.

Table 2. The cutting and mixing unit linear speed

Motor pulley (rpm)	Cutting pulley (rpm)	Cutting pulley (m/s)	Auger pulley (rpm)	Auger pulley (m/s)
2400	847	7.540	720	7.540
3000	1059	9.426	900	9.425
3600	1270	11.304	1080	11.310

2.2 Study of performance parameters

The performance parameters of the designed machine are described as follows:

1) Three cutting speeds (V) of 7.540, 9.426 and 11.304 m/s which changed according to the transmission system.
2) Three feeding rates (F) of 0.3, 0.6 and 0.9 ton/h which settled experimentally by adapting the feeding quantity with the time using the merged cutting unit trays as listed in Table 3.
3) Three knife interferences (I) of 5, 10 and 15 mm which according to lateral controlling lever that gauge the interference distance between the two cutting rotors (Figure 2).

Table 3. The used feed ingredients at the changed feeding rates

Feeding rate (ton/h)	Feed ingredients		
	Straw (kg)	Dried clover (kg)	Supplement liquid (litre)
0.3 (5 kg/min)	3.0	1.5	0.5
0.6 (10 kg/min)	6.0	3.0	1.0
0.9 (15 kg/min)	9.0	4.5	1.5

2.3 Measurements

Three experiments were conducted and replicated three times. The developed feed equipment was studied to evaluate the developed unit without modification (Wm) and after distributing the additional blades in the vertical (Vd) and helical (Hd) distributions to measure the following:

1) The cutting lengths percentages (CL, %): After each cutting treatment, a sample of 1 kg weight from cutting crop material was taken and separated into three categories, i.e. less than 5, more than or equal 5-10 and more than 10 cm. Each cutting length in the sample was weighed and calculated as a percentage from the total sample weight. The mean length cutting straw was calculated using the following equation according to Wanapat *et al.* [7]:

$$M.L.S = \frac{\Sigma_i^n . X_i . W_i}{W_{i-n}} \quad (1)$$

Where: M.L.S is the mean length cutting straw,
Xi is the mean length of each division (Wm, Vd, Hd) and
Wi is the sample weight of each division, g.

2) The mixing efficiency (M, %): After every treatment the outlet of mixed feed random sample was analyzed. Each ingredient weight (straw, dried forage and supplement liquid) was dived into the total weight to measure the mixing efficiency percentages by the following equation:

$$M = \frac{S_w \times D_w \times L_w}{T_w} \times 100\ \% \quad (2)$$

Where: M% is the mixing efficiency,
S_w is the straw weight (g),
D_w is the dried clover weight (g),
L_w is the supplement liquid weight (g) and
T_w is the total sample weight (1000 g).

3) The machine productivity (P, ton/h): The machine productivity was calculated by using the following equation:

$$P = \frac{M \times 60 \times 1}{1000} ton/h \quad (3)$$

Where: P is the machine productivity (ton/h), M is straw feed mass (kg), 60 is minutes, 1 is one ton and 1000 is constant.

4) The fuel consumption (F), L/min: Fuel consumption was determined by measuring the volume of fuel consumed during the operation time for each run and calculated in liter per hour. It was measured by completely filling the fuel tank before each end run and refilling the fuel tank was used as a scaled container. The fuel consumption rate was calculated by the following equation:

$$F = \frac{V}{T} \quad L/h \quad (4)$$

Where: F: rate of fuel consumption, L/h, V: rate of consumed fuel, L and T: time, h.

5) The consumed power requirements (Pr, kW.h/ton): The consumed power requirements were calculated by using the following equation [19]:

$$Pr = \left(\frac{Fs \times \rho_f \times C.V}{3600} \right) \times \left(\frac{427 \times \eta_{th} \times \eta_m}{75 \times 1.36 \times P} \right) kW.h/ton \quad (5)$$

Where: Pr is energy requirements (kW.h/ton),
Fs is fuel consumption rate (L/h),
ρf is density of fuel (kg/L) (for diesel = 0.85 kg/L),
C.V is calorific value of fuel (Kcal/kg,),
427 is thermal-mechanical equivalent (kg.m/Kcal),
ηth is thermal efficiency of the engine, assumed 40 % for diesel engine,
ηm is mechanical efficiency to engine, assumed 80 % for diesel engine and
P is machine productivity (ton/h).

6) The operating cost (C, Pound/ton): The operating cost was determined using the following formula:

$$\text{Operating cost (C)} = \frac{\text{Machine hourly cost (Pound/h)}}{\text{Actual machine capacity (ton/h)}} \text{ Pound/ton} \quad (6)$$

3. Results and Discussion

3.1 Factors affecting mean cutting length percentages

In general, the obtained first percentage category of cutting length < 5 cm at the effect of the cutting speed (V) within the tested variables; the different feeding rates (F) and also the knife interferences (I). Figure 14 shows From these figures, it could be cleared that, there are high effect for V at the new development for the new knife distribution on the beneath cutting rotor from the vertical to the helical arrangements which improves significantly the desired cutting length category < 5 cmmore than the other categories > 5-10 and >10 cm.

The results indicated that increasing the cutting speeds from 7.540 to 11.304 m/s would directly increase the percentage of cutting length < 5 cm at the both variable levels for F and I. As shown in Figure 14, the maximum values of the cutting length percentages for the 1st category distribution of soften length (< 5 cm) were 83.83, 89.41 and 92.82 % for the (Wm, Vd and Hd), respectively and the highest value (F) 0.9 ton/h at the highest (V) of 11.304 m/s while the minimum values for the 1st category were 71.39, 76.97 and 80.38 % for the (Wm, Vd and Hd) distributions, respectively at the lowest value of (F) 0.3 ton/h and (V) of 7.540 m/s. Also, as shown in Figure 14(b), the maximum values of the cutting length percentages for 1st category were 82.85, 88.43 and 91.84 % for the (Wm, Vd and Hd) distributions, respectively, at the highest value (V) of 11.304 m/s and the highest value (I) of 15 mm while the minimum values for the 1st category were 72.50, 78.08 and 81.49 % for Wm, Vd and Hd distributions, respectively at the lowest value (V) of 7.540 m/s and (I) of 5 mm. It could be stated that the distribution percentage of cutting length less than 5 cm were increased by increasing both knife interference and feeding rate levels. There are high significance differences between the tested treatments and the total interaction between it to CL %. The analysis of variance for the data of 1st category for CL % at different tested factors indicated highly significant differences between the treatments. A simple power regression analysis is applied to relate the change in the 1st category < 5 cm with the change in the tested factors in the form of:

(Wm) Without modification	[<5 cm] = (50.178, 55.758 and 59.168)+ 2.498 V + 4.854 F + 0.0983 I	
	R^2= 0.9977	C.V. = (0.306, 0.286 and 0.0274)

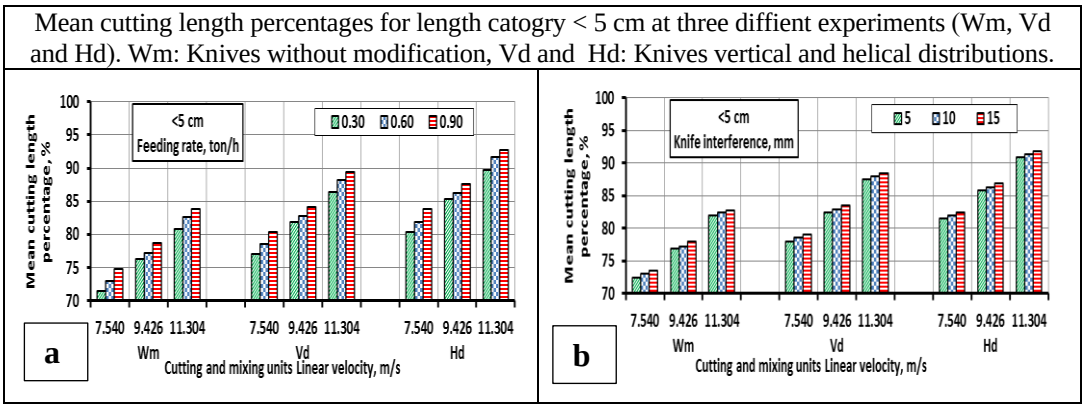

Figure 14. The effect of cutting and mixing unit linear velocity on the mean cutting length percentages of category < 5 cm at the different feeding rates and knife interference

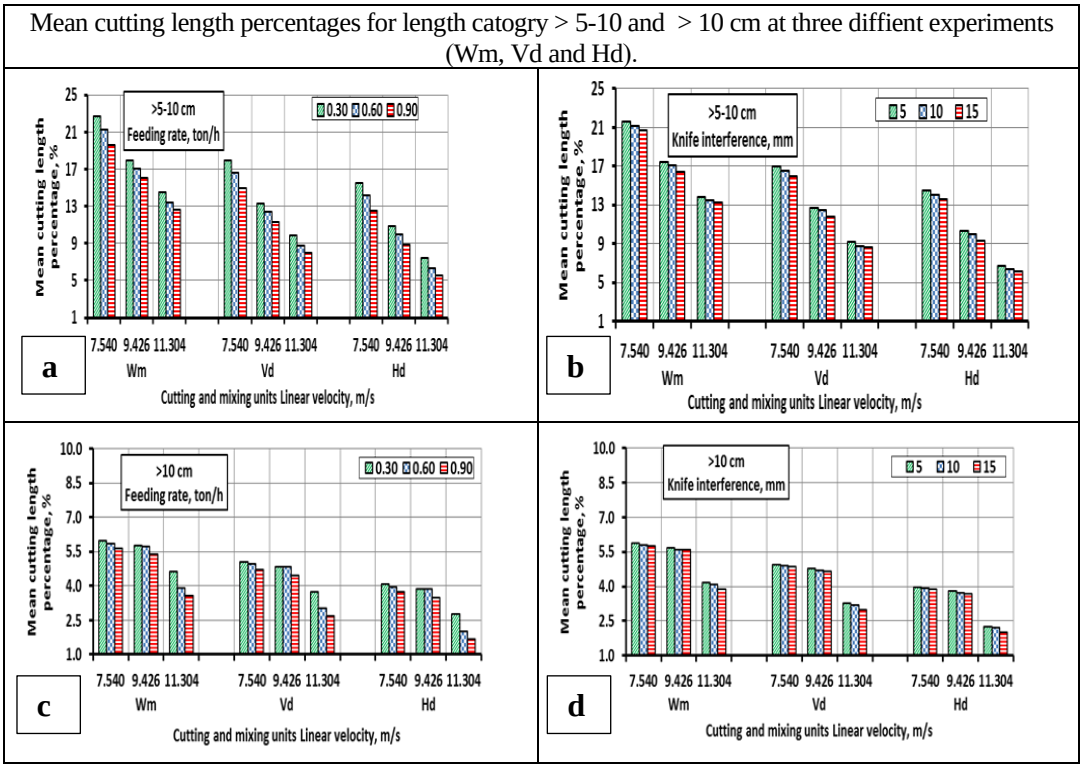

Figure 15. The effect of cutting and mixing unit linear velocity on the mean cutting length percentages of category > 5-10 and > 10 cm at the different feeding rates and knife clearances

Figure 15 showed that there are an oppositely relationship by increasing the cutting speed the (CL) percentages decreased with increasing both of the F and the I. The results showed that increasing the cutting speeds from 7.540 to 11.304 m/s adversely decreased the percentage of cutting length (> 5-10 and > 10 cm) at both variable levels for F and I. The maximum values of the

CL% for 2nd and 3th categories (> 5-10 and > 10 cm) as shown in Figure 15 (a and b), were (22.63, 17.95 and 15.53 %) and (5.98, 5.08 and 4.09 %), respectively, for the lowest feeding rate (F) 0.3 ton/h and the lowest cutting speed (V) of 7.540 m/s while the minimum values were (12.58, 7.90 and 5.48 %) and (3.59, 2.69 and 1.70 %) for the (Wm, Vd and Hd), respectively, at the highest value of (F) 0.9 ton/h and (V) of 11.304 m/s.

In that manner, as shown in Figure 15 (c and d), the maximum values of the CL% for 2nd and 3th categories were (21.63, 16.95 and 14.53 %) and (5.87, 4.97 and 3.98 %), respectively, for the lowest (V) of 7.540 m/s and the minimum (I) of 5 mm. The minimum values were (13.26, 8.58 and 6.16 %) and (3.89, 2.99 and 2.00 %) for the (Wm, Vd and Hd), respectively, at the maximum value (V) of 11.304 m/s and (I) of 15 mm. From the results, the new CL% with ($P < 0.05$) could be clarified. The analysis of variance for the data of 2nd and 3th categories showed highly significant differences. The power regression equations for 2nd and 3th categories are as follows:

(Vd) Knives distribution

$$[>5\text{-}10\ \text{cm}] = (39.479, 34.799 \text{ and } 32.379) - 2.029\ V - 3.864\ F - 0.0826\ I$$

$R^2 = 0.9967$ C.V. = (1.347, 1.850 and 2.293)

(Hd) Knives distribution

$$[>10\ \text{cm}] = (10.343, 9.443 \text{ and } 8.453) - 0.469V - 0.990\ F - 0.0157\ I$$

$R^2 = 0.9908$ C.V. = (1.939, 2.347 and 3.056)

3.2 Factors affecting feed mixing efficiency (M %)

As shown in Figure 16(a), the maximum values of M were 88.38, 94.63 and 95.45 %, respectively, at the highest (F) 0.9 ton/h and the highest (V) of 11.304 m/s. The minimum values of M were 75.94, 82.19 and 83.01 % for the (Wm, Vd and Hd), respectively, at the lowest value of (F) 0.3 ton/h and (V) of 7.540 m/s. Also, as shown in Figure 16(b), the maximum values of M were (87.40, 93.65 and 94.47 %), respectively, at (V) of 11.304 m/s and (I) of 15 mm. The minimum values of M were (77.05, 83.30 and 84.12 %) for the (Wm, Vd and Hd), respectively, at the lowest value (V) of 7.540 m/s and (I) of 5 mm. The use of two- part auger with high rotational speed and screw pitch led to the efficiency of feed mixing at the highest speeds with the maximum levels of (F and I). There are significance differences between the tested factors and the total interaction between it to M with ($P < 0.05$). The power regression equations for M% are as follows:

Wm, Vd and Hd Knives distributions

$$[M\%] = (54.728, 60.978 \text{ and } 61.798) + 2.498\ V + 4.854\ F + 0.098\ I$$

$R^2 = 0.9977$ C.V. = (0.289, 0.269 and 0.266)

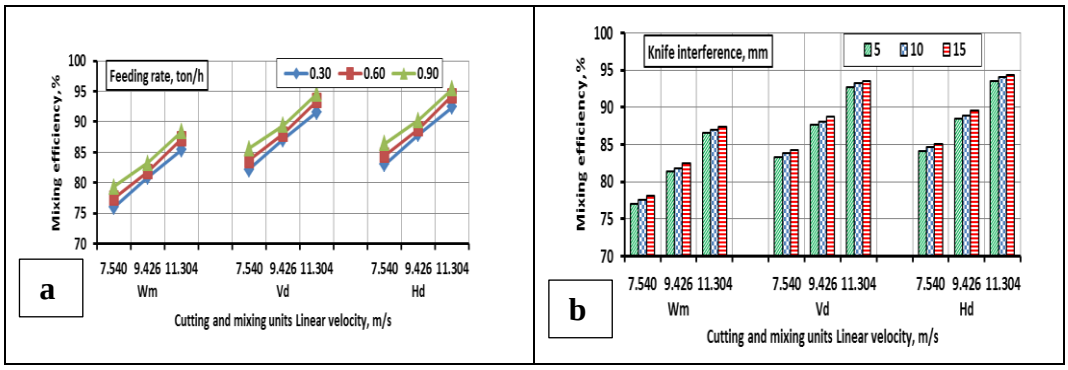

Figure 16. The effect of cutting and mixing unit linear velocity on the feed mixing efficiency at the different feeding rates and knife interference

3.3 Factors affecting the machine productivity (P, ton/h)

As shown in Figure 17(a), there are direct relations between the highest values of P (0.79, 0.84 and 0.85 ton/h), respectively, at (F) 0.9 ton/h and (V) of 11.304 m/s while the minimum values of P were (0.23, 0.24 and 0.25 ton/h) for the (Wm, Vd and Hd), respectively, at the lowest value of (F) 0.3 ton/h and (V) of 7.540 m/s. Moreover, the maximum values of P were (0.52, 0.56 and 0.57 ton/h), respectively, at (V) of 11.304 m/s and (I) of 15 mm as shown in Figure 17(b). The minimum values of P were (0.46, 0.49 and 0.50 ton/h) for the (Wm, Vd and Hd), respectively, at the lowest value (V) of 7.540 m/s and (I) of 5 mm. The application of the maximum cutting speed, feeding rates and knife interferences allowed relatively mass production and improved the cutting unit to contain large capacity of the feed to produce these values of huge capacities.

The statistical analysis showed high significance differences between the tested treatments and the total interaction between it to P with ($P < 0.05$) and highly significant differences between the treatments. The obtained regression equations for P were in the form of:

Wm, Vd and Hd

$$[P(ton/h)] = (-0.161, -0.161 \text{ and } -0.161) + 0.0149\ V + 0.841\ F + 6.037e\text{-}4\ I$$

Knives distributions

$$R^2 = 0.9999 \qquad C.V. = (0.328, 0.321 \text{ and } 0.311)$$

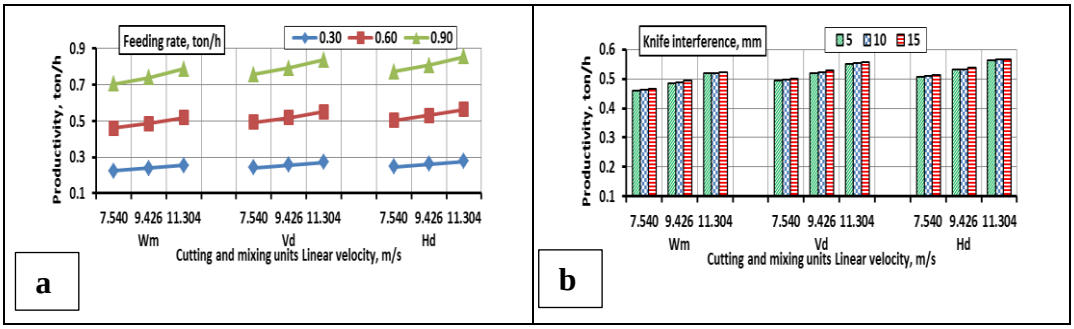

Figure 17. The effect of cutting and mixing unit linear velocity on the total machine productivity at the different feeding rates and knife interference

3.4 Factors affecting power requirements (Pr, kWh/fed)

As shown in Table 4, the fuel consumption rates range from 0.49 to 0.62 l/h which is more economical for the operating of the designed feed equipment.

Table 4. The fuel consumption rates at the tested factors

Distribution	V and F	Wm	Vd	Hd	V and I	Wm	Vd	Hd
Fuel cons. Max l/h	11.304m/s 0.9 ton/h	0.57	0.61	0.62	11.304m/s 15 mm	0.56	0.60	0.61
Fuel cons. Min l/h	7.540m/s 0.3ton/h	0.49	0.52	0.54	7.540 m/s 5 mm	0.49	0.53	0.54

Generally, there are a direct relation as shown in Figure 18 (a) that the maximum values of Pr were equaled at 6.85 kWh/ton for the (Wm, Vd and Hd) distributions, respectively, at the lowest feeding rate (F) of 0.3 ton/h and the lowest cutting speed (V) of 7.540 m/s while the minimum values for Pr was equaled at (2.28kWh/ton) for the (Wm, Vd and Hd) distributions, respectively at the maximum value (F) of 0.9 ton/h and (V) of 11.304 m/s. From the results it could be stated that the consumed fuel was not affected by the machine loads unless the changing of machine speed was decreased by the power requirements at the higher values of V than the lowest speeds. Figure 18(b) shows a linear relationship between Pr and V at the different values of F and I which explains that there were no significant differences between the tested factor I and Pr but the significant difference was found between the changing of the cutting speed and the feeding rate. The obtained regression equations for Pr were in the form of:

(Wm), (Vd) and (Hd) distributions [Pr kW.h/ton] = (8.757, 8.757 and 8.757) - 4.929e -17 V -7.615 F +1.266e-19 I R^2= 1

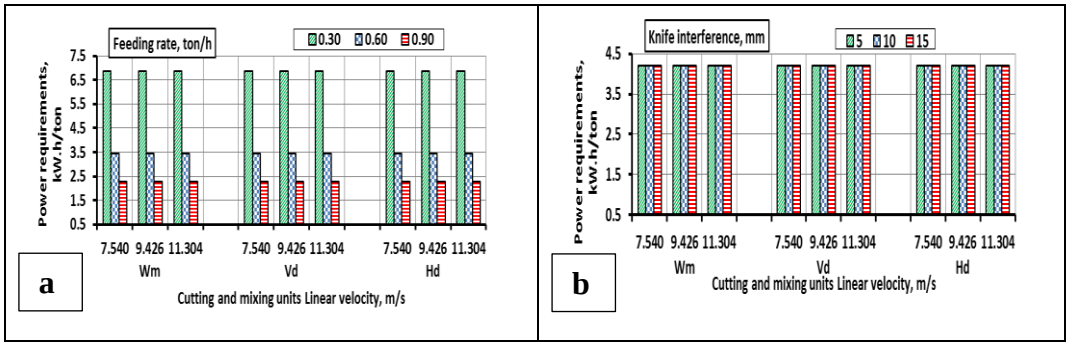

Figure 18. The effect of cutting and mixing unit linear velocity on the power requirements at the different feeding rates and knife interference

3.5 Factors affecting operating cost (C, Pound/ton)

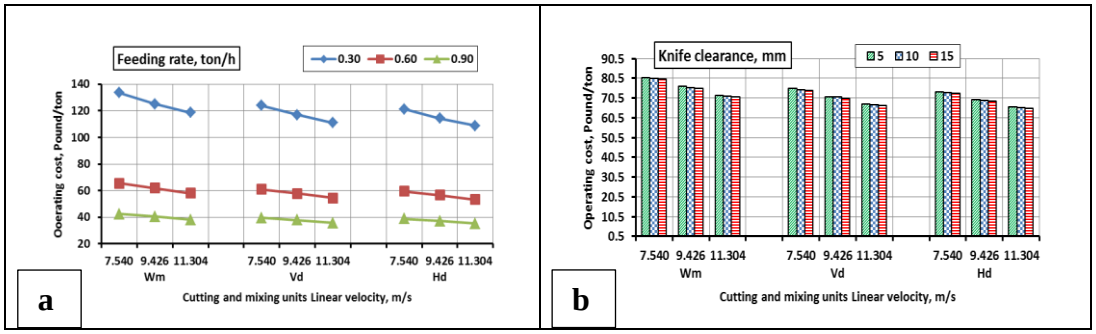

Figure 19. The effect of cutting and mixing unit linear velocity on the machine operating cost at the different feeding rates and knife interference

As shown in Figure 19 (a), there are inverse relations. The maximum values of C were (133.35, 123.93 and 121.20 Pound/ton), respectively, at (F) of 0.3 ton/h and (V) of 7.540 m/s. The minimum values of C were (38.13, 35.79 and 35.11 Pound/ton) for the (Wm, Vd and Hd), respectively, at the maximum value of (F) 0.9 ton/h and (V) of 11.304 m/s. However, the maximum values of C were (80.91, 75.23 and 73.59 Pound/ton), respectively, at (V) of 7.540 m/s and (I) of 5 mm while the minimum values of C were (71.13, 66.70 and 65.40 Pound/ton), respectively at (V) of 11.304 m/s and (I) 15 mm as shown in Figure 19(b). The manufacturing cost was 10 thousand Egyptian pounds in 2018. The results showed that the use of minimum cutting speeds, feeding rates and knife interferences could increase the operating costs more than the levels of economical operation for the developed machine. The power regression equations for (C) were in the form of:

(Wm), (Vd) and (Hd) Knives distributions: [C (Pound/ton)] = (184.334, 170.540 and 166.554) – (2.362, 2.060 and 1.975) V – (142.088, 132.423 and 129.607) F – (0.0898, 0.07821 and 0.0751) I

R^2= 0.9999 C.V. = (0.310, 0.289 and 0.283)

4. Conclusions

It could be concluded that the maximum percentage in the soften cutting (length > 5 cm) was 92.82 % at the helical distribution with the maximum speed of 11.304 m/s, feeding rate of 0.9 ton/h and the largest knife interference of 15 mm. Besides, the maximum feed mixing efficiency of 95.45 % was recorded at the highest adaptable settings. The maximum machine productivity was recorded at 0.85 ton/h at the same variables. The maximum power consumption value at 6.85 kWh/ton was obtained at the lowest cutting speed of 7.540 m/s, feeding rate of 0.85 ton/h and knife interference of 5 mm. In addition, the maximum operation cost was 121.20 Pound/ton with the same factors. It is recommended to establish this modified system in the small barns.

5. Acknowledgements

Many thanks for Prof. Mohamed El Kholy and Prof. Gamal Hasan Elsayed, Agriculture Engineering Research Institute, Egypt.

References

[1] Chenost, M. and Kayouli, C., 1997. Roughage utilisation in warm climates. *FAO Animal Production and Health Paper 135*, Rome

[2] Church, D.C., 1991. *Livestock Feeds and Feeding*. 3rd ed. Englewood Cliffs: Prentice Hall.

[3] Devendra, C., 1997. Crop residues for feeding animals in Asia: technology development and adoption in crop/livestock Systems. In: C. Renard, ed. *Crop Residues in Sustainable Mixed Crop/Livestock Farming System*. Wallingford: CAB International, pp. 241-267.

[4] De Leeuw, P.N., 1997. Crop residues in tropical Africa : trends, in supply, demand and use. In : C. Renard, ed. *Crop Residue in Sustainable Mixed Crop/Livestock Farming Systems*. New York : CAB International.

[5] Philip, D., Nkonya, E., Pender, J. and Oni, O.A., 2009. Constraints to increasing agricultural productivity in Nigeria: a review. *NSSP Working Paper 6*. Abuja: International Food Policy Research Institute (IFPRI).

[6] Walli, T.K, Garg, M.R. and Makka, H.P.S., 2012. Crop Residue Based Densified Total Mixed Ration- A User friendly Approach to Utilise Food Crop By-products for Ruminant Production. *FAO Animal Production and Health Paper No. 172*, Rome.

[7] Wanapat, M., Polyrach, S., Boonnop, K., Mapato, C. and Cherdthong, A., 2009. Effect of treating rice straw with urea and calcium hydroxide upon intake, digestibility, rumen fermentation and milk yield of dairy cows. *Livestock Science*, 125(2), 238-243.

[8] Senthilkumar, S., Suganya, T., Deepa, K., Muralidharan, J. and Sasikala, K., 2016. Supplementation of molasses in livestock feed. *International Journal of Science, Environment and Technology*, 5(3), 1243-1250.

[9] Akamittath, J.G., Brekke, C.J. and Schanus, E.G., 1990. Lipid oxidation and colour stability in restructured meat systems during frozen storage. *Journal of Food Science*, 55(10), 1513-1517.

[10] Przybylski, R., and Eskin, N.A.M., 1995. Methods to measure volatile compounds and flavor significance of volatile compounds. In: K. Warner and N.A.M. Eskin, eds. *Methods to Assess Oil Quality and Stability of Oils and Fat- Containing Foods*. Champaign: AOCS Press, pp. 107-133.

[11] Rawls, H.R. and Van Santen, P.J., 1990. A possible role for singlet oxygen in the initiation of fatty acid autoxidation. *Journal of the American Oil Chemists' Society*, 47(1), 121-125.

[12] Mathers, J.O. and Otchere, E.O., 2012. Research on the nutrition of working animals: needs, experiences and methods. *FAO Document*, p 9.

[13] Hoque, M., Sokhansanj, S., Naimi, L., Bi X and Lim, J., 2007. Review and analysis of performance and productivity of size reduction equipment for fibrous materials. *ASABE Paper Number: 076164*. Paper presented at ASABE Annual International Meeting Minneapolis, Minnesota.

[14] El-Berry, A.M., Baiomy, A., Radwan, H.A. and Arif, E.M., 2001. Evaluation of (Hematol) machine in rice straw chopping. *9th Conference of MISR Society of Agricultural Engineering*, September 9-11, 2001, 65-76.

[15] El-Iraqi, M. and El-Khawaga, S., 2003. Design and test performance of cutting machine for some crop residues. *MISR Journal of Agricultural Engineering*, 20(1), 85-101.
[16] Abo-Habaga, M.M and Khader, M.O., 2005. Developed of a combined cutting unit with rice harvesting combine machine for utilization in field waste. Journal of Agricultural Science, 30(3), 1481-1487.
[17] El-Hanfy, E.H. and Shalby, S.A., 2009. Performance evaluation and modification of the Japanese combine chopping unit. *MISR Journal of Agricultural Engineering*, 26(2), 1021-1035.
[18] Abo-Habaga, M.M., Yehia, I. and Abo-Elasaad, G.A., 2015. Development of a rice straw bales chopper. *Journal of Soil Science and Agricultural Engineering*, 6(10), 1249 -1262.
[19] Hunt, D., 1983. *Farm Power Machinery Management*. 8th ed. Ames: Iowa State University Press.

Production of Fiber Hydrolysate from Bamboo Shoot with Antioxidative Properties by Enzymatic Hydrolysis

Supatra Karnjanapratum[1], Pensiri Kaewthong[1], Sirima Takeungwongtrakul[2], Thanasak Sae-leaw[3], Jeong Hwa Hong[4] and Sitthipong Nalinanon[1*]

[1]Faculty of Agro-Industry, King Mongkut's Institute of Technology Ladkrabang, Bangkok, Thailand
[2]Department of Agricultural Education, Faculty of Industrial Education and Technology, King Mongkut's Institute of Technology Ladkrabang, Bangkok, Thailand
[3]Department of Food Technology, Faculty of Agro-Industry, Prince of Songkla University, Hat Yai, Songkhla, Thailand
[4]Department of Smart Foods and Drugs, School of Food and Life Science, Inje University, Gimhae, South Korea

Received: 18 March 2019, Revised: 24 June 2019, Accepted 4 July 2019

Abstract

Bamboo shoots possess a rich source of dietary fiber for Asian countries as well as Thailand, which give various beneficial physiological effects for human beings. Dietary fibers in soluble form could provide better texture and would be easier to apply in food products. This study aimed to prepare fiber hydrolysate with high solubility and antioxidant activity from bamboo (*Bambusa vulgaris*) shoot. The fiber hydrolysate from bamboo shoot (FHBS) was prepared by stepwise enzymatic hydrolysis including amylase (1%, w/w), cellulase (1, 2, 3%, w/w) and papain (1%, w/w). The released fiber yield of FHBS increased with increasing cellulose levels in dose dependent manner ($P \leq 0.05$). It was found that the process with 1% (w/w) amylase for 1 h and 3% (w/w) cellulase for 3 h followed by 1% (w/w) papain for 1 h at 50 ºC, rendered the highest released fiber yield (92.10±1.10%). The resultant FHBS contained 5.76±0.21 % of total dietary fiber with total sugar and reducing sugar contents of 1431.22±46.01 and 918.91±10.57 mg/g solid, respectively. The FHBS exhibited antioxidant activities including ABTS radical scavenging activities (ABTS), DPPH radical scavenging activities (DPPH), ferric reducing antioxidant power (FRAP) and oxygen radical absorbance capacity (ORAC). Therefore, FHBS with antioxidant activities could be effectively prepared by using enzymatic hydrolysis and suitable to apply in the fiber fortified products.

Keywords: bamboo shoot, fiber hydrolysate, antioxidative properties, enzymatic hydrolysis
DOI 10.14456/cast.2019.19

*Corresponding author: Tel.: +66 2329 8000 ext 7253 Fax: +66 2329 8527
E-mail: sitthipong.na@kmitl.ac.th

1. Introduction

Dietary fiber is part of daily food intake, normally from part of plant material that is resistant for digestion by human digestive system [1]. Even though it is carbohydrate including cellulose, noncellulosic polysaccharides and non-carbohydrate component lignin, fiber cannot be broken down into sugar molecules like other typical carbohydrates due to its structure [2]. High-fiber diets are growing in popularity as compared to low-fat or low-calorie diets and integrating healthy nutrition within regular daily routines via small changes to consumer's lifestyles are needed. Fiber also comes in two forms; soluble and insoluble [3]. Insoluble form cannot be digested or absorbed by human bodies and is insoluble in water, which can be used as bulk agent for products to prevent constipation. Soluble fibers dissolve in water and can be used by human bowel bacteria as their food source. The soluble form has outstanding health promotion functions [3, 4]. Moreover, soluble dietary fiber could properly be fortified as functional ingredient in food products, especially in beverages, which are a convenient and efficient delivery vehicle for many essential nutrients such as antioxidant plant extracts and protein/peptides as well as soluble dietary fiber [1, 5-7].

Non-starch polysaccharides in plant, particularly fiber, with antioxidant properties have been exploited as potential novel antioxidants. Several rice bran fiber fractions offer protection against the superoxide radical, hydroxyl free radical, lipid peroxidation and exhibit good potential for reducing power and chelating ferrous ions [8]. Besides nutrients, bamboo shoots also contain lethal concentration of oxalate content and the anti-nutrient (cyanogen) that need to be removed before human consumption, which could effectively be removed by boiling in water [9, 10]. Bamboo shoot dietary fiber is an inexpensive alternative fiber apart from wheat, oat, corn, soybean and apples, especially for Asian people. There are many studies reported on its extensive biological activities such as antibacteria, antitumor, anticancer, immune regulation and so on [11]. However, the dietary fiber in bamboo shoots is mostly insoluble, which limits its applications in food products. There are several techniques used to modify and increase soluble dietary fiber of bamboo shoot and the enzymatic hydrolysis was found as an effective method to improve physicochemical properties and the bioactivity of resulting fiber [3, 12, 13]. Xiao-bing *et al.* [12] evaluated the effects of different preparation methods, including water-washing, acid-base treatment, fermentation and enzyme treatment, on the quality of dietary fiber from bamboo shoot. They found that the highest contents of soluble, insoluble and total dietary fibers were obtained from enzyme treatment with alpha-amylase and papain. Song *et al.* [13] reported that the incorporation of extrusion with enzymatic hydrolysis by cellulase could increase the contents of soluble dietary fiber (22.17 g/100 g dry solids) of amylase and papain pretreated bamboo shoots, and the resulting fiber can be useful as a fiber-rich ingredient in functional foods. Alpha-amylase could rapidly increase starch hydrolysis [14]. Papain is a cheap cysteine protease obtained from the latex of papaya, which can cleave protein and peptide in bamboo shoot matrix. These two enzymes have been used for pretreatment of the bamboo shoot and provided the matrix which is prone to be modified by extrusion, chemical or enzymatic methods [13, 15] In addition, cellulase can hydrolyze cellulose and hemicellulose components, which most likely leads to increase exposure of functional groups and influences the bioactivity of dietary fiber [16]. Therefore, the aim of this study was to prepare the soluble dietary fiber from bamboo shoot by stepwise hydrolysis with several enzymes. The antioxidative activities of resultant fiber hydrolysate were then evaluated.

2. Materials and Methods

2.1 Chemicals

Amylase (enzyme activity: 10,000 U/g) and papain (enzyme activity: 100,000 U/g), were obtained from Shaanxi Orient Industrial Co., Ltd. (Shaanxi, China). Cellulase (enzyme activity: 20,000 U/g) was purchased from the Beijing Aoboxing Biotechnology Co., Ltd. (Beijing, China). The other reagents were of analytical grade.

2.2 Bamboo shoot preparation

The fresh bamboo shoots were purchased from local market in Ladkrabang, Bangkok, Thailand and transported to Faculty of Agro-Industry, King Mongkut's Institute of Technology Ladkrabang. The bamboo shoots were peeled and washed with running water before cut into pieces with a diameter of 5 cm. Bamboo shoots were then boiled in hot water (95 ºC) for 15 min prior to storage in polyethylene bag with vacuum seal. The prepared bamboo shoot was stored at -20 ºC until used for analysis within 6 months.

2.3 Pretreatment

Two hundred grams of prepared bamboo shoot were mixed with 400 ml of distilled water and homogenized into slurry. The slurry was then boiled for 15 min and filtered through two-layer of cheesecloth. This process was done twice. The moisture content of pretreated bamboo shoot was analyzed and calculated to be 88.94 ± 2.41%.

2.4 Preparation of fiber hydrolysate by enzymatic hydrolysis

The pretreated bamboo shoot (150 g) was homogenized into slurry with 450 ml water (pH 5.1-5.5). The slurry was preheated at 50°C in water bath. Then, the bamboo shoot slurry was hydrolyzed at 50°C by stepwise enzyme treatment including α-amylase (1% w/w) for 1 h, cellulase (1, 2 and 3% w/w) for 3 h and papain 1% (w/w) for 1 h, respectively. The resultant mixture was heated at 95°C for 15 min for enzyme inactivation prior to filter to remove insoluble debris. The filtered mixture was referred to as "fiber hydrolysate" and collected for analysis.

2.5 Released fiber hydrolysate yield

The released fiber hydrolysate yield was calculated based on initial weight (wet weight) of the starting material using the following equation:

$$\text{Released fiber hydrolysate yield (\%)} = \frac{\text{Total solid of fiber hydrolysate (g)}}{\text{Total weight of bamboo shoot (g)}} \text{x100}$$

2.6 Proximate analysis

The methods for determining the chemical composition of bamboo shoot and its hydrolysate from selected condition, including moisture, protein, fat and ash contents are outlined in the Official Methods of Analysis [17]. Total carbohydrate was calculated by subtraction sum of protein, fat moisture and ash from total weight of sample [18].

2.7 Total sugar and reducing sugar contents

Total sugar content was determined by the phenol-H_2SO_4 method [19] by measuring the absorbance at 490 nm, using sucrose as a standard. The reducing sugar contents was evaluated as per DNS (3,5-dinitrosalicylate) method [20] using glucose as a standard.

2.8 Fiber composition analysis

The fiber compositions of the fiber hydrolysate from bamboo shoot (FHBS) were evaluated from the hydrolysate without filtration. The insoluble dietary fiber (IDF), soluble dietary fiber (SDF), and total dietary fiber (TDF) were determined using the Megazyme TDF Test Kit (K-TDFR, Megazyme International Ireland, Bray Business Park, Bray, Co., Wicklow, Ireland) exactly according to enzymatic gravimetric method with MES-TRIS buffer, based on the AOAC991.43 [21].

2.9 Antioxidative activities

Antioxidative activities of the sample were determined for ABTS radical scavenging activity (ABTS) [22], DPPH radical scavenging activity (DPPH) [22] and ferric reducing antioxidant power (FRAP) [23]. The oxygen radical absorbance capacity (ORAC) was also determined as per method of Kittiphattanabawon *et al.* [24]. Trolox (50 mg/ml) was plotted between relative fluorescence intensity (%) and time (min). All activities were expressed as mmol Trolox equivalent (TE)/g sample.

2.10 Statistical analysis

All experiments were done in triplicate using three different lots of bamboo shoot. Pairwise T-Tests were performed for evaluating the differences in chemical composition of boiled bamboo shoot and FHBS. Significant differences among means within each experiment were evaluated by Duncan's multiple range test at a significance level of $\alpha = 0.05$ [25]. Statistical analysis was performed using the Statistical Package for Social Science (SPSS 11.0 for windows, SPSS Inc., Chicago, IL, USA).

3. Results and Discussion

3.1 Released fiber hydrolysate yield

Fiber hydrolysates from bamboo shoot (FHBS) obtained by stepwise enzymatic hydrolysis with variation of cellulase concentrations, are shown in Figure 1 and those released fiber hydrolysate yield counterparts are presented in Figure 2. The result showed that greater amount of bamboo shoot hydrolysis occurred with higher amount of enzyme used, as monitored by the decreasing of sample mass (Figure 1). The remained sample masses were 17.53±1.35%, 10.89±1.13% and 5.04±0.67% after enzymatic hydrolysis using 1%, 2% and 3% of cellulase, respectively, which were significantly lower than that from control (0% cellulase; 94.36±5.53%). From control, the lowest yield of soluble fraction was obtained ($P \leq 0.05$), compared to enzymatic treatments (Figure 2). The yield of FHBS increased with increasing cellulase levels in dose dependent manner ($P \leq 0.05$). The highest cellulase concentration used (3%) resulted in the highest yield (92.10±1.10%). This result indicated that the cellulose in bamboo shoot matrix could be cleaved by cellulase, in which the short chain fractions

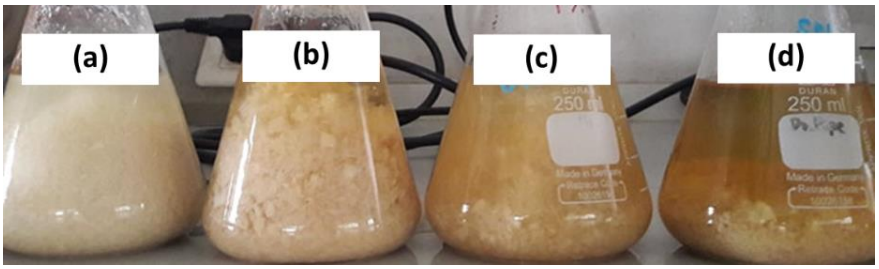

Figure 1. Fiber hydrolysate of bamboo shoot (FHBS) prepared by stepwise enzymatic hydrolysis with different concentrations of cellulase. (a) 1% (w/w) α-amylase and 1% (w/w) papain, (b) 1% (w/w) α-amylase, 1% (w/w) cellulase and 1% (w/w) papain, (c) 1% (w/w) α-amylase, 2% (w/w) cellulase and 1% (w/w) papain, (d) 1% (w/w) α-amylase, cellulase (3% (w/w) of shoot mass) and 1% (w/w) papain

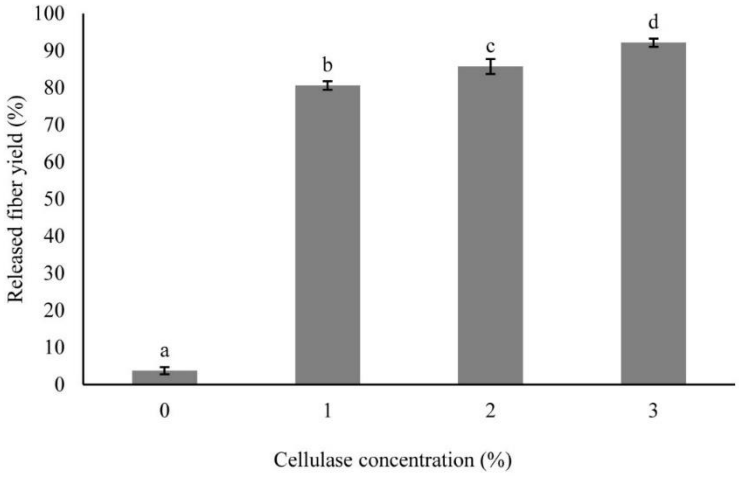

Figure 2. Released fiber hydrolysate yield (%) from bamboo shoot by stepwise enzymatic hydrolysis with different concentrations of cellulase. Different small letters on the bars indicate significant differences ($P \leq 0.05$).

with greater solubility could be obtained. Glucose and cellobiose are two major products from enzymatic hydrolysis of cellulose by cellulase [26]. Two major steps (including adsorption of enzymes onto surfaces of cellulose and breakage of β-1,4-glucosidic bond between glucose) are involved in enzymatic hydrolysis of cellulose [27]. The result was in accordance with those reported by Shafiei *et al.* [28] who prepared palm date fibers by using enzymatic hydrolysis. Cellulase with higher concentration (50 FPU/g activity) was able to hydrolyse glucan in the fibers with higher degree (67.1%), compared with those from 20 FPU/g activity (37.5%). Therefore, the stepwise enzymatic hydrolysis using 1% (w/w) α-amylase, 3% (w/w) cellulase and 1% (w/w) papain was the suitable enzyme treatment condition and was also selected to use for the production of FHBS for further analysis.

3.2 Chemical compositions

Chemical compositions of boiled bamboo shoot and the selected fiber hydrolysate (FHBS) obtained from stepwise enzymatic hydrolysis using 1% α-amylase, 3% cellulase and 1% papain, are shown in Table 1. Both samples (boiled bamboo shoot and FHBS) had carbohydrate as a major composition, followed by protein and ash contents, respectively. No fat content was detected from bamboo shoot and FHBS. These results were in accordance with chemical compositions of bamboo shoot reported by Nongdam and Tikendra [29] and Wang *et al*. [15]. Carbohydrate and protein are main composition found from boiled bamboo shoot with various amount depended on types and cooking processes, in which fat content could not be detected from all boiled shoot tested [29]. It was noted that FHBS had higher protein and ash contents, compared with those of substrate used (boiled bamboo shoot) ($P \leq 0.05$). This might indicate the residue of protein and ash content from enzyme added during stepwise enzymatic hydrolysis.

Table 1. Chemical compositions of boiled bamboo (*Bambusa vulgaris*) shoot and the selected fiber hydrolysate from bamboo shoot (FHBS).

Chemical compositions	Boiled bamboo shoot	FHBS	t-test
Ash (% dry basis)	1.23 ± 0.01	2.35 ± 0.12	*
Protein (% dry basis)	5.23 ± 0.11	6.19 ± 0.12	*
Fat (% dry basis)	ND	ND	-
Carbohydrate (% dry basis)	93.5 ± 0.10	91.5 ± 0.14	*

Values are expressed as means ± standard deviation. * Significant differences between means of boiled bamboo shoots and FHBS ($P \leq 0.05$). ND = not detected.

3.3 Sugar and fiber composition

Sugar and fiber compositions of FHBS prepared by selected condition are shown in Table 2. The FHBS contained 892 ±14.2 mg/g of total sugar. In addition, this hydrolysate consisted of high content of reducing sugar, relating to the high degree of degradation of starch and cellulose by amylase and cellulase, respectively, in which the glucose and oligomers could be released. Some enzymes produced naturally by microorganisms could reduce the molecular weight and improve the solubility of dietary fiber [30].

After stepwise hydrolysis, the FHBS without filtration had 5.76±0.21% of total dietary fiber, including 1.30±0.09% and 4.46±0.20% of soluble and insoluble dietary fiber, respectively. This result indicated that bamboo shoot fiber was almost cleaved during enzymatic hydrolysis to generate soluble fraction in the extracted fractions. The presence of monomer sugars and oligomers from complete and incomplete hydrolysis of polysaccharides could be obtained from palm date fiber hydrolysate by using cellulase and resulted the soluble fraction [28]. Enzymatic treatment hydrolyzes the insoluble fiber into soluble fraction, which could improve the prebiotic health benefits of the developed product [31]. Ramos *et al.* [32] found that a product from cocoa husks treated with the enzyme mixture Ultraflo L® resulted in soluble cocoa fiber which showed the potential application as a functional food ingredient. Therefore, FHBS might exhibit some promising biological activities.

Table 2. Sugar and fiber compositions of the selected fiber hydrolysate from bamboo shoot (FHBS)

Characteristics	Contents*
Total sugar[£] (mg/g solid)	892 ± 14.2
Reducing sugar content[£] (mg/g solid)	735 ± 8.45
Total dietary fiber content[¥] (g/100 g solid)	5.76 ± 0.21
Soluble dietary fiber content[¥] (g/100 g solid)	1.30 ± 0.09
Insoluble dietary fiber content[¥] (g/100 g solid)	4.46 ± 0.20

*Values are expressed as means ± standard deviation (n = 3). [£] The data was determined from soluble fraction. [¥] The data was determined from FHBS without filtration.

3.4 Antioxidative activities

Antioxidative activities of the selected FHBS were evaluated using different assays and presented in Table 3. It was found that the enzymatic hydrolysis produced antioxidative components that could both scavenge the radicals and work as electron donator. The bioactive oligosaccharides for regulation of plant cell growth and induction of phytoalexins were reportedly produced from primary cell-wall polysaccharides [33]. Reddy and Krishnan [34] reported on the production of prebiotics and antioxidants as health food supplements from lignocellulosic materials using multi-enzymatic hydrolysis. They found that a multi-enzyme mix produced from a new strain of *Bacillus subtilis* KCXOO6 could effectively produce prebiotic functional oligosaccharides and antioxidants from wheat bran, sugarcane bagasse, rice husk and bamboo bagasse. Previous researches have demonstrated that degraded polysaccharides by enzymatic hydrolysis process exhibited superior free radical scavenging effect [35, 36]. Moreover, the biological activities of polysaccharides are closely related to their Mw distributions. Theoretically, low Mw polysaccharides are more active than high Mw polysaccharides, which is attributed to the greater surface area and better water solubility [37-39]. Tabarsa *et al.* [40] found that the lower molecular weight of water-soluble polysaccharide fraction from *Ulva intestinalis* was very pivotal for its high bioactivity. Chen *et al*. [37] showed that the degraded polysaccharide from *Sargassum fusiforme* possesses superior anti-tyrosinase activity and antioxidant activity than the original polysaccharide. The different antioxidative properties may be due to the combined effects of the different sizes of the electron cloud density and the different accessibility between free radical and low molecular polysaccharides which, in turn, depends upon the different hydrophobicities of the constituent sugars [41]. The uncontrolled production of free radicals is involved in various diseases, including cancer, atherosclerosis and degenerative aging processes. These results clearly establish the possibility that water- soluble polysaccharides fractions from enzymatic hydrolysate of bamboo shoot might effectively be employed as ingredient in health or functional food to alleviate oxidative stress.

Table 3. Antioxidative activities of the selected fiber hydrolysate from bamboo shoot (FHBS)

Antioxidative activities	Content
ABTS (mmol TE/g solid)	16.4 ± 1.55
DPPH (μmol TE/g solid)	25.4 ± 0.01
FRAP (mmol TE/g solid)	6.24 ± 0.32
ORAC (mmol TE/g solid)	3.39 ± 0.04

* Values are expressed as means ± standard deviation (n = 3). ABTS: ABTS radical scavenging activity; DPPH: DPPH radical scavenging activity; FRAP: Ferric reducing antioxidant power; ORAC: Oxygen radical absorbance capacity.

4. Conclusions

The production of fiber hydrolysate from bamboo shoot with antioxidative activity was simply done by using stepwise enzymatic hydrolysis. Cellulase tended to be the key enzyme used in the hydrolytic process. The information gained could be used for soluble fiber production with antioxidative activity from bamboo shoot and other fiber sources, which had the potential to apply into food products.

References

[1] Dhingra, D., Michael, M., Rajput, H. and Patil, R.T., 2012. Dietary fibre in foods: a review. *Journal of Food Science and Technology*, 49, 255-266.

[2] Tungland, B.C. and Meyer, D., 2002. Nondigestible oligo and polysaccharides (dietary fibre): their physiology and role in human health and food. *Comprehensive Reviews in Food Science and Food Safety*, 1, 73-92.

[3] Yang, Y.-Y., Ma, S., Wang, X.-X. and Zheng, X.-L., 2017. Modification and application of dietary fiber in foods. *Journal of Chemistry*, 2017, 1-8. http://doi.org/10.1155/2017/9340427

[4] Prosky, L., 2000. When is dietary fiber considered a functional food?. *BioFactors*, 12, 289-297.

[5] Benjakul, S, Chantakun, K. and Karnjanapratum, S., 2018. Impact of retort process on characteristics and bioactivities of herbal soup based on hydrolyzed collagen from seabass skin. *Journal of Food Science and Technology*, 55, 3779-3791.

[6] Karnjanapratum, S. and Benjakul, S., 2017. Antioxidative and sensory properties of instant coffee fortified with galactose- fish skin gelatin hydrolysate Maillard reaction products. *Carpathian Journal of Food Science and Technolog*, 9 (1), 90-99.

[7] Thongsombat, W., Sirichote, A. and Chanthachum, S., 2007. The production of guava juice fortified with dietary fiber. *Songklanakarin Journal of Science and Technology*, 29, 187-196.

[8] Zha, X.-Q., Wang, J.-H., Yang, X.-F., Liang, H., Zhao, L.-L., Bao, S.H., Luo, J.-P., Xu, Y.-Y. and Zhou, B.-B., 2009. Antioxidant properties of polysaccharide fraction with different molecular mass extracted with hot-water from rice bran. *Carbohydrate Polymers*, 78, 570-575.

[9] Judprasong, K., Charoenkiatkul, S., Sungpuag, P., Vasanachitt, K. and Nakjamanong,Y., 2006. Total and soluble oxalate contents in Thai vegetables, cereal grains and legume seeds and their changes after cooking. *Journal of Food Composition and Analysis*, 19(4), 340-347.

[10] Pandey, A.K. and Ojha, V., 2014. Precooking processing of bamboo shoots for removal of anti-nutrients. *Journal of Food Science and Technology*, 51(1), 43-50.

[11] He, M.-X., Wang, J.-L.,Qin, H., Shui, Z., Zhu, Q. and Wu, B., 2014. Bamboo: a new source of carbohydrate for biorefinery. *Carbohydrate Polymers*, 111(20), 645-654.

[12] Xiao-bing, H., Ji-hua, L., Shao-dan, P. and Li-Jing, L., 2015. Effect of preparation methods on the composition and structure of dietary fiber from bamboo shoot. *International Conference on Chemical, Material and Food Engineering*, Kunming, Yunnan, China, July 25-26, 2015, 182-186. doi: 10.2991/cmfe-15.2015.43.

[13] Song, Y., Su, W. and Mu, Y.C., 2018. Modification of bamboo shoot dietary fiber by extrusion-cellulase technology and its properties. *International Journal of Food Properties*, 21, 1219-1232.

[14] Konovalova, V., Guzikevich, K., Burban, A, Kujawski, W., Jarzynka, K. and Kujawa, J., 2016. Enhanced starch hydrolysis using α-amylase immobilized on cellulose ultrafiltration affinity membrane. *Carbohydrate Polymers*, 152, 710-717.

[15] Wang, C.-H., Ma, Y.-L., Zhu, D.-Y., Wang, H., Ren, Y.-F. and Zhang, J.-G., 2017. Physicochemical and functional properties of dietary fiber from bamboo shoot (*Phyllostachys praecox*). *Emirates Journal of Food and Agriculture*, 29(7), 509-517.

[16] Ullah, I., Yin, T., Xiong, S., Zhang, J., Din, Z.-U., 2017. Structural characteristics and physicochemical properties of okara (soybean residue) insoluble dietary fiber modified by high-energy wet media milling. *LWT-Food Science and Technology*, 82, 15-22.

[17] AOAC, 2002. *Official Methods of Analysis.* 16thed. Washington DC: Association of Official Analytical Chemists.

[18] Ellefson, W., 1993. Provision of the nutrition labelling and education act. In: D.M. Sullivan and D.E. Carpenter, eds. *Methods of Analysis for Nutrition Labeling*. Virginia: AOAC International.

[19] Dubois, M., Gilles, K.A., Hamilton, J.K., Rebers, P.A. and Smith, F., 1956. Colorimetric method for determination of sugars and related substances. *Analytical Chemistry*, 28, 350-356.

[20] Marsden, W.L., Gray, P.P., Nippard, G.J. and Quinlan, M.R., 2006. Evaluation of the DNS method for analysing lignocellulosic hydrolysates. *Journal of Applied Sciences and Environmental Management*, 10, 93-96.

[21] Horwitz, W., 1995. *Total, Soluble and Insoluble Dietary Fiber in Foods*. 16th ed. Arlington, Virginia: AOAC Official Methods of Analysis.

[22] Binsan, W., Benjakul, S., Visessanguan, W., Roytrakul, S. Tanaka, M. and Kishimura, H., 2008. Antioxidative activity of Mungoong, an extract paste, from the cephalothorax of white shrimp (*Litopenaeus vannamei*). *Food Chemistry*, 106(1), 185-193.

[23] Benzie, I.F. and Strain, J., 1996. The ferric reducing ability of plasma (FRAP) as a measure of "antioxidant power": The FRAP assay. *Analytical Biochemistry*, 239(1), 70-76.

[24] Kittiphattanabawon, P., Benjakul, S., Visessanguan, W. and Shahidi, F., 2012. Gelatin hydrolysate from blacktip shark skin prepared using papaya latex enzyme: Antioxidant activity and its potential in model systems. *Food Chemistry*, 135, 1118-1126.

[25] Steel, R.G.D., Torrie, J.H. and Dicky, D.A., 1980. *Principles and Procedures of Statistics: A Biometrical Aproach*. New York: McGraw-Hill.

[26] Yeh, A.-I., Huang, Y.-C. and Chen, S.H., 2010. Effect of particle size on the rate of enzymatic hydrolysis of cellulose. *Carbohydrate Polymers*, 79, 192-199.

[27] Peri, S., Karra, S., Lee, Y.Y. and Karim, M.N., 2007. Modeling intrinsic kinetics of enzymatic cellulsoe hydrolysis. *Biotechnology Progress*, 23, 626-637.

[28] Shafiei, M., Karimi, K., and Taherzadeh, M.J., 2010. Palm date fibers: analysis and enzymatic hydrolysis. *International Journal of Molecular Sciences*, 11, 4285-4296.
[29] Nongdam, P. and Tikendra, L., 2014. The nutritional facts of bamboo shoots and their usage as important traditional foods of Northeast India. *International Scholarly Research Notices*, 2014. http://dx.doi.org/10.1155/2014/679073.
[30] Nakajima, N., Ishihara, K. and Matsuura, Y., 2002. Dietary-fiberdegrading enzymes from a human intestinal *Clostridium* and their application to oligosaccharide production from nonstarchy polysaccharides using immobilized cells. *Applied Microbiology and Biotechnology*, 59, 182-189.
[31] Charalampopoulos, D. and Rastall, R.A., 2012. Prebiotics in foods. *Current Opinion in Biotechnology*, 23, 187-191.
[32] Ramos, S., Moulay, L., Granado-Serrano, A.B., Vilanova, O., Muguerza, B., Goya, L. and Bravo, L., 2008. Hypolipidemic effect in cholesterol-fed rats of a soluble fiber-rich product obtained from cocoa husks. *Journal of Agricultural and Food Chemistry*, 56, 6985-6993.
[33] Fry S.C., 1989. Cellulases, hemicelluloses and auxin-stimulated growth: a possible relationship. *Physiologia Plantarum*, 75, 532-536.
[34] Reddy, S.S., and Krishnan, C., 2010. Production of prebiotics and antioxidants as health food supplements from lignocellulosic materials using multi enzymatic hydrolysis. *International Journal of Chemical Science*, 8(3), S535-S549.
[35] Liu, Z.-J., Wang, Y.-L., Li, Q.-L. and Yang, L., 2018. Improved antimelanogenesis and antioxidant effects of polysaccharide from *Cuscuta chinensis* Lam seeds after enzymatic hydrolysis. *Brazilian Journal of Medical and Biological Research*, 51(7), e7256. http:// dx. doi.org/10.1590/1414-431X20187256
[36] Xu, J., Xu, L.L., Zhou, Q.W., Hao, S.X., Zhou, T. and Xie, H.J., 2016. Enhanced *in vitro* antioxidant activity of polysaccharides from *Enteromorpha prolifera* by enzymatic degradation. *Journal of Food Biochemistry*, 40, 275-283.
[37] Chen, B.J., Shi, M.J., Cui, S., Hao, S.X., Hider, R.C. and Zhou, T., 2016. Improved antioxidant and anti-tyrosinase activity of polysaccharide from *Sargassum fusiforme* by degradation. *International Journal of Biological Macromolecule*, 92, 715-722.
[38] Zhou, J., Hu, N., Wu, Y.L., Pan, Y.J. and Sun, C.R., 2008. Preliminary studies on the chemical characterization and antioxidant properties of acidic polysaccharides from *Sargassum fusiforme*. *Journal of Zhejiang University-Science B*, 9, 721-727.
[39] Wu, Q., Zheng, C., Ning, Z.X. and Yang, B., 2007. Modification of low molecular weight polysaccharides from *Tremella fuciformis* and their antioxidant activity *in vitro*. *International Journal of Molecular Sciences*, 8, 670-679.
[40] Tabarsa, M., You, S.G., Dbaghian, E.H. and Surayot, U., 2018. Water-soluble polysaccharides from *Ulva intestinalis*: Molecular properties, structural elucidation and immunomodulatory activities. *Journal of Food and Drug Analysis*, 26(2), 599-608.
[41] Chen, S.K., Tsai, M.L. Huang, J.R. and Chen, R.H., 2009. *In vitro* antioxidant activities of low-molecular-weight polysaccharides with various functional groups. *Journal of Agricultural and Food Chemistry*, 57, 2699-2704.

Antimicrobial Activity of Edible Electrospun Chitosan/Cellulose Acetate/Gelatin Hybrid Nanofiber Mats Incorporating Eugenol

Jaruayporn Somsap[1], Kobsak Kanjanapongkul[2], Chuenjit Chancharoonpong[3], Suriyan Supapvanich[4] and Racha Tepsorn[1*]

[1]Department of Food Science and Technology, Faculty of Science and Technology, Thammasat University (Rangsit Center), Phatumthani, Thailand
[2]Department of Food Engineering, Faculty of Engineering at Kamphaeng Saen, Kasetsart University, Kamphaeng Saen Campus, Nakhon Pathom, Thailand
[3]Department of Food Technology and Nutrition, Faculty of Natural Resource and Agro-Industry, Kasetsart University, Chalermprakiat Sakon-Nakhon Province Campus, Sakon Nakhon, Thailand
[4]Department of Agricultural Education, Faculty of Industrial Education and Technology, King Mongkut's Institute of Technology Ladkrabang, Bangkok, Thailand

Received: 11 April 2019, Revised: 6 July 2019, Accepted: 9 July 2019

Abstract

Antimicrobial nanofiber mats were successfully fabricated via electrospinning. Polymer solutions of chitosan, cellulose acetate and gelatin were blended at a volume ratio of 4:1:5. Eugenol at concentrations of 0 to 10.0% (v/v) was directly incorporated into the mixed polymer solutions. Electrospinning was performed at 23 kV with a flow rate at 0.7 ml/h and collector distance of 10 cm. The average diameters of fibers incorporated with eugenol ranged from 152.32±41.48 to 288.92±77.69 nm. Fibers with larger diameters and junctions appeared when the concentration of eugenol was increased. Eugenol release was observed within 300 min. The burst release of eugenol at 0.1, 0.75, and 1.5% (v/v) reached equilibrium after 60 min while the burst release at 3.0, 5.0 and 10.0% (v/v) continued to increase gradually. The phase transition temperatures of nanofiber mats incorporated with eugenol ranged from 129.69 to 161.84 °C. The thermal characteristic demonstrated that the melting point decreased in accordance with the increase of incorporated eugenol. The nanofiber mats with eugenol at less than 5.0% (v/v) showed better thermostability than mats incorporated with eugenol concentrations greater than 5.0% (v/v). Antibacterial activity was tested against *Salmonella* Typhimurium and *Staphylococcus aureus*. The results demonstrated that the edible electrospun CS/CA/Gel nanofiber mats incorporated with eugenol could effectively retard the growth of both bacteria. Our results suggest that eugenol incorporated nanofibers have potential applications as antimicrobial materials in active food packaging, air filtration, antibacterial textiles, wound dressing, drug delivery and others.

Keywords: antimicrobial nanofibers, electrospinning, edible electrospun, eugenol, chitosan
DOI 10.14456/cast.2019.20

*Corresponding author: Tel.: +66850640161 Fax: +6625644486
E-mail: rtepsorn@tu.ac.th

1. Introduction

Public concern on health issues has increased due to foodborne pathogen contamination and environmental problems associated with plastic packaging. *Salmonella* Typhimurium and *Staphylococcus aureus* are the cause of foodborne diseases in both developed and developing countries [1- 3]. *Salmonella* Typhimurium belongs to the enterobacteriaceae living in human digestive tract and causes salmonellosis [4]. According to a report from the CDC (2013), it is estimated to cause 1.2 million cases each year in the USA with more than 23,000 hospitalizations. Among these, 450 deaths were recorded. Foods are the major source of these illnesses [1]. Likewise, *S. aureus* can cause gastroenteritis, accounting for an estimated 241,000 cases per year in the USA [5] due to the consumption of enterotoxin contaminated food [2, 3]. *Staphylococcus aureus* is a normal flora on the skin and in nasal passages. In addition, it can be found in the air, dust, sewage, water and on environmental surfaces [3, 6]. Improper preparation, handling and storage are the cause of foodborne contamination. 'To prevent the growth and spread of foodborne pathogens, the use of antimicrobial material from natural substances could reduce the growth of microorganisms and extend the shelf-life of food. Additionally, it should be biodegradable, eco-friendly, nontoxic and safe for consumers [7-9].

Nanofiber mats can be produced via electrospinning. The outstanding properties of nanofibers are a large surface area to volume ratio, superior mechanical performance, flexibility in surface functionality and high porosity [10-12]. They can be used for applications such as filtration membranes, scaffolds in tissue engineering, drug delivery, wound dressing and food packaging [13-15]. Electrospinning is an interesting process for production of nanofibers [10, 11, 15]. The device contains a high voltage power supply, blunt-ended stainless needle, syringe pump and ground collector [11, 16, 17]. When polymer solution is placed in the syringe connected to the stainless needle, a positive charge is connected to the stainless needle and the negative charge is connected to the ground collector. A droplet of the polymer solution at the end of the needle changes from a semicircle to a conical shape when a high voltage is applied. These phenomena can occur due to charge-charge repulsion [10, 11, 18]. The electrostatic repulsion force overcomes the surface tension of the polymer solution causing the polymer to be ejected towards the ground collector. The solvent evaporates and a continuous fiber is laid on the collector as a nonwoven membrane [12, 19, 20].

Chitosan (CS), cellulose acetate (CA) and gelatin (Gel) were natural polymers selected for this study as they are edible, biocompatible, biodegradable, eco-friendly with low toxicity. Chitosan is a derivative of chitin made of glucosamine and N-acetyl glucosamine [21, 22]. It is antimicrobial due to the availability of the positive change on the C-2 of the glucosamine monomer, which reduces the permeability of bacterial membrane [15]. However, chitosan is hard to electrospin as it mainly gives rise to droplets of nanometer and micrometer sizes [23, 24]. Therefore, gelatin was used as copolymer to improve the electrospinnability of the chitosan. Gelatin contains abundant amino and carboxyl hydrophilic groups that can be ionized by acidic agents or hydrolyzed to carry positive or negative charges [14, 25]. Gelatin can be used alone or as a blend to fabricate nanofibers for a range of applications [25-27]. However, electrospun nanofiber mats from chitosan-gelatin hybrid are often susceptible to moisture and rapidly dissolve when submerged in water. Consequently, cellulose acetate was used to improve the physical properties due to its thermostability, chemical resistance, biodegradability and so on [28, 29]. Electrospun nanofibers containing an antimicrobial agent can be used as food coating membranes, filter membranes and food packaging with antimicrobial properties [15, 30, 31]. Eugenol (4-allyl-2-methoxyphenol), which is categorized as GRAS (Generally Recognized as Safe) by the FDA, was used as the antimicrobial agent [4, 32]. Eugenol inhibits microorganisms by disruption of the cytoplasmic membrane, proton motive force, electron flow, active transport and protein synthesis [4, 8, 32-34]. Previous studies have demonstrated success in producing electrospun antimicrobial nanofibers [15, 30, 35, 36]. However, no edible

electrospun nanofibers have been reported. The aim of this research was to fabricate edible antimicrobial nanofiber mats with incorporated eugenol via electrospinning. The morphology of the electrospun CS/CA/Gel nanofiber mats, the release of eugenol and the thermal properties were determined. Additionally, the antimicrobial activity of the mats against foodborne pathogens was also investigated. The edible antimicrobial material may have potential applications as active food packaging and in biomedical products.

2. Materials and Methods

2.1 Materials

Shrimp chitosan powder (deacetylation 95.04%) was purchased from Taming Enterprises Co. Ltd., China. Gelatin powder (250 bloom) was purchased from Xiamen Huaxuan Gelatin Co. Ltd., China. Cellulose acetate (average Mn ~ 30,000) and eugenol 99% (v/v) were purchased from Sigma-Aldrich Co. Ltd, USA. Glacial acetic acid (>99%) was purchased from QRec, New Zealand. Peptone, Tryptic Soy Broth (TSB), and Tryptic Soy Agar (TSA) were used as bacterial culture media and purchased from Becton Dickinson and Company, USA. Bacterial strains of *Salmonella* Typhimurium ATCC 13311 and *S. aureus* ATCC 25923 were obtained from the Department of Medical Science, the Ministry of Public Health, Thailand.

2.2 Electrospinning of CS/CA/Gel nanofibers with incorporated eugenol

The preparation of the nanofiber mats was described previously in Somsap *et al.* [37]. Briefly, chitosan (CS), cellulose acetate (CA) and gelatin (Gel) were dissolved separately in acetic acid 80.0% (v/v) under continuous stirring at room temperature until completely dissolved. Then, CS (5.0% wt), CA (18.0% wt), and Gel (30.0% wt) were blended at a volume ratio of 4:1:5. Final concentration of polymer solution was 18.8% wt. Eugenol at concentrations of 0, 0.1, 0.75, 1.5, 3.0, 5.0, and 10.0% (v/v) of polymer solution was added. In the electrospinning process, the polymer solution with incorporated eugenol was loaded into a 10 ml plastic syringe with 18 gauge metal needle. The positive electrode was clasped to the needle while the negative electrode was clasped to the ground collector. The flow rate of polymer solution was controlled at 0.7 ml/h by a syringe pump (New Era NE-300, USA). A high voltage DC power supply (Gamma High Voltage Research, USA) was applied at 23 kV. The distance between needle and collector was 10 cm. Electrospinning was performed at room temperature and all electrospun nanofiber samples were dried overnight to remove residual solvent.

2.3 Scanning electron microscopy

The morphology of the electrospun nanofibers was observed using scanning electron microscopy (SEM JSM-7800F, JEOL, MA, USA) after coating the nanofiber samples with a thin gold layer to provide electrical conductivity. In total, 50 counts were used to calculate the average diameter of the nanofibers.

2.4 Eugenol release characteristics from electrospun nanofiber mats

The mats were cut into pieces of approximately 50 mg and immersed in 10 ml of distilled water. Eugenol release studies were carried out at room temperature. Samples of 5 ml were taken from distilled water after every 10 min until 300 min. After sampling, 5 ml of fresh distilled water was

added to sustain incubation. The amount of eugenol present in the water samples was determined by UV-vis spectrophotometry (Unicam, England) at a wavelength of 280 nm. The amount of eugenol release was determined from a standard calibration curve. The results were presented in terms of cumulative release as a function of time.

2.5 Differential scanning calorimetry

Thermal analysis was carried out by differential scanning calorimetry (Mettler Toledo, DSC 1 Module, Switzerland) at 30 to 180 ºC and a heating rate of 5 ºC/min. The samples, weighing about 3 mg each, were placed in an aluminum pan with holes in the lid.

2.6 Antibacterial activity

Salmonella Typhimurium and *S. aureus* were cultivated in sterilized TSB and incubated overnight at 37 °C. The culture was then diluted with sterile peptone solution 0.1% (w/v) to a concentration of 4 $\log_{10}$ colony forming units / milliliter (CFU/ml). Next, 5 ml of bacterial suspension was transferred to a flask containing 45 ml of sterilized TSB. The bacterial suspensions employed for the tests contained between 2 to 3 $\log_{10}$ CFU/ml. Antibacterial activity assays were conducted using a modified ASTM dynamic shake test [38]. The mats were cut into 50 mg rectangles and sterilized under ultraviolet (UV) radiation for 2 h (each side for 1 h) then placed into bacterial suspension flasks. The bacterial suspensions were shaken at 200 rpm in an orbital shaker for 0, 15, 30, 60, 120, 240, 480, 720, and 1,440 min. At the end of each period, 1.0 ml of bacterial suspension was transferred from the flask and serial dilutions were plated on TSA plates using the spread plate method [15, 38]. The numbers of viable bacteria were determined by counting colonies after 24 h of incubation at 37 °C. Bacterial suspension without mat was also used as control. The results were analysed by the number of viable bacteria as a function of contact time and compared with the control. The percentage reduction of bacteria was calculated using Equation (1) as follows :

$$\text{Reduction of bacteria (\%)} = (B\text{-}A)/B \times 100 \quad (1)$$

Where A and B are the numbers of surviving bacteria in the test samples and blank control after the specific contact time, respectively.

2.7 Statistical analysis

Results were subjected to statistical analysis using the SPSS package. One-way ANOVA with three replicates was applied. Duncan's multiple range test was used to analyze differences at a *p*-value ≤ 0.05.

3. Results and Discussion

3.1 Morphology of nanofibers

CS/CA/Gel nanofibers incorporating eugenol were successfully fabricated. The morphology of these nanofibers is shown in Figure 1. The results from Figures 1A, D, E from our previous study [39] were also used for comparison. The average fiber diameters incorporating eugenol at 0, 0.1, 0.75, 1.50, 3.0, 5.0 and 10.0 % (v/v) (n=50) were 152.32±41.48 nm, 156.11±17.10, 231.16±54.96 nm, 233.11±53.21 nm, 246.05±84.36 nm, 203.47±99.71 and 288.92±77.69 nm, respectively.

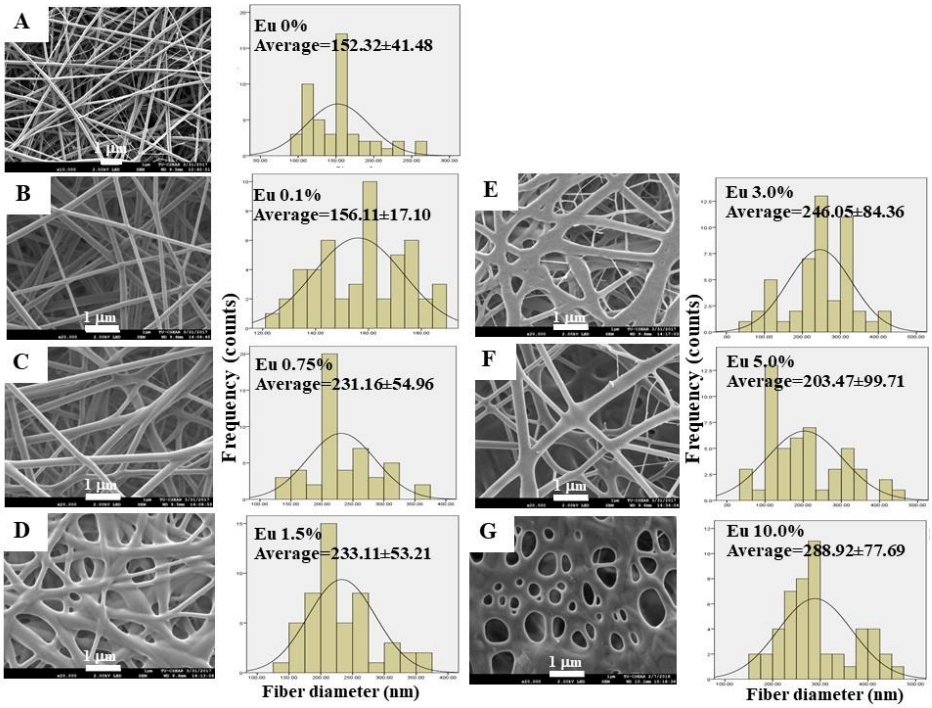

Figure 1. SEM images of morphology and fiber diameter distribution of CS/CA/Gel nanofibers containing different amounts of eugenol: 0% (A), 0.1% (B), 0.75% (C), 1.5% (D), 3.0% (E), 5.0% (F) and 10.0% (G). Magnification:10,000x (A) and 20,000x (B-G)

When the concentration of eugenol was higher, larger fiber diameters with junctions were observed. The control (eugenol 0.0%) exhibited smooth fibers with the smallest average diameter while the largest average fiber diameter was obtained at 10.0% (v/v) of eugenol. The diameter of fibers was later decreased when the concentration of eugenol was increased to 5.0% (v/v). No significant difference (p>0.05) in fiber diameter was found between samples containing 0.75, 1.5, 3.0 and 5.0% (v/v) eugenol. However, a significant difference (p<0.05) was observed at 10.0% (v/v) incorporation. Eugenol insertion into the nanofibers caused them to expand, accounting for the difference. As eugenol is a volatile organic compound, it induced melting of the CS/CA/Gel blend, producing junctions between the nanofibers. The electrospinning process and morphology of the electrospun nanofibers depend on the solution properties (concentration, viscosity, surface tension and conductivity) and processing conditions [11, 17]. When the processing condition was fixed, the solution properties influenced the fiber diameter and morphology. Increasing the concentration of eugenol leads to larger fiber diameters with junctions. Likewise, a polyurethane solution containing 10.0 wt% of olive oil has been reported to produce nanofibers with junctions because of the low volatility of the oil [2]. This might also be related to the electric conductivity of the polymer solution. When the processing condition was fixed, the addition of essential oil into the polymer solution decreased electrical conductivity, causing elongation of the jet as the electric force was insufficient, producing large nanofibers with junctions [11, 40-41]. Rieger and Schiffman [15] reported that electrospun chitosan/PEO nanofibers incorporating cinnamaldehyde essential oil at 0, 0.5 and 5.0% had average fiber diameters of 55±8 nm, 52±9 nm and 38±9 nm, respectively. A smaller fiber diameter was obtained when the concentration of cinnamaldehyde was increased. Incorporation of

antimicrobial agents directly into polymer solution prior to electrospinning is a simple method for loading antimicrobial agents or drugs [7, 42]. However, this process could have an effect on the electrospinnability and morphology of the nanofibers because of changes in the viscosity, surface tention and conductivity of the solution [42].

3.2 Release of eugenol from CS/CA/Gel electrospun nanofiber mats

The release of eugenol from the electrospun nanofiber mats at different time periods is shown in Figure 2. As the mats absorbed water, they expanded, producing burst release of eugenol. The cumulative release of eugenol from 0.1, 0.75, 1.5, 3.0, 5.0 and 10.0% (v/v) incorporated samples at 60 min were $1.21x10^{3}\pm1.2x10^{-3}$ µg, $1.35x10^{3}\pm1.1x10^{-1}$ µg, $1.45x10^{3}\pm1.4x10^{-1}$ µg, $2.61x10^{3}\pm3.2x10^{1}$ µg, $2.70x10^{3}\pm5.8x10^{-2}$ µg and $3.35x10^{3}\pm5.1x10^{-2}$ µg, respectively. At 300 min, it was $1.37x10^{3}\pm8.2x10^{-3}$ µg, $1.60x10^{3}\pm8.2x10^{-4}$ µg, $1.69x10^{3}\pm8.2x10^{-4}$ µg, $3.25x10^{3}\pm1.4x10^{-3}$ µg, $3.74x10^{3}\pm4.5x10^{-3}$ µg and $6.23x10^{3}\pm8.8x10^{-2}$ µg, respectively. The burst release of eugenol at 0.1, 0.75, and 1.5% (v/v) reached a plateau after 60 min indicating that equilibrium had been reached. The burst release of eugenol at 3.0, 5.0, and 10.0% (v/v) continued to increase gradually.

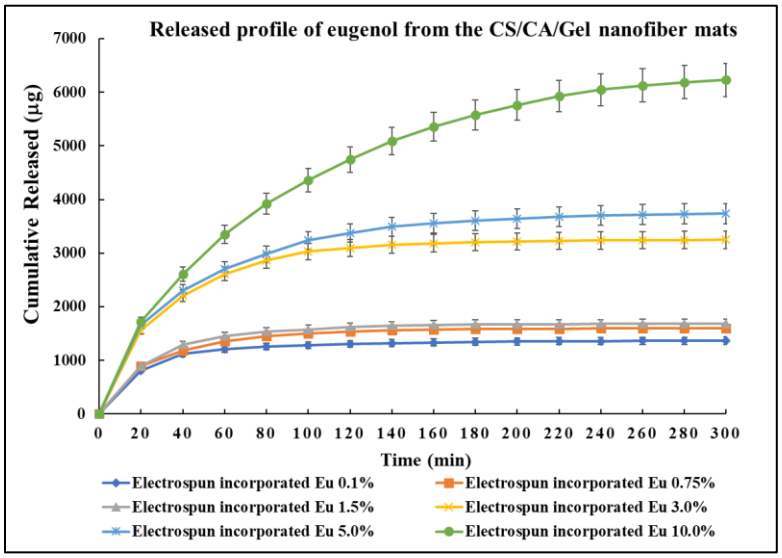

Figure 2. Released profile of eugenol from CS/CA/Gel electrospun nanofiber mats at different time periods

As the eugenol concentration was increased, the cumulative release of eugenol from the CS/CA/Gel nanofiber mats increased. For the cumulative release at 0.1, 0.75 and 1.5% (v/v), neither significant difference ($p>0.05$) in cumulative release were found between samples with 0.1, 0.75 and 1.5% (v/v) nor between samples with 3.0% and 5.0% (v/v). However, a significant difference ($p<0.05$) was found between the two groups and between samples with 10.0% (v/v) eugenol and all other samples.

The release rate of active agents from electrospun nanofibers depends on the method of inclusion into the polymer solution. A previous study reported that the direct inclusion of cinnamaldehyde into polymer solution presented the releasing phenomena into the aqueous solution within 180 min [15]. The release mechanisms can be classified into three categories; swelling-

controlled, diffusion-controlled, and reaction-controlled [15, 43, 44]. In this study, the electrospun chitosan/ gelatin nanofiber mats could easily be dissolved in water. When the networks of chitosan/gelatin hybrid are composed of cellulose acetate, the solubility is reduced because cellulose acetate is water- insoluble. This causes the CS/ CA/ Gel nanofiber mats to swell, eliminating degradability in water. The factors affecting drug release from the matrix depend on the solubility of the drug, the geometry of the particle and drug diffusion through the polymer and /or erosion of polymers [45]. The expansion of the matrix depends on the water absorption, which regulates the degree of swelling. When the matrix is inflated, the porosity of the coating material is larger. This will result in better diffusion [43]. In this study, the presumed release mechanism of eugenol from the CS/CA/Gel nanofiber mats is the diffusion through the matrix polymer network. However, the release behavior is intimately related to the swelling behavior [46]. Moreover, the release rate depends on the type and composition of the polymer and structure of the electrospun nanofiber mats [42].

3.3 Thermal property of electrospun nanofiber mats

The thermal properties of the mats were investigated using DSC analysis (Figure 3). The phase transition temperatures of samples incorporating eugenol at 0%, 0.1%, 0.75%, 1.5%, 3.0%, 5.0 % and 10.0% (v/v) were 152.71, 161.79, 161.84, 155.72, 153.15, 140.37 and 129.69°C, respectively. It was found that the melting point of samples with eugenol concentrations of 0.1 and 0.75 % was increased (~162°C) when compared to the control (152.71°C). The melting point of the 5.0% and 10. 0% eugenol samples was then decreased to 140. 37°C and 129. 69°C, respectively. This demonstrated that mats incorporating eugenol at less than 5.0% (v/v) had better thermostability. Additionally, the melting point correlated with time. As the eugenol concentration was increased, both melting point and time decreased.

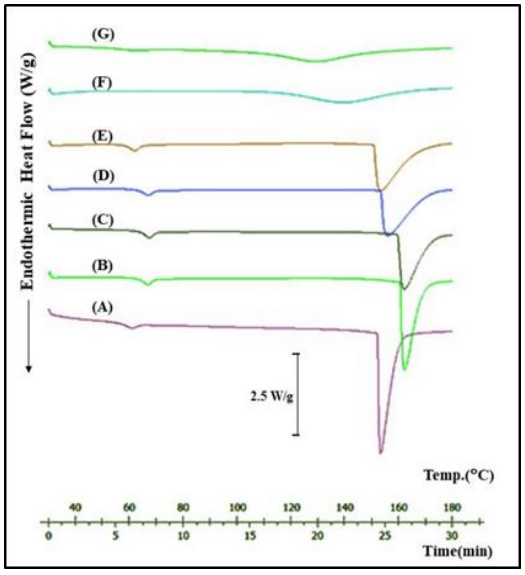

Figure 3. DSC thermograms of CS/CA/Gel electrospun nanofiber mats containing different amounts of eugenol: 0% (A), 0.1% (B), 0.75% (C), 1.5% (D), 3.0% (E), 5.0% (F) and 10.0% (G)

3.4 Antibacterial activity of nanofiber mats

Antibacterial activity was evaluated by dynamic shake test using two strains of foodborne pathogenic bacteria: gram negative (*Salmonella* Typhimurium) and gram positive (*S. aureus*). Figures 4 and 5 show the growth and reduction of bacteria after different contact times. Control AA (without eugenol or nanofiber mat) was the growth control each bacteria test, and control A (nanofiber mat without eugenol) was used in the comparison of CS/CA/Gel nanofiber mats containing different amounts of eugenol.

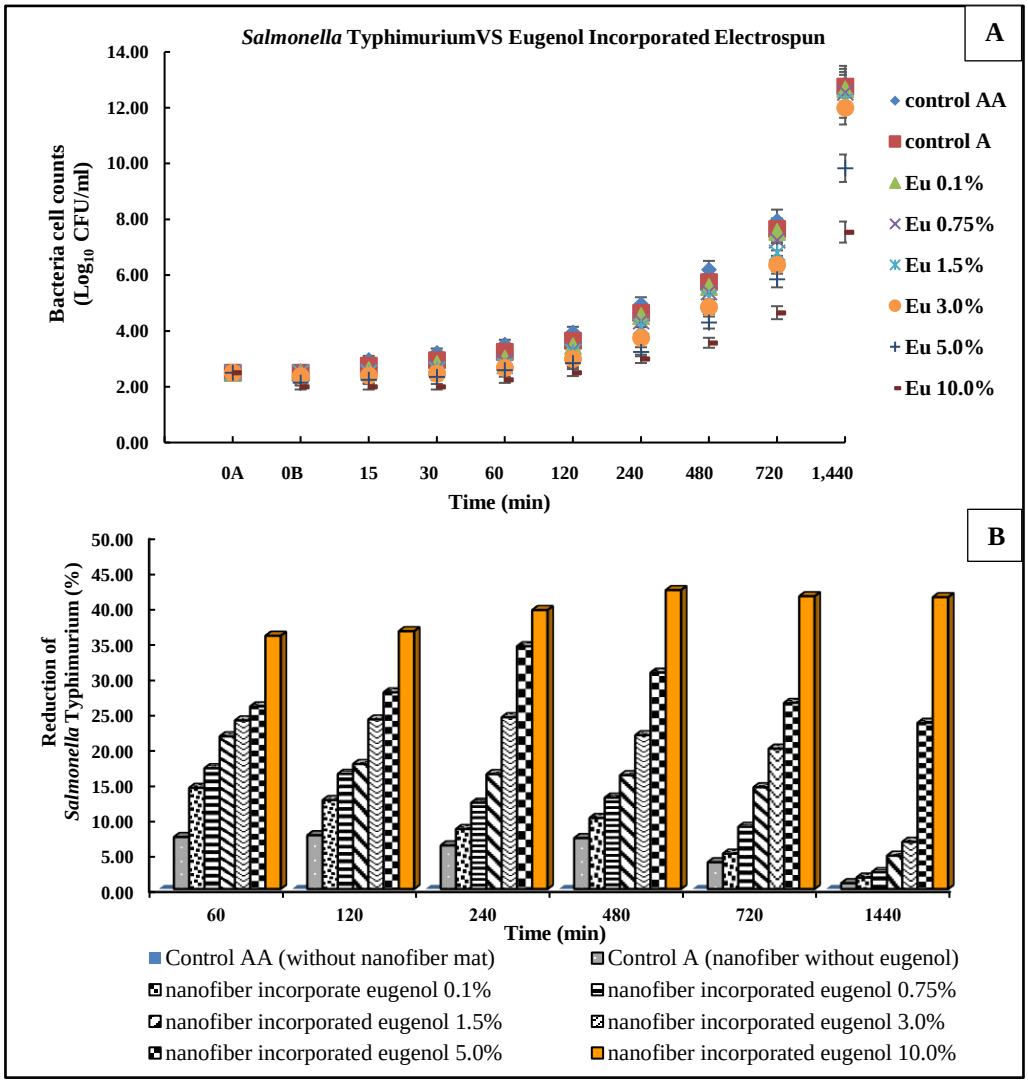

Figure 4. Growth and reduction of *Salmonella* Typhimurium at different time periods

Time 0A min is the initial population of each test with approximately 2 – 3 Log_{10} CFU/ml. and Time 0B min is the population of each test after contact with nanofiber mats incorporating eugenol for 15 sec. In Figure 4 A, the initial population of *Salmonella* Typhimurium was 2.51 log_{10} CFU/ml. At 60 min, the growth of *Salmonella* Typhimurium reached 3.51 log_{10} CFU/ml in control AA and 3.25 log_{10} CFU/ml in control A. As for the test samples, bacterial growth on mats containing eugenol at 0.1%, 0.75%, 1.5%, 3.0%, 5.0% and 10.0% (v/v) was 3.01, 2.91, 2.75, 2.67, 2.60 and 2.25 log_{10} CFU/ml, respectively. At 1,440 min, bacterial growth reached 12.86 log_{10} CFU/ml in control AA and 12.75 log_{10} CFU/ml in control A. As for the test samples, bacterial growth on mats containing eugenol at 0.1%, 0.75%, 1.5%, 3.0%, 5.0% and 10.0% (v/v) contained colonies of 12.65, 12.55, 12.25, 12.00, 9.83, and 7.54 log_{10} CFU/ml, respectively.

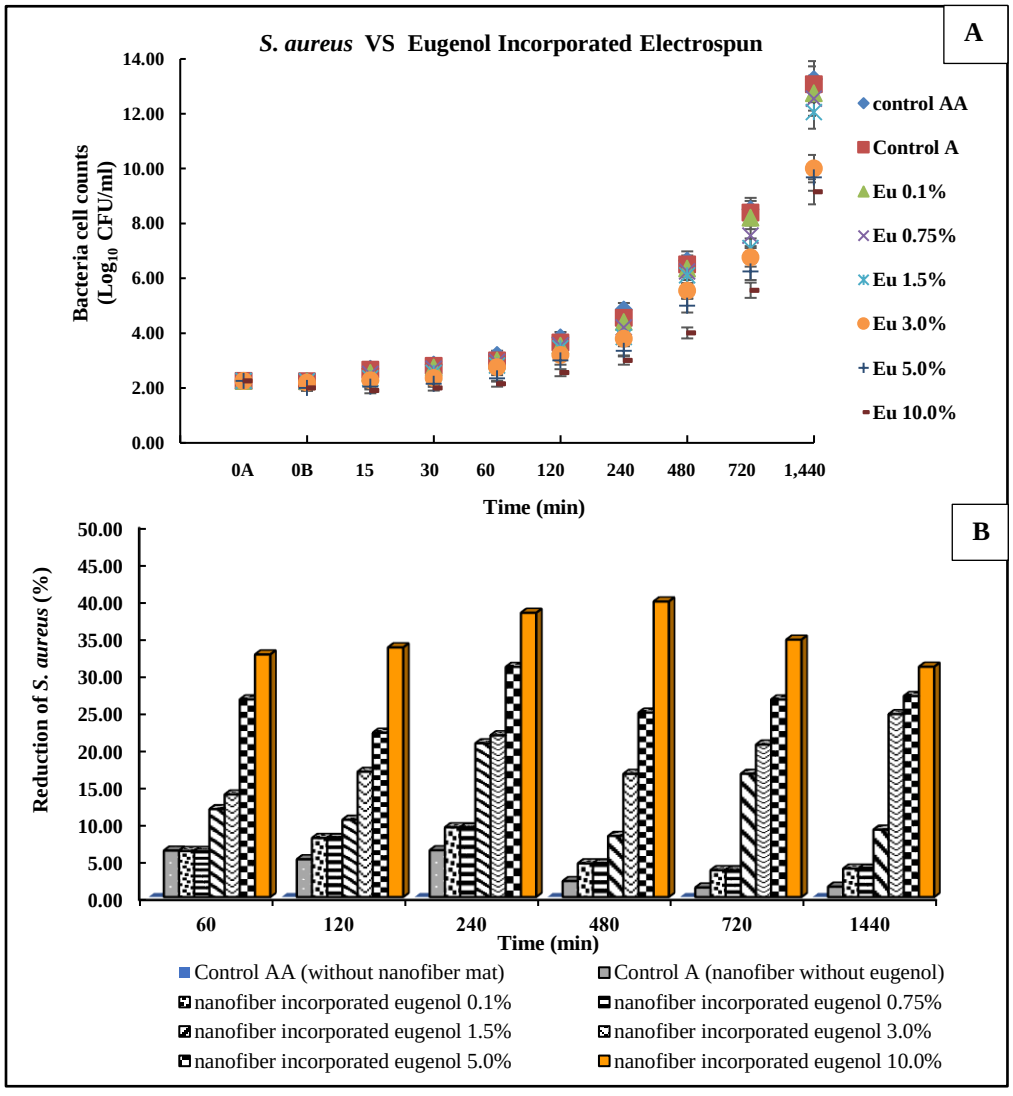

Figure 5. Growth and reduction of *S. aureus* at different time periods

From Figure 4 B, in every time period the growth of *Salmonella* Typhimurium reduced as the eugenol loading of the samples increased. At 1,440 min, reductions of 0.81, 1.61, 2.37, 4.71, 6.67, 23.53, and 41.33% were observed at eugenol concentrations of 0.0% (control A), 0.1%, 0.75%, 1.5%, 3.0%, 5.0% and 10.0% (v/v), respectively.

From Figure 5 A, the initial population of *S. aureus* was 2.25 $\log_{10}$ CFU/ml. At 60 min, the growth of *S. aureus* reached 3.20 $\log_{10}$ CFU/ml in control AA and 3.00 $\log_{10}$ CFU/ml in control A. As for the test samples, mats containing eugenol at 0.1%, 0.75%, 1.5%, 3.0%, 5.0% and 10.0% (v/v) contained colonies of 3.00, 2.96, 2.82, 2.76, 2.35 and 2.16 $\log_{10}$ CFU/ml, respectively. At 1,440 min, the colonies reached 13.26 $\log_{10}$ CFU/ml in control AA and 13.08 $\log_{10}$ CFU/ml in control A. As for the test samples, mats containing eugenol at 0.1%, 0.75%, 1.5%, 3.0%, 5.0% and 10.0% (v/v) contained colonies of 12.75, 12.55, 12.06, 10.00, 9.68 and 9.16 $\log_{10}$ CFU/ml, respectively. From Figure 5 B, in every time period the growth of *S. aureus* reduced as the eugenol loading of the samples increased. At 1,440 min, reductions of 1.38, 3.81, 5.31, 9.05, 24.57, 27.01 and 30.95% were observed at eugenol concentrations of 0.0% (control A), 0.1%, 0.75%, 1.5%, 3.0%, 5.0% and 10.0% (v/v), respectively. The results demonstrated that up to 240 min, the populations of both *Salmonella* Typhimurium and *S. aureus* increased gradually and then increasing more rapidly in all samples. The mat incorporating eugenol at 10.0% (v/v) showed the maximum growth reduction compared to control A.

Previous studies have suggested that eugenol may disrupt the cytoplasmic membrane of bacteria as well as increasing its permeability [4, 47]. The cell membrane of Gram-negative bacteria is sensitive to the hydrophobic property of eugenol. Eugenol can penetrate the lipopolysaccharide of the bacterial membrane and alter the cell structure. This phenomenon can cause leakage of intracellular components and lead to the death of bacterial cell [4, 32, 48, 49]. Moreover, the chitosan offer positively charged free amino group, which can interact with the negative bacterial cell wall causing membrane to rupture. Consequently, intracellular proteins were released due to membrane deterioration [15, 24, 50].

4. Conclusions

The results of this study showed that eugenol essential oil could directly be incorporated into a CS/CA/Gel polymer solution without the use of surfactant. Edible electrospun nanofiber mats were succesfully fabricated via electrospinning. The release of eugenol was related to eugenol diffusion through the polymer and/ or erosion of the polymer. Thermal analysis demonstrated better thermostability when the concentration of eugenol was less than 5.0% (v/v). The CS/CA/Gel edible electrospun nanofiber mats with incorporated eugenol showed enhanced activity against *Salmonella* Typhimurium and *S. aureus.* This approach may effectively extend the shelf-life of food with potential applications in active food packaging and others products.

5. Acknowledgements

This research was financially supported by a research grant for graduate dissertation (Year 2017) from the National Research Council of Thailand. The authors would like to thank Faculty of Science and Technology, Thammasat University for scholarship in the Year of 2015.

References

[1] Centers for Disease Control and Prevention, 2013. *An Atlas of Salmonella in the United States, 1968-2011: Laboratory-based Enteric Disease Surveillance*. Atlanta, Georgia: US Department of Health and Human Services, CDC.

[2] Amna, T., Yang, J., Ryu, K.S. and Hwang, I.H., 2015. Electrospun antimicrobial hybrid mats: Innovative packaging material for meat and meat-products. *Journal Food Science Technology*, 52(7), 4600-4606.

[3] Ercoli, L., Gallina, S., Nia, Y., Auvray, F., Primavilla, S., Guidi, F., Pierucci, B., Graziotti, C., Decastelli, L. and Scuota, S., 2017. Investigation of a Staphylococcal food poisoning outbreak from a Chantilly cream dessert, in Umbria (Italy). *Foodborne Pathogens and Disease*, 14(7), 407-413.

[4] Devi, K.P., Nisha, S.A., Sakthivel, R. and Pandian, S.K., 2010. Eugenol (an essential oil of clove) acts an antibacterial agent against *Salmonella typhi* by disrupting the cellular membrane. *Journal of Ethnopharmacology*, 130, 107-115.

[5] Kadariya, J., Smith, T.C. and Thapaliya, D., 2014. *Staphylococcus aureus* and Staphylococcal food-borne disease: An ongoing challenge in public health. *BioMed Research International*, 2014, 1-9. http://dx.doi.org/10.1155/2014/827965

[6] Hennekinne, J.A., Buyser, M.L.D. and Dragacci, S., 2012. *Staphylococcus aureus* and its food poisoning toxins: characterization and outbreak investigation. *FEMS Microbiology Reviews*, 36, 815-836.

[7] Appenendini, P. and Hotchkiss, J. H., 2002. Review of antimicrobial food packaging. *Innovative Food Science & Emerging Technologies*, 3, 113-126.

[8] Sung, S.Y., Sin, L.T., Tee, T.T., Bee, S.T., Rahmat, A.R., Rahman, W.A.W.A., Tan, A.C. and Vikkraman, M., 2013. Antimicrobial agents for food packaging applications. *Trends in Food Science & Technology*, 33, 110-123.

[9] Wen, P., Zhu, D.H., Wu, H., Zong, M.H., Jing, Y.R. and Han, S.Y., 2016. Encapsulation of cinnamon essential oil in electrospun nanofibrous film for active food packaging. *Food Control*, 59, 366-376.

[10] Kriegel, C., Kit, K.M., McClements, D.J. and Weiss, J., 2009. Nanofibers as carrier systems for antimicrobial microemulsions. Part I: Fabrication and characterization. *Langmuir*, 25, 1154-1161.

[11] Bhardwaj, N. and Kundu, S.C., 2010. Electrospinning: A fascinating fiber fabrication technique. *Biotechnology Advances*, 28, 325-347.

[12] Zargham, S., Bazgir, S., Tavakoli, A., Rashidi, A.S. and Damerchely, R. 2012. The effect of flow rate on morphology and deposition area of electrospun nylon 6 nanofiber. *Journal of Engineered Fibers and Fabrics*, 7, 42- 49.

[13] Zong, X., Kim, K., Fang, D. and Ran, S., 2002. Structure and process relationship of electrospun bioabsorbable nanofiber membranes. *Polymer*, 43, 4403-4412.

[14] Oraby, M.A., Waley, A.I., El-Dewany, A.I., Saad, E.A. and Abd El-Hady, B.M., 2013. Electrospun gelatin nanofibers: Effect of gelatin concentration on morphology and fiber diameters. *Journal of Applied Sciences Research*, 9, 534-540.

[15] Rieger, K.A. and Schiffman, J.D., 2014. Electrospinning an essential oil: Cinnamaldehyde enhances the antimicrobial efficacy of chitosan/ poly (ethylene oxide) nanofibers. *Carbohydrate Polymers*, 113, 561-568

[16] Pelipenko, J., Kristl, J., Jankovic, B., Baumgartner, S. and Kocbek, P., 2013. The impact of relative humidity during electrospinning on the morphology and mechanical properties of nanofibers. *International Journal of Pharmaceutics*, 456, 125-134.

[17] Rogina, A., 2014. Electrospinning process: Versatile preparation method for biodegradable and natural polymers and biocomposite systems applied in tissue engineering and drug delivery. *Applied Surface Science*, 296, 221-230.
[18] Baji, A., Mai, Y.W., Wong, S.C., Abtahi, M. and Chen, P., 2010. Electrospinning of polymer nanofibers: Effects on oriented morphology, structures and tensile properties. *Composites Science and Technology*, 70, 703-718.
[19] Frenot, A. and Chronakis, I.S., 2003. Polymer nanofibers assembled by electrospinning. *Current Opinion in Colloid and Interface Science*, 8, 64-75.
[20] Sener, A.G., Altay, A.S. and Altay, F., 2011. Effect of voltage on morphology of electrospun nanofibers. *Electrical and Electronics Engineering (ELECO) 7th International Conference*, Bursa, Turkey, December 1- 4, 2011, P. I-324-I-328.
[21] Elsabee, M.Z., Naguib, H.F. and Morsi, R.E., 2012. Chitosan based nanofibers, review. *Materials Science and Engineering C*, 32, 1711-1726.
[22] Mendes, A.C., Stephansen, K. and Chronakis, I.S., 2017. Electrospinning of food proteins and polysaccharides. *Food Hydrocolloids*, 68, 53-68.
[23] Geng, X., Kwon, O.H. and Jang, J., 2005. Electrospinnping of chitosan dissolved in concentrated acetic acid solution. *Biomaterials*, 26, 5427-5432.
[24] Arkoun, M., Daigle, F., Heuzey, M.C. and Ajji, A., 2017. Antibacterial electrospun chitosan-based nanofibers: A bacterial membrane perforator. *Food Science and Nutrition*, 5, 865-874.
[25] Jafari, J., Emami, S.H., Samadikuchaksaraei, A., Bahar, M.A. and Gorjipour, F., 2011. Electrospun chitosan-gelatin nanofiberous scaffold: Fabrication and *in vitro* evaluation. *Bio-Medical Materials and Engineering*, 21, 99-112.
[26] Huang, Z.M., Zhang, Y.Z., Ramakrishna, S. and Lim, C.T., 2004. Electrospinning and mechanical characterization of gelatin nanofibers. *Polymer*, 45, 5361-5368.
[27] Haider, S., Al-Massry, W.A., Bukhari, N. and Javid, M., 2010. Preparation of the chitosan containing nanofibers by electrospinning chitosan-gelatin complexes. *Polymer Engineering and Science*, 50, 1887-1893.
[28] Han, S.O., Youk, J.H., Min, K.D., Kang, Y.O. and Park, W.H., 2008. Electrospinning of cellulose acetate nanofibers using a mixed solvent of acetic acid/water: effects of solvent composition on the fiber diameter. *Material Letters*, 62, 759-762.
[29] Unnithan, A.R., Gnanasekaran, G., Sathishkumar, Y., Lee, Y.S. and Kim, C.S., 2014. Electrospun antibacterial polyurethane-cellulose acetate-zein composite mats for wound dressing. *Carbohydrate Polymers*, 102, 884-892.
[30] Wang, S., Marcone, M.F., Barbut, S. and Lim, L.T., 2013. Electrospun soy protein isolate-based fiber fortified with anthocyanin-rich red raspberry (*Rubus strigosus*) extracts. *Food Research International*, 52, 467-472.
[31] Blanco-Padilla, A., Soto, K.M., Iturriaga, M.H. and Mendoza, S., 2014. Food antimicrobials nanocarriers. *The Scientific World Journal*, 2014, 1-11.
[32] Li, Z., Zhou, P., Zhou, F., Zhao, Y., Ren, L. and Yuan, X., 2018. Antimicrobial eugenol-loaded electrospun membranes of poly(Ɛ-caprolactone)/gelatin incorporated with REDV for vascular graft applications. *Colloids and Surfaces B: Biointerfaces*, 162, 335-344.
[33] Oussalah, M., Caillet, S., Saucier, L. and Lacroix, M., 2007. Inhibitory effects of selected plant essential oils on the growth of four pathogenic bacteria: *E. coli* O157:H7, *Salmonella* Typhimurium, *Staphylococcus aureus* and *Listeria monocytogenes*. *Food Control*, 18, 414-420.
[34] Bevilacqua, A., CorBo, M.R. and Sinigaglia, M., 2010. In vitro evaluation of the antimicrobial activity of eugenol, limonene, and citrus extract against bacteria and yeasts, representative of the spoiling microflora of fruit juices. *Journal of Food Protection*, 73(5), 888-894.

[35] Wang, X., Yue, T. and Lee, T.C., 2015. Development of Pleurocidin-poly (vinyl alcohol) electrospun antimicrobial nanofibers to retain antimicrobial activity in food system application. *Food Control*, 54, 150-157.
[36] Wen, P., Zhu, D.H., Feng, K., Liu, K.F., Lou, W.Y., Li, N., Zong, M.H. and Wu, H., 2016. Fabrication of electrospun polylactic acid nanofilm incorporating cinnamon essential oil/β-cyclodextrin inclusion complex for antimicrobial packaging. *Food Chemistry*, 196, 996-1004.
[37] Somsap, J., Kanjanapongkul, K. and Tepsorn, R., 2018. Effect of parameters on the morphology and fibre diameters of edible electrospun chitosan-cellulose acetate-gelatin hybrid nanofibers. *MATEC Web of Conferences*, 192, 03038. https://doi.org/10.1051/matecconf/201819203038
[38] ASTM E2149-01, 2004. *Standard Test Method for Determining the Antimicrobial Activity of Immobilized Antimicrobial Agents under Dynamic Contact Conditions*. American Society for Testing and Materials.
[39] Tepsorn, R. and Somsap, J. 2018. Morphology of edible nanofibers based chitosan-cellulose acetate-gelatin blend fortified with eugenol by electrospinning and electrospinning-spraying technique. *Thai Science and Technology Journal*, 26(7), 1130-1140.
[40] Angammana, C.J. and Jayaram, S.H., 2011. Analysis of the effects of solution conductivity on electrospinning process and fiber morphology. *IEEE Transactions on Industry Applications*, 47, 1109-1117.
[41] de Oliveria Mori, C.L.S., dos Passos, N.A., Oliveira, J.E., Altoé, T.F., Mori, F.A., Mattoso, L.H.C., Scolforo, J.R. and Tonoli, G.H.D., 2015. Nanostructured polylactic acid/candeia essential oil mats obtained by electrospinning. *Journal of Nanomaterials*, 2015, 1-9. http://dx.doi.org/10.1155/2015/439253
[42] Gao, Y., Truong, Y.B., Zhu, Y. and Kyratzis, I.L., 2014. Electrospun antibacterial nanofibers: Production, activity, and *In vivo* application. *Journal of Applied Polymer Science*, 2014, 1-13. doi:10.1002/app.40797
[43] Peppas, N.A., Bures, P., Leobandung, W. and Ichikawa, H., 2000. Hydrogels in pharmaceutical formulations. *European Journal of Pharmaceutics and Biopharmaceutics*, 50, 27-46.
[44] Kabay, G., Meydan, A.E., Can, G.K., Demirci, C. and Mutlu, M., 2017. Controlled release of a hydrophilic drug from electrospun amyloid-like protein blend nanofibers. *Materials Science & Engineering C*, 81, 271-279.
[45] Varma, M.V.S., Kaushal, A.M., Garg, A. and Garg, S., 2004. Factors affecting mechanism and kinetics of drug release from matrix-based oral controlled drug delivery systems. *American Journal of Drug Delivery*, 2(1), 43-57.
[46] Huang, X. and Brazel, C.S., 2001. On the importance and mechanisms of burst release in matrix-controlled drug delivery systems. *Journal of Controlled Release*, 73, 121-136.
[47] Bennis, S., Chami, F., Chami, N., Rhayour, K., Tantaoui-Elaraki, A. and Remmal, A., 2004. Eugenol induces damage of bacterial and fungal envelope. *Moroccan Journal of Biology*, 1, 33-39.
[48] Burt, S., 2004. Essential oils: their antibacterial properties and potential applications in foods-a review. *International Journal of Food Microbiology*, 94, 223-253.
[49] Marchese, A., Barbieri, R., Coppo, E., Orhan, I.E., Daglia, M., Nabavi, S.F., Izadi, M., Abdollahi, M., Nabavi, S.M. and Ajami, M., 2017. Antimicrobial activity of eugenol and essential oils containing eugenol: A mechanistic viewpoint. *Critical Reviews in Microbiology*, 43(6), 668-689.
[50] Cooper, A., Oldinski, R., Ma, H., Bryers, J.D. and Zhang, M., 2013. Chitosan-based nanofibrous membranes for antibacterial filter applications. *Carbohydrate Polymers*, 92, 254-259.

Indoor Nitrogen Dioxide Investigation and Health Risk Assessment in Primary Schools at Rayong City, Thailand

Susira Bootdee[1*], Suganya Phantu[2], Pawit Lamlongrat[1] and Thanin Khumphai[1]

[1]Industrial Chemical Process and Environment Program, Faculty of Science, Energy and Environment, King Mongkut's University of Technology North Bangkok, Rayong Campus, Rayong, Thailand
[2]Energy Technology and Management Program, Faculty of Science, Energy and Environment, King Mongkut's University of Technology North Bangkok, Rayong Campus, Rayong, Thailand

Received: 25 April 2019, Revised: 29 June 2019, Accepted: 31 July 2019

Abstract

Indoor air pollution in schools adversely affects children's health due to the inhalation of nitrogen dioxide (NO_2), which is a toxin released by motor vehicles. This research aims to measure NO_2 levels around schools in an attempt to evaluate indoor air quality within the framework of a health risk assessment. Air samples were collected in schools from indoor and outdoor locations. The results for indoor NO_2 concentrations in urban, industrial and rural areas ranged between 12.8 - 32.9, 11.7 - 36.6 and 7.0 - 17.5 μg/m^3, while the values for outdoor areas ranged between 13.0 - 43.7, 15.5 - 37.6 and 10.1 - 32.6 μg/m^3, respectively. The indoor NO_2 concentrations measured in urban and industrial areas were significantly higher than those in rural areas ($p<0.05$), while the values for urban and industrial areas were not significantly different ($p>0.05$). The mean of indoor and outdoor NO_2 concentrations were not significantly different ($p>0.05$) and these values were more significantly correlated ($r = 0.526$). Moreover, the values of NO_2 concentrations and meteorological factors were not significantly correlated, thereby rejecting the hypothesis that meteorological factors might have affected indoor NO_2 concentrations. These findings clearly stress the relationship that exists between NO_2 concentrations and the level of local activity, for example traffic intensity. Hazard quotient (HQ) values indicated that human health risks linked to NO_2 inhalation were of the low hazard type. It can be concluded that local activities played a significant role in the emission of NO_2 and the level of indoor air quality in classrooms.

Keywords: indoor air pollution, nitrogen dioxide, passive sampling, hazard quotient (HQ)
DOI 10.14456/cast.2019.21

1. Introduction

Indoor air pollution in schools represents one of the most serious environmental and public health concerns in the world. Indoor pollutants such as particulate matter (PM), volatile organic compounds

*Corresponding author: Tel.: 66 83 570 4960
E-mail: susira.b@sciee.kmutnb.ac.th

(VOCs), formaldehyde, carbon dioxide (CO_2), nitrogen dioxide (NO_2), sulfur dioxide (SO_2) and polycyclic aromatic hydrocarbons (PAHs)have often been measured in schools [1-3]. Major sources of pollutants in schools can originate from outdoor pollution sources like motor vehicle traffic, industry and combustion, while other sources are related to indoor human activities including painting, cleaning, equipment building and furnishings [4, 5].

The measured level of nitrogen dioxide commonly is often a major indicator of traffic air pollution [1, 6]. It is the most toxic form of nitrogen oxides (NO_X). Boulter *et al.* [7] reported that the proportion of NO_2 within the total NO_X for diesel burning (20-70%) in an engine was 7-10 times higher than for petrol burning (2-10%). Relations between NO_2 levels inside primary schools and urban areas of Italy were studied by Cibella *et al*. [6], who established that the mean of indoor NO_2 concentrations during winter and spring seasons were 32.2 ± 16.3 $\mu g/m^3$ and 31.9 ± 14.9 $\mu g/m^3$, respectively. Moreover, during 25.2 % of the time in winter and 24.5% of the time in spring, indoor NO_2 concentrations in primary schools exceeded the World Health Organization indoor limit of 40 $\mu g/m^3$. An investigation into indoor NO_2 levels inside primary schools located in the centre of cities and in the suburban area of Aveiro in Portugal was undertaken. The researchers revealed that indoor NO_2 concentrations during a one-week time-frame ranged from 12.81 ± 0.59 to 16.46 ± 0.98 $\mu g/m^3$ and from 12.92 ± 0.59 to 16.57 ± 0.99 $\mu g/m^3$ in city centre and sub-urban areas, respectively. The researchers further concluded that the levels of NO_2 observed were related to vehicular exhaust emissions from nearby intense traffic [1]. Rivas *et al* [8] revealed the presence of NO_2 concentrations in classrooms and playgrounds in 39 schools in Barcelona, Spain. It was found that the levels of NO_2 concentrations in classrooms (5-69 $\mu g/m^3$) were lower than those in playgrounds (14-98 $\mu g/m^3$). The intensity of road traffic was identified as the main cause of pollution.

Each day, children spend most of their time in schools, where they are primarily exposed to indoor pollution rather than outdoor pollution. Children while still growing up have an immune system that is not yet fully developed. Therefore, they are more vulnerable to various indoor environmental pollutants than are adults [1, 9, 10]. Previous studies reported that a relationship existed between exposure to NO_2 and health effects in schoolchildren such as respiratory illnesses, impaired lung function, and asthma [6, 11-13]. Furthermore, Norbäck *et al*. [3] revealed that indoor NO_2 concentrations in schools were associated with ocular symptoms and fatigue. Giffin *et al*. [13] reported that 10 ppb increase in NO_2 levels was associated with a 5% decrease in pulmonary function. An increment of 21.9 $\mu g/m^3$ in the 7-day-average concentrations of NO_2 was associated with a 6.1 % increase in pneumonia hospitalizations [14]. Ayuni and Juliana [12] found that exposure to indoor NO_2 concentrations might increase the risk of respiratory problems among schoolchildren living near petrochemical industries. Furthermore, girls may be more susceptible to indoor NO_2 than boys [11].

Indoor air quality in schools is regarded as a serious issue because air pollutants can be the cause of adverse health effect in students. Consequently, the main objective of this research is to accurately determine indoor NO_2 concentrations in various primary schools located within the vicinities of intense traffic areas so as to assess the level of quality of indoor air and its possible risks to health.

2. Materials and Methods

2.1 Sampling sites

Rayong province is located in the eastern part of Thailand. It is famous for its natural resources, which include various kinds of tropical fruit and seafood. Moreover, an industrial estate is also situated there. Sampling sites were surveyed and randomly selected within three areas of the Rayong

province. There are 12 primary schools (Figure 1 and Table 1) included in the study and they can be divided into urban areas (4 sites), industrial areas (4 sites) and rural areas (4 sites). Air-quality samples were randomly collected inside three primary school classrooms surrounded by communal ambient air. The selection of locations for the sampling sites was based on criteria like school roadside infrastructure, traffic intensity, population density, and human activities. The sampling sites as seen in Figure 1 are defined as follows :

Urban area (UB) : This urban area is identified as the Rayong municipality. It is a community area which includes residential and business buildings, a transportation network and high traffic intensity.

Industrial area (ID) : This is the Map ta phut industrial estate in Map ta phut municipality. Most of the area is occupied by industrial plants and included are petroleum plants, a coal-fired power plant, petrochemical and plastics facilities, community areas and various transportation networks.

Rural area (RR) : This is the Wong Chan district. Most of the area is used for agricultural purposes such as rubber trees and pineapples fields. There is a low level of vehicle traffic.

The samples were subjected to continual exposure over a week from September 2017 to February 2018 (except for the entire month of October 2017, which was the primary school semester break).

2.2 NO_2 sampling and analysis

The indoor and outdoor NO_2 concentrations were collected using lab made passive samplers sourced from the Environmental Chemistry Research Laboratory (ECRL), Chemistry Department, Faculty of Science, Chiang Mai University. The polypropylene (PP) passive sampler (7.70 cm length and 1.50 cm inner diameter) containing 50 µl of 20% triethanolamine (TEA) was directly added onto the Whatman GF/A filter paper. A sample set consisted of 5 sampling tubes and 3 blank tubes, which were attached to a shelter and hung at 1.5 – 2.0 m above ground level for 1 week. After sampling, the NO_2 concentration was determined colorimetrically as nitrite (NO_2^-). For extraction, the NO_2 samplers were extracted with 2 ml of deionized water, shaken and held for 15 min. One ml of the extracted sample solution was filtered through a 0.45 µm cellulose acetate membrane. Then, the solution was mixed with 2 ml of Saltzmann reagent and allowed to stand for 10 min until color development was completed. After extraction, the absorbance was measured by spectrophotometer (Shimadzu UV 2600, Japan) at 540 nm [15].

2.3 Statistical analysis

The data were statistically analyzed by T-test to determine the difference between indoor and outdoor nitrogen dioxide levels. One-way ANOVA was used to analyze the mean difference between the spatial variations. The NO_2 concentrations were log–transformed to achieve normal distribution. Pearson correlation analysis was used to assess the relationship between the meteorological data and the NO_2 concentrations. The meteorological data were received from Rayong Meteorological Station (RMS) and from the Thai Meteorological Department (TMD) (Figure 1).

2.4 Health risk assessment

Health risk assessment is a process estimating the exposure risk linked to pollutant inhalation on the basis of the hazard quotient (HQ). The hazard quotient (HQ) is widely used to assess the effects of non-carcinogenic risk exposure to a known pollutant. It reflects the probability of an adverse health outcome occurring among healthy or sensitive individuals [16-18]. Human exposure was explained in terms of the average daily dose (ADD). ADD was quantified as described in equation 1 :

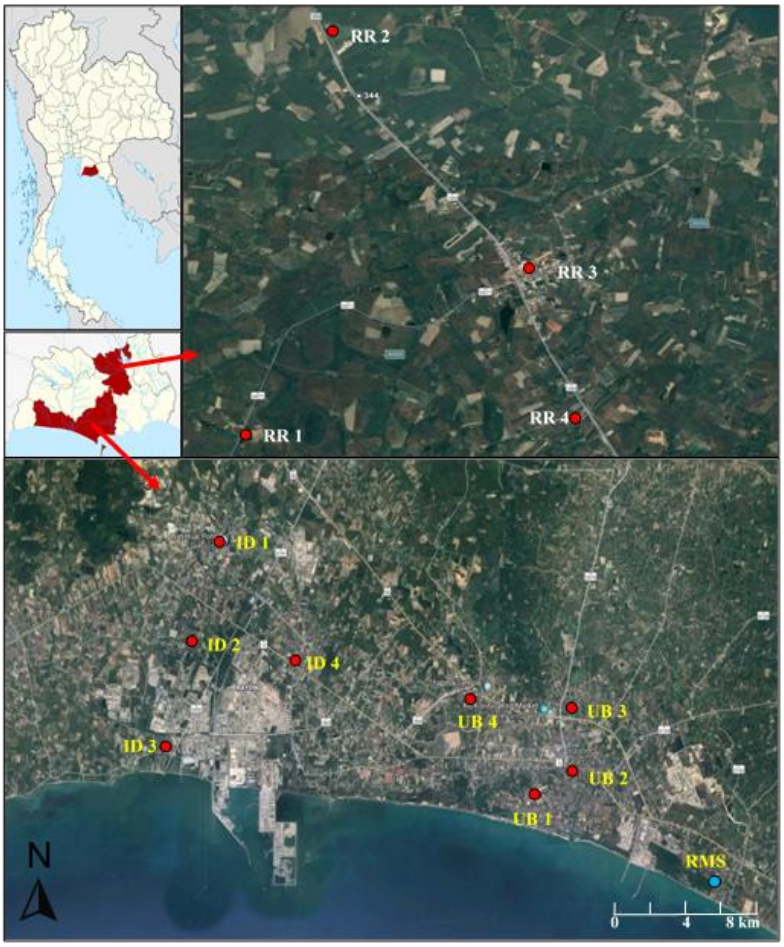

Note: Applied from Google map

Figure 1. Map of NO_2 sampling sites; (A) Wang Chan district and (B) Maung district of Rayong province.

Table 1. Sampling sites and land-use patterns of primary schools in Rayong province

Site	Code	Classrooms characteristics	GPS position Lat-Long
Urban area	UB 1	The school is located along a road of approximately 8 m in width. A high level of traffic intensity occurs during rush hours. It is surrounded by many government offices. Its buildings have 3 floors and are constructed from concrete.	12° 40' 29.73" 101°16' 44.79"
	UB 2	The school is located in a temple area, ~200 m distant from a road of 8 m in width with a high level of traffic intensity. Its buildings are of 3-4 floors and are constructed from concrete.	12° 40' 47.88" 101° 16' 59.94"

Table 1. (cont.)

	UB 3	The school is located behind a temple area. The buildings are of 2 floors and are constructed from concrete. The school is near the local market and department store. It is approximately 1 km away from a highway road.	12° 42' 1.278" 101° 16' 29.44"
	UB 4	The school is located close to a highway intersection or interchange road that has a high level of traffic intensity during rush hours. Its buildings are of 2-3 floors and are constructed from concrete.	12° 42' 16.938" 101° 14' 24.69"
Industrial area	ID 1	The sampling site is near an intersection and a temple. Its buildings have 2-4 floors and are constructed from concrete. It is located close to a tapioca flour manufactory.	12° 45' 15.96" 101° 8' 11.76"
	ID 2	The school is located on the premises of a temple near a petrochemical plant. It is built from wooden and concrete materials and consist of 2 floors. It is near an intersection and approximately 100 meters away from a road where a high level of traffic intensity occurs especially during rush hours.	12° 41' 6.6768" 101° 6' 58.88"
	ID 3	The school is located at the back of the Maptaphut municipality. It is built from wooden materials and has 2 floors. This site is surrounded by governmental offices.	12° 43' 23.37" 101° 7' 35.58"
	ID 4	The school is located on a highway road. There are 4-6 floor buildings that are constructed from concrete. It is surrounded by commercial buildings and a local market. This site is a residential area close to an intersection with a high level of traffic intensity.	12° 42' 55.63" 101° 10' 0.45"
Rural area	RR 1	The school is located on a local road in a small residential area surrounded by rubber tree fields and orchards. The school has 2 floors and it is built of wooden and concrete materials.	12° 54' 38.28" 101° 28' 47.61"
	RR 2	The sampling site is located on a highway. Its buildings are constructed with wooden materials and have 2 floors. It is surrounded by rubber tree fields.	12° 58' 50.63" 101° 29' 32.88"
	RR 3	The school is located near a hospital. It is surrounded by commercial buildings and a local market. Its buildings have 2 floors and are constructed from concrete and wooden materials.	12° 56' 23.874" 101° 31' 38.82"
	RR 4	The school is located in a temple area. It has 2 floors and its buildings are constructed from concrete and wooden materials. The sampling site is surrounded by rubber tree fields.	12° 54' 47.264" 101° 31' 54.42"

$$\mathrm{ADD} = \frac{\mathrm{C} \times \mathrm{Inh\ R} \times \mathrm{EF} \times \mathrm{ED}}{\mathrm{BW} \times \mathrm{AT}} \quad (1)$$

where ADD is the ADD of pollutants; C is the concentration of NO_2 ($\mu g/m^3$); ED is the exposure duration (days); BW is the body weight of the exposed group (Kg); AT is the average time (days); InhR is the inhalation rate (m^3/day) and EF is the exposure frequency (days/year). The values of these parameters were reported [16-18] as shown in Table 2.

Table 2. Parameters of the average daily dose (ADD) for NO_2

Parameters	**Exposed group**	
	Child (6-12 years)	**Adult (19-75 years)**
Exposure frequency (EF)	350 days/year	350 days/year
Exposure duration (ED)	12 years	30 years
Averaging time (AT) AT = ED ×365 days	4,380 days	10, 950 days
Body weight (BW)	45.3 Kg	71.8 Kg
Inhalation rate (InhR)	16.6 m^3/day [19]	21.4 m^3/day

The HQ was calculated from the ratio of ADD and the reference dose (RfD) of each pollutant using the following equation 2.

$$\mathrm{HQ} = \frac{\mathrm{ADD}}{\mathrm{RfD}} \quad (2)$$

The reference concentrations (RfD) allowable for human exposure are shown in Table 3. When the HQ < 0.1, there is no hazard or only negligible risk. When the HQ values are situated between 0.1-1.0, there are low hazard risks. When the HQ values are situated between 1.1-10.0, there are moderate risks. When the HQ values are situated above the threshold of 10, there are high hazard risks [16].

Table 3. The indoor air quality standard of nitrogen dioxide (NO_2)

Organization or country	**Indoor air quality standards for NO_2 ($\mu g/m^3$)**		
	1 h	**8 h**	**Annual mean**
NAAQ-US-EPA[20]	200	-	40
WHO[21]	200	-	40
Thailand[22]	-	150	-
Hong Kong[23]	200	150	40

3. Results and Discussion

3.1 NO_2 concentrations in primary schools

The mean concentrations of NO_2 were measured inside classrooms at primary schools in Rayong city as shown in Figure 2. The highest indoor NO_2 concentrations were found in the urban area at the UB4 site (15.1-52.0 $\mu g/m^3$). It is located close to a highway intersection with high traffic

intensity. However, the indoor NO_2 concentrations were not significantly different ($p>0.05$) from one site to another. The highest indoor NO_2 concentration in the industrial area was found at the ID1 site (20.7±7.3 to 32.9±15.6 µg/m^3), while that in the rural area was found at the RR2 site (12.9±3.3 to 18.5±10.8 µg/m^3).

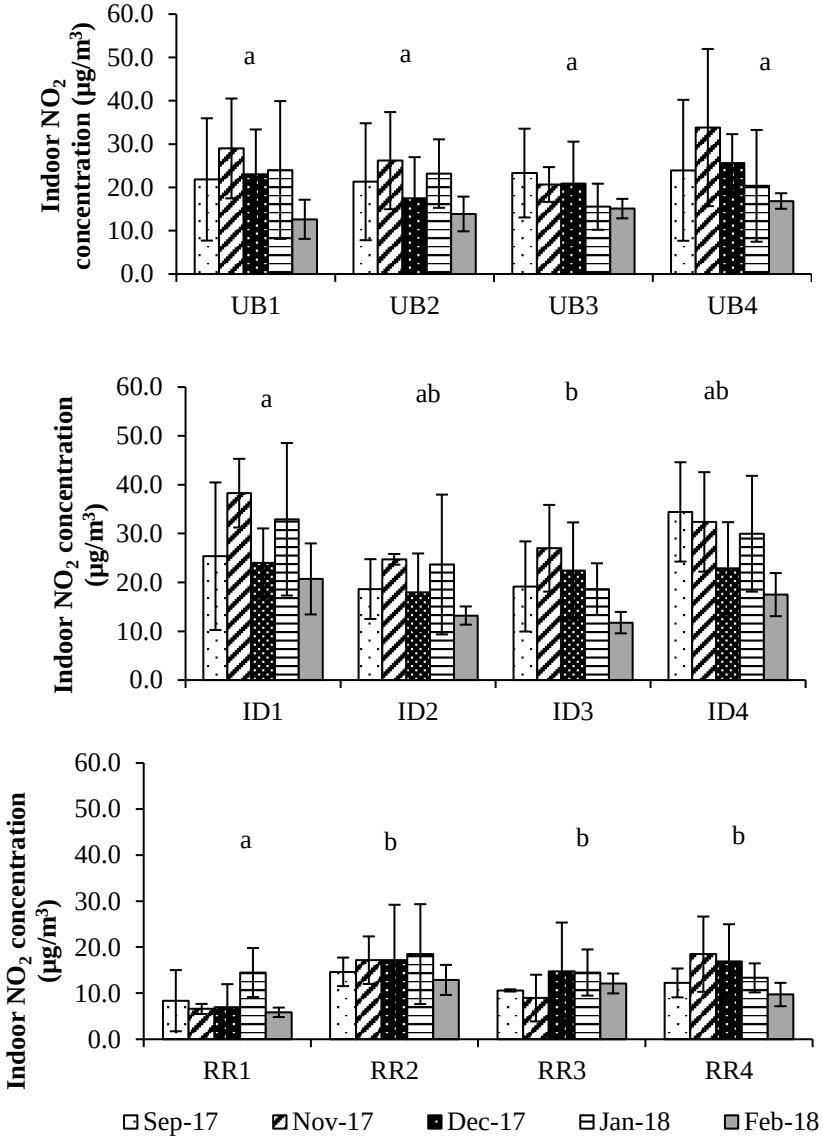

Note: a, b = Significant differences ($p < 0.05$) among groups of primary school within the same period

Figure 2. Indoor NO_2 concentrations in school at urban area (UB), industrial area (ID) and rural area (RR)

The cause of NO_2 concentrations in the industrial area may well be related to traffic and industrial plants, while the values in the rural area are likely due to traffic and open burning. Moreover, One-Way ANOVA was used to determine the differences in indoor NO_2 concentrations between each primary school. It was found that the indoor NO_2 concentrations in the primary schools of the urban area were not significantly different (p>0.05), and the values of the rural area from RR2 to RR4 were not significantly different (p>0.05). In the industrial area, the indoor NO_2 concentrations in the ID1 site were significantly different from the ID3 site (p>0.05). The values at the ID3 site were the lowest of indoor NO_2 concentrations in the industrial area despite the fact that this site was surrounded by government offices (Table 1). The buildings were made from wooden materials and an advantage of using them as building materials is that they cause a lower input of contaminants [4]. Therefore, the schools located within the vicinities of high traffic intensity are exposed to pollutants that may adversely affect the health of students and teachers.

The mean concentrations of NO_2 that were measured both indoors and outdoors at primary schools in Rayong province in the urban area, industrial area and rural area are shown in Table 4. The ranges of indoor NO_2 concentrations in the urban area, industrial area and rural area were 12.8-32.9 (mean: 21.4±4.6), 11.7-36.6 (mean: 23.8±5.5) and 7.0 - 17.5 μg/m^3 (mean: 12.7±2.0), while the values of outdoor were 13.0-43.7 (mean: 26.8±5.7), 15.5-37.6 (mean: 23.9±4.2) and 10.1-32.6 μg/m^3 (mean: 21.4±2.1), respectively. Further, the indoor NO_2 concentrations in the urban area, industrial area and rural area found in this study were higher than those found inside primary schools in Spain [24]. They reported that the indoor NO_2 concentrations in the urban area, industrial area and rural area ranged between 7.5-23.1, 9.8-15.8 and 1.4-29.3 μg/m^3, while the outdoor NO_2 concentrations were between 1.0-16.8, 3.7 0-9.2 and 1.0-2.2 μg/m^3, respectively. Guerriero *et al.* [25] reported indoor NO_2 concentrations in the suburban area (9.1-22.5 μg/m^3) and in the urban area (25.5-41.2 μg/m^3) of London, UK. It was found that the levels of indoor NO_2 were higher than those in this study. Moreover, the indoor and outdoor NO_2 values in this study were also lower than the levels of indoor (2.9-47.0 μg/m^3) and outdoor (1.7-50.9 μg/m^3) values in six schools in Stockholm, Sweden that were exposed to traffic [26]. Blaszczyk *et al*. [27] investigated the indoor and outdoor NO_2 concentrations of urban and rural kindergartens in Silesia, Poland. They found that the values from the urban area were 6.8-9.8 μg/m^3 (indoor) and 19.0-55.0 μg/m^3 (outdoor), whereas the values in the rural area were 4.2-13.5 μg/m^3 (indoor) and 8.0-17.0 μg/m^3 (outdoor), which were lower values than those in this study. It appears that the wooden materials used to construct primary schools in the rural area of Rayong allowed ventilation and in turn NO_2 contamination inside classrooms [4]. Significantly, the mean values of NO_2 concentrations collected from both indoor and outdoor areas were lower than the National Ambient Air Quality Standard (NAAQS) in the USA per annum, which is 40 μg/m^3[20]. The mean indoor NO_2 concentrations in the urban area, industrial area and rural area from September 2017 to February 2018 were 21.4±4.6, 23.8±5.5 and 12.7±2.0 μg/m^3, while the mean values of outdoor areas were 26.8±5.7, 23.9±4.2 and 21.4±2.1 μg/m^3, respectively.

For our statistical analyses, differences in the means of NO_2 concentrations between indoor and outdoor areas were calculated using paired T-tests. It was found that the concentrations of NO_2 measured indoors were not significantly different from outdoor concentrations in urban and industrial areas ($p>0.05$), whereas the values in the rural area were significantly different ($p<0.05$). However, the outdoor NO_2 concentrations in urban, industrial and rural areas were higher than those in indoor ones. One-Way ANOVA was used to differentiate the average NO_2 concentrations between the different sampling areas for each month. The indoor NO_2 concentrations measured in urban and industrial areas were significantly higher than those in the rural area ($p<0.05$), while the values of urban and industrial areas were not significantly different ($p>0.05$). The outdoor NO_2 concentrations in the urban area were significantly higher than those in the rural area ($p<0.05$). However, the outdoor NO_2 values in the industrial areas and the rural areas were not significantly different.

Table 4. Indoor and outdoor NO_2 concentrations ($\mu g/m^3$) and metrological data from sampling sites between September 2017 - February 2018

Study site			Concentrations of NO_2 ($\mu g/m^3$)					
			Sep. 2017	**Nov. 2017**	**Dec. 2017**	**Jan. 2018**	**Feb. 2018**	**Sep. 2017 -Feb. 2018**
			(n=4)	**(n=3)**	**(n=4)**	**(n=4)**	**(n=4)**	
Indoor	Urban area[A] (N=4)	Max	23.9	33.8	25.6	24.0	16.9	27.4
		Min	21.3	20.7	17.4	15.5	12.6	14.6
		Mean	22.6 [ab]	27.4 [a]	21.7 [ab]	20.8 [ab]	14.6 [b]	21.4
		SD	1.2	5.5	3.4	3.8	1.8	4.6
	Industrial area[A] (N=4)	Max	34.4	38.3	24.0	32.9	20.7	30.6
		Min	18.6	24.7	18.0	18.6	11.8	15.8
		Mean	24.4 [ab]	30.6 [a]	21.8 [ab]	26.3 [a]	15.8 [b]	23.8
		SD	7.4	6.0	2.6	6.4	4.1	5.5
	Rural area[B] (N=4)	Max	14.6	18.5	17.2	18.5	12.9	15.2
		Min	8.4	6.6	7.0	13.3	5.8	10.1
		Mean	11.5[a]	12.8 [a]	14.0 [a]	15.2 [a]	10.1 [a]	12.7
		SD	2.6	5.9	4.8	2.3	3.2	2.0
Outdoor	Urban area[A] (N=4)	Max	35.6	54.0	32.1	42.6	37.2	33.7
		Min	15.2	24.4	13.0	19.3	15.0	21.0
		Mean	23.1 [a]	32.0 [a]	21.0 [a]	33.7 [a]	24.1 [a]	26.8
		SD	8.7	14.7	8.0	10.0	9.4	5.7
	Industrial area[AB] (N=4)	Max	27.7	40.8	25.6	38.4	28.8	30.6
		Min	13.4	25.8	15.3	15.7	13.2	19.8
		Mean	22.1 [a]	30.6 [a]	19.8 [a]	25.3 [a]	21.8 [a]	23.9
		SD	7.0	7.0	4.3	9.7	7.2	4.2
	Rural area[B] (N=4)	Max	27.9	38.2	38.2	32.7	30.3	23.4
		Min	9.7	14.5	12.6	14.8	14.7	18.2
		Mean	18.2 [a]	22.9 [a]	21.0 [a]	23.4 [a]	21.4 [a]	21.4
		SD	8.1	10.7	11.6	9.2	7.0	2.1
Ratio I/O	Urban area		0.98	0.86	1.03	0.62	0.61	0.80
	Industrial area		1.10	1.00	1.10	1.04	0.72	0.99
	Rural area		0.63	0.55	0.66	0.65	0.47	0.59
Total precipitation (mm)* (precipitation date)			276.9 (17)	100.7 (10)	11.6 (3)	1.4 (3)	16.6 (4)	411.4 (37)
Relative humidity (%)*			82.1 ±3.3	80.1 ±11.7	69.3 ±5.1	78.9 ±7.0	78.2 ±5.3	77.6 ±7.4
Wind speed (Knot)*			2.8±1.4	2.3±1.7	2.9±0.8	2.0±0.8	2.4±0.4	2.5±1.0
Ambient temperature (ºC)*			28.2 ±0.7	26.9 ±0.4	25.7 ±1.3	26.6 ±1.4	26.9 ±1.0	26.9 ±1.3

Notes; N = Number of school days
n = Number of weeks
A, B = Range of significant discrepancy ($p < 0.05$) among clusters of sampling areas (vertical direction)
a, b = Range of significant discrepancy ($p < 0.05$) among clusters of sampling months (horizontal direction)
* Thai Meteorological Department, 2017-2018

Table 4 shows that the indoor NO_2 concentrations in urban and industrial areas in November 2017 were significantly different from those in February 2018 ($p<0.05$), whereas the values in the rural area from September 2017 to February 2018 were not significantly different. The outdoor NO_2 concentrations in all areas from September 2017 to February 2018 were not significantly different ($p>0.05$).

The indoor/outdoor (I/O) ratio of NO_2 concentrations is specifically defined to be greater than 1, which shows that the exposure of NO_2 values can be higher indoors when compared to the extended outdoor area. Table 4 presents the I/O ratio means for NO_2 concentrations in the urban area, industrial area and rural area of primary schools in the Rayong province. It was found that the I/O ratios of NO_2 concentrations in descending order were: urban area (0.61-1.03 and mean: 0.80) > industrial area (0.72-1.10 and mean: 0.99) > rural area (0.47-0.66 and mean: 0.59). Guerriero *et al.* [25] reported that the I/O ratios of NO_2 levels in primary schools of London in the urban area were (0.6-0.8; mean 0.7±0.1) and in the sub-urban area were (0.3-0.7, means 0.5±0.2), results that were very similar to the values obtained in this study. Moreover, the I/O ratios of NO_2 concentrations in this study were lower than those in the primary schools of Stockholm, Sweden (0.44-2.17 and mean: 0.96±0.36) [26]. Bruno *et al.* [28] and Poupard *et al.* [29] revealed that the I/O values vary within a narrow range, from 0.88 to 1, as shown by the positive relationship that exists between indoor and outdoor NO_2 concentrations. On the whole, indoor concentrations reflect the outdoor concentrations irrespectively of the level of airtightness of the building.

3.2 Effects of meteorological factors on NO_2 concentrations

The climate in Thailand is under the influence of monsoon winds of seasonal character, such as the southwest monsoon (SW) and the northeast monsoon (NW). When the SW monsoon prevails over Thailand, the rainy season occurs, and abundant rain falls over the country. This happens from mid-May to mid-October. Winter, which starts in mid-October and ends in mid-February, is influenced by the NE monsoon. The NE monsoon brings cold and dry air from the anticyclone in mainland China over the Northern and Northeastern parts of Thailand [30]. Figure 3 presents the different wind directions and levels of wind speed in the Rayong province during the sampling periods. The major SW-NE wind direction dominated throughout September 2017 and January to February 2018, whereas in November and December 2017 the N-S (north to south) wind prevailed. The wind speed range from September to December 2017 was 2-10 knots whereas it was about 2-9.9 knots in January and February 2018. The calmness index was averaging a level nearing 50% and above. Overall wind speed was poor.

Pearson's correlations of NO_2 concentrations and meteorological factors including total precipitation (total-P), relative humidity (RH), wind speed (WS) and ambient temperature (Temp.) are shown in Table 5. The results suggested significantly strong correlations between indoor and outdoor NO_2 concentrations as r = 0.526 ($P<0.001$). These results were similar to those of Bozkurt *et al.* [31] and Blaszczyk *et al.* [27], who studied the correlation values of NO_2 in schools in industrial cities in Turkey (r = 0.9-1.0) and rural kindergartens in Silesia, Poland (r = 0.430) observed. Moreover, the positive correlations of relative humidity with total precipitation and ambient temperature were significant (r = 0.512 and 0.654), while wind speed levels and relative humidity were negatively correlated with any level of significance (r = -0.576). On the other hand, the indoor NO_2 concentrations were weak and hence negatively related to wind speed and ambient temperature. The relationships between outdoor NO_2 concentrations and wind speed or ambient temperature were weak, and hence negative. Nevertheless, previously published studies demonstrated that NO_2 concentrations were negatively related to rainfall, temperature and wind speed (r = -0.929, -0.819 and -0.950, respectively) with any level of significance [32]. Ahmad and Aziz [33] revealed that outdoor NO_2 concentrations were significantly related to temperature

($r = -0.839$) and rainfall ($r = -0.928$). In general, increasing levels of wind speed facilitate the dilution of air pollutants at the ground level and a reaction of the indoor level as well. Decreasing atmospheric temperature supports low mixing height, which prevents the dispersion of pollutants. Consequently, indoor values were found to rise to such a high level. The increase in total precipitation is linked to relative humidity, as rain cleanses and eliminates pollutants from the atmosphere [34]. Moreover, low wind speed together with calm conditions constitute important factors that condition the accumulation of air pollutants [35]. It seems that meteorological factors might not have affected NO_2 concentrations since the correlation of NO_2 concentrations with different meteorological factors did not identify any significant relationships. Importantly, however, the obtained results indicated that indoor NO_2 concentrations and outdoor NO_2 ones are primarily dependent upon the level of local activity i.e. traffic intensity and industrial plant operations. According to Wichman *et al.* [26], the main source (64-71%) of indoor NO_2 at schools and pre-schools was outdoor NO_2 that had infiltrated indoors.

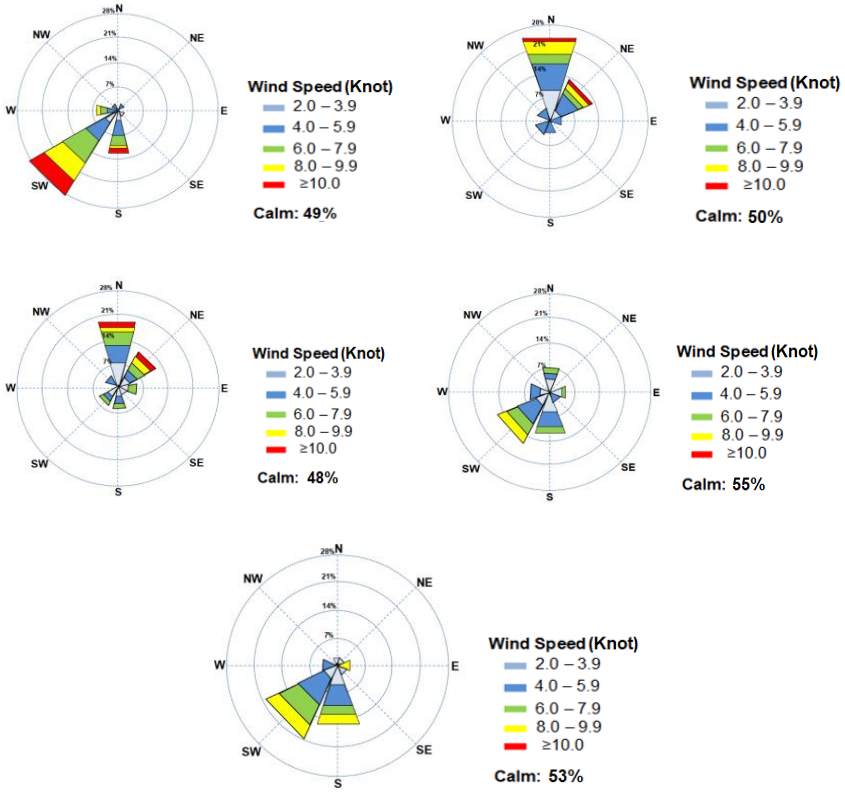

Figure 3. Wind Speed in Rayong province during sampling in each month: A. September 2017, B. November 2017, C. December 2017, D. January 2018 and E. February 2018

Table 5. Pearson correlations of meteorological factors and NO_2 concentrations in primary schools

N = 57	Indoor NO_2	Outdoor NO_2	Total-P	RH	WS	Temp.
Indoor NO_2	1.000					
Outdoor NO_2	**0.526****	1.000				
Total-P	0.241	-0.021	1.000			
RH	0.062	-0.004	**0.512****	1.000		
WS	-0.132	-0.165	0.002	**-0.576****	1.000	
Temp.	-0.190	-0.291*	**0.392****	**0.654****	-0.048	1.000

*Correlation is significant at the 0.05 level (2- tailed)
**Correlation is significant at the 0.01 level (2- tailed)

3.3 Human health risk of indoor NO_2 concentration

The hazard quotient (HQ) is used for the estimation of non-carcinogenic risks to human health that derive from NO_2. The HQ of NO_2 is calculated by equations 1 and 2. Students spend most of their time indoors, in the classroom. They are more exposed to pollutants when they are inside than when they are outside in playgrounds. Therefore, human health risk was assessed according to the level of inhalation of NO_2 in indoor environments only. Table 6 presents the HQ of short-term (1- 8 hours) and long-term (annual mean) non-carcinogenic health risks for indoor NO_2 exposure in urban, industrial and rural areas. The results for all HQ values deriving from exposure to indoor NO_2 over a period of 5 months via the inhalation pathway were less than 1.0, which indicates the existence of a low hazard. In the same way, Olufemi *et al.* [18] studied HQ values pertaining to exposure to NO_2 indoors among students in schools located within the vicinities of coal mines in Emalahleni, South Africa. They found that HQ values deriving from exposure to NO_2 were less than 1.0. The HQ values per annum in relation to children and adults in the industrial area of Rayong city were higher than those for individuals in urban and rural areas of Rayong city. However, many health risk studies have established that exposure to low concentrations of NO_2 may increase the risks of pneumonia, hospitalization, asthma problems, respiratory problems and decreased lung function in children [6, 14, 36, 37]. Zhang *et al.* [38] revealed that an increase of 10 $\mu g/m^3$ in NO_2 concentration contributed towards an increase of 2.0 % in associated chronic obstructive pulmonary disease (COPD) in adults, an increase of 1.3 % in hospital admissions and an increase of 2.6 % in mortality.

Table 6. ADD and HQ values for indoor NO_2 at primary schools in each area of Rayong city

Sampling site	ADD (µg/Kg)		HQ					
			Child			Adult		
	Child	Adult	1 h	8 h	Annual	1 h	8 h	Annual
Urban area	7.5±1.6	6.1±1.3	0.04	0.05	0.19	0.03	0.04	0.15
Industrial area	8.4±1.9	6.8±1.6	0.04	0.06	0.21	0.03	0.04	0.17
Rural area	4.5±0.7	3.6±0.6	0.02	0.03	0.11	0.02	0.02	0.09

4. Conclusions

The concentrations of indoor NO_2 in primary schools at Rayong city were found to be directly associated with outdoor pollution caused by road traffic intensity. It was clearly seen that the values of NO_2 in urban and industrial areas were significantly higher than those in the rural area. Moreover, a positive correlation for NO_2 concentrations between indoor and outdoor premises in primary schools was identified within the relevant range of significance. Meteorological factors might not have affected indoor NO_2 concentrations. The obtained results indicate that indoor NO_2 concentrations levels are much more dependent upon local activities such as traffic intensity than upon meteorological factors. Students sitting in classrooms in proximity to zones of high traffic intensity may be exposed to NO_2. However, the HQ values in relation to a non-carcinogenic risk to human health deriving from NO_2 exposure have indicated the existence of a low hazard.

5. Acknowledgements

Financial supports from King Mongkut's University of Technology North Bangkok (Contract no. KMUTNB-61-NEW-019) are gratefully acknowledged. The authors are grateful to the Thai Meteorological Department for Meteorological data in the Rayong province, Thailand.

References

[1] Pegas, P.N., Nunes, T., Alves, C.A., Silva, J.R., Vieira, S.L.A., Caseiro, A. and Pio, C.A., 2012. Indoor and outdoor characterization of organic and inorganic compounds in city centre and suburban elementary schools of Aveiro, Portugal. *Atmospheric Environment*, 55, 80-89.

[2] Ferreira, A.M.C. and Cardoso, S.M., 2013. Exploratory study of air quality in elementary schools, Coimbra, Portugal. *Revista de Saúde Pública*, 47(6), 1059-1068.

[3] Norbäck, D., Hashim, J.H., Hashim, Z. and Ali F., 2017. Volatile organic compounds (VOC), formadehyde and nitrogen dioxide (NO_2) in schools in Johor Bahru, Malaysia: Associations with rhinitis, ocular, throat and dermal symptoms, headache and fatigue. *Science of the Total Environment*, 592, 153-160.

[4] Freitas, Md.C., Canha, N., Martinho, M., Almeida-Silva, M., Almeida, S.M., Pegas, P., Alves, C., Trancoso, M., Sousa, R., Mouro, F. and Contreiras, T. 2011. IndoorAir Quality in Primary Schools. In Moldoveanu, A.M., ed. *Advanced Topics in Environmental Health and Air Pollution Case Studies;* 1st ed. Rijeka, Croatia: InTech, pp. 361-384.

[5] Gül, H., Gaga, E.O., Döğeroğlu, T., Özden, Ö., Ayvaz, Ö., Özel, S. and Güngör, G., 2011. Respiratory health symptoms among students exposed to different levels of air pollution in a Turkish city. *International Journal of Environmental Research and Public Health*, 8, 1110-1125.

[6] Cibella, F., Cuttitta, G., Maggiore, R.D., Ruggieri, S., Panunzi, S., Gaetana, A.D., Bucchieri, S., Drago, G., Melis, M.R., Grutta, S.L. and Viegi, G., 2015. Effect of indoor nitrogen dioxide on lung function in urban environment. *Environmental Research*, 138, 8-16.

[7] Boulter, P.G., Barlow, T.J. and McCrae, I.S., 2009. *Emissions factors 2009: Report 3 - Exhaust Emissions Factors for Road Vehicles in the United Kingdom*. Published Project Report PPR 356. TRL Limited, 200 pages.

[8] Rivas, I., Querol, X., Wright, J. and Sunyer, J., 2018. How to protect school children from the neurodevelopmental harms of air pollution by interventions in the school environment in the urban context. *Environment International*, 121, 199-206.

[9] Faustman, E.M., Silbernagel, S.M., Fenske, R.A., Burbacher, T.M. and Ponce, R.A., 2000. Mechanisms underlying children's susceptibility to environmental toxicants. *Environmental Health Perspectives*, 108(1), 13-21.
[10] Mendell, J.M. and Health, G.A., 2005. Do indoor pollutants and thermal condotions in schools influence student performance? A critical review of the literature. *Indoor Air*, 15, 27-52.
[11] Shima, M. and Adachi, M., 2000. Effect of outdoor and indoor nitrogen dioxide on respiratory symptoms in schoolchildren. *International Journal of Epidemiology*, 29(5), 862-870.
[12] Ayuni, N.A. and Juliana, J., 2014. Exposure to PM_{10} and NO_2 and association with respiratory health among primary school children living near petrochemical industry area at Kertih, Terengganu. *Journal of Medical Biological Engineering*, 3(4), 282-287.
[13] Gaffin, J.M., Hauptman, M., Petty, C.R., Sheehan, W.J., Lai, P.S., Wolfson, J.M., Gold, D.R. and Coull, B.A., 2018. Nitrogen dioxide exposure in school classrooms of inner-city children with asthma. *Journal of Allergy and Clinical Immunology*, 141(6), 2249-2255.
[14] Nhung, N.T.T., Schindler, C., Dien, T.M., Probst-Hensch, N., Perez, L. and Künzli, N., 2018. Acute effects of ambient air pollution on lower respiratory infections in Hanoi children: An eight-year time series study. *Environment International*, 110, 139-148.
[15] Bootdee, S., Chalemrom, P. and Chantara, S., 2012. Validation and field application of tailor-made nitrogen dioxide passive sampler. *International Journal of Environmental Science and Technology*, 9(3), 519-526.
[16] Thabethe, N.D.L., Engelbrecht, J.C., Wright, C.Y. and Oosthuizen, M.A., 2014. Human health risks posed by exposure to PM10 for four life stages in a low socio-economic community in South Africa. *The Pan African Medical Journal*, 18(206), 1-12.
[17] Morakinyo, O.M., Adebowals, A.S., Mokgobu, M.I. and Mukhola, M.S., 2017. Health risk of inhalation exposure to sub-10 µm particulate matter and gaseous pollutants in an urban-industrial area in South Africa: an ecological study. *British Medical Journal*, 7, 1-9.
[18] Olufemi, A.C., Mji, A. and Mukhola, M.S., 2018. Health risks of exposure to air pollutants among students in schools in the vicinities of coal mines. *Energy Exploration & Exploitation*, 0(0), 1-19. https ://doi.org/10.1177/0144598718765489
[19] US-EPA, 2011. *Exposure Factors Handbook: 2011 Edition.* U.S. Environmental Protection Agency, Washington DC. [Online] Available at: https: / / cfpub. epa. gov/ ncea/ risk/ recordisplay. cfm? deid=236252
[20] United State Environmental Protection Agency (US-EPA), 2017. *National Ambient Air Quality Standards* (*NAAQS*) table. [Online] Available at: https://www.epa.gov/criteria-air-pollutants/naaqs-table#2.
[21] World Health Organization (WHO), 2010. WHO guidelines for indoor air quality: selected pollutants. [Online] Available at: http://www.euro.who.int/en/health-topics/environment-and-health/air-quality/policy/who-guidelines-for-indoor-air-quality.
[22] Bureau of Environmental Health, Department of Health, 2016. Indoor air quality sampling. [Online] Available at: http://env.anamai.moph.go.th/ewt_dl_link.php?nid=824
[23] Environmental Protection Department, 2003. *The Government of the Hong Kong Special Administrative Region. A guide on indoor air quality certification scheme for offices and public places*. [Online] Available at: http://www.iaq.gov.hk/en/publications-and-references/guidance-notes.aspx.
[24] Villanueva, F., Tapia, A., Lara, S. and Amo-Salas, M., 2018. Indoor and outdoor air concentrations of volatile organic compounds and NO_2 in schools of urban, industrial and rural areas in Central-Southern Spain. *Science of the Total Environment*, 622-623, 222-235.
[25] Guerriero, C., Chatzidiakou, L., Cairns, J. and Mumovic, D., 2016. The economic benefits of reducing the levels of nitrogen dioxide (NO_2) near primary schools: The case of London. *Journal Environmental Management*, 181, 615-622.

[26] Wichmann, J., Lind, T., Nilsson, M.A.-M. and Bellandder, T., 2010. $PM_{2.5}$, soot and NO_2 indoor- outdoor relationships at homes, pre- schools and schools in Stockholm, Sweden. *Atmospheric Environment*, 44, 4536-4544.

[27] Blaszczyk, E., Rogula-Kozlowska, W., Klejnowski, K., Kubiesa, P., Fulara, I. and Mielżyñska-Švach, D., 2017. Indoor air quality in urban and rural kindergartens: short-term studies in Silesia, Poland. *Air Quality Atmosphere and Health*, 10, 1207-1220.

[28] Bruno, P., Caputi, M., Caselli, M., de Gennaro, G. and de Rienzo, M., 2005. Reliability of a BTEX radial diffusive sampler for thermal desorption: field measurements. *Atmospheric Environment*, 39, 1347-1355.

[29] Poupard, O., Blondeau, P., Iordache, V. and Allard, F., 2005. Statisical analysis of parameters influrencing the relationship between outdoor and indoor air quality in schools. *Atmospheric Environment*, 39, 2071-2080.

[30] Thai Meteorological Department, 2015. The climate of Thailand. [Online]. Available at: https://www.tmd.go.th/en/archive/thailand_climate.pdf.

[31] Bozkurt, Z., Doğan, G., Arslanbaş, D., Pekey, B., Pekey, H., Dumanoğlu, Y., Bayram, A. and Tuncel, G., 2015. Determination of the personal, indoor and outdoor expoure levels of inorgaic gaseous pollutants in different microenvironments in an industrial city. *Environmental Monitoring and Assessment*, 187 (590), 1-17.

[32] Ahmad, S.S., Biiker, P., Emberson, L. and Shabbir, R., 2011. Monitoring nitrogen dioxide levels in urban areas in Rawalpindi, Pakistan. *Water, Air and Soil Pollution*, 220, 141-150.

[33] Ahmad, S.S. and Aziz, N., 2013. Spatial and temporal analysis of ground levels ozone and nitrogen dioxide concentration across the twin cities of Pakistan. *Environmental Monitoring and Assessment*, 185, 3133-3147.

[34] Chithra, V.S. and Shiva Nagendra, S.M., 2014. Impact of outdoor meteorology on indoor PM10, PM2.5, and PM1 concentrations in a naturally ventilated classroom. *Urban Climate*, 10, 77-91.

[35] Ratto, G. and Nico, A., 2012. Preliminary wind analysis regarding different speed ranges in the city of La Plata, Argentina. *Revista Brasileira de Meteorologia*, 27(3), 281-290.

[36] He, B., Huang, J.V., Kwork, M.K., Yeung, S.L.A., Hui, L.L., Li, A.M., Leung, G.M. and Schooling, C.M., 2019. The association of early-life exposure to air pollution with lung function at ~17.5 years in the "Children of 1997" Hong Kong Chinese Birth Cohort. *Environment International*, 123, 444-450.

[37] Mudway, I.S., Dundas, I., Wood, H.E., Marlin, N., Jamaludin, J.B., Bremner, S.A., Cross, L., Grieve, A., Nanzer, A., Barratt, B.M., Beevers, S., Dajnak, D., Fuller, G.W., Font, A., Colligan, G., Sheikh, A., Walton, R., Grigg, J., Kelly, F.J., Lee, T.H. and Griffiths, C.J., 2019. Impact of London's low emission zone on air quality and children's respiratory health: a sequential annual cross-sectional study. *Lence*, 4, 28-40.

[38] Zhang, Z., Wang, J. and Lu, W., 2018. Exposure to nitrogen dioxide and chronic obstructive pulmonary disease (COPD) in adults: a systematic review and meta-analysis. *Environmental Science and Pollution Research*, 25, 15133-15145.

Iron-modified Biochar Derived from Rice Straw for Aqueous Phosphate Removal

Usarat Thawornchaisit*, Korawan Donnok, Natchaphat Samphoanoi and Pimwimon Pholsil

Department of Chemistry, Faculty of Science
King Mongkut's Institute of Technology Ladkrabang, Bangkok, Thailand

Received: 17 May 2019, Revised: 19 July 2019, Accepted: 7 August 2019

Abstract

Conversion of rice straw to biochar, followed by chemical modification of the biochar with iron salts under alkaline conditions can turn agricultural biomass waste into a useful adsorbent material for phosphorus removal. Study of the rice straw-to-biochar conversion process at various pyrolysis temperatures showed that biochar yield decreased with increased pyrolysis temperature: The yield of stable organic matter and specific surface area was found to be optimum at 400°C. An Fe coating process, through direct precipitation of $FeCl_3.6H_2O$ or co-precipitation of $FeCl_3.6H_2O$ and $FeSO_4.7H_2O$ on biochar, led to Fe-modified rice straw biochars. Based on physical appearance, SEM, FT-IR and XRF, we confirmed that Fe was well retained in the biochar. The pH_{pzc} was approximately 7.6 and 8.0 for Fe(III)+Fe(II)-modified biochar and Fe(III) modified biochar. Therefore, the modified biochar could attract negatively charged phosphate species in a system, like natural water or domestic wastewater, where pH is normally less than their pH_{pzc}. In laboratory batch adsorption tests, phosphate removal efficiency was enhanced, rising from about 35.4% in the unmodified biochar to 69.5% in Fe(III)+Fe(II)-modified biochar and 83.0% in Fe(III) modified biochar.

Keywords: biochar modification, phosphorus removal, pyrolysis
DOI 10.14456/cast.2019.22

1. Introduction

Phosphorus is an essential nutrient, which is vital for the growth of aquatic plants. However, phosphorus becomes a pollutant, when it is present in excessive amounts in aquatic environments. Excess phosphorus from runoff into water bodies, such as lakes, creeks and rivers, can cause eutrophication an environmental problem caused by excessive growth of algae and other aquatic plants. This phenomenon often leads to deterioration in the aquatic ecosystem quality, for example, development of anoxic conditions and decreased biodiversity [1, 2]. Discharge of municipal wastewaters is one of the main causes of eutrophication, since the wastewaters are rich in

*Corresponding author: E-mail: usarat.th@kmitl.ac.th

phosphorus [1]. Therefore, wastewater treatment is important in order to reduce phosphorus levels from the effluent, limit phosphorus load in receiving water bodies, and subsequently protect public health.

Phosphorus in water occurs in both dissolved and particulate forms. However, most of the phosphorus discharged by wastewater treatment facility plants (WWTPs) is in the dissolved form and is mainly orthophosphate [3]. Previously, phosphorus removal, rather than recovery, emerged with the primary attention given to lowering phosphorus levels in effluents for safe discharge into surface waters [4], which, in turn, would inhibit undesirable algal growth in sensitive surface waters [3, 5]. Thus, technologies for phosphorus pollution control tended to be more focused and oriented towards phosphorus removal, whereas technologies that focus on recovery have received less attention [4]. In 2015, a report on "World Fertilizer Trend and Outlook to 2018", published by the United Nations Food and Agriculture Organization, showed an increasing world phosphate fertilizer demand between 2014 and 2018, with 58 % of the increase expected to be in Asia. Today, the primary source of phosphorus in fertilizers is natural minerals, for example, mined phosphate rock [4]. Unfortunately, phosphate rock is a finite, nonrenewable resource [4] and is listed as one of the critical raw materials for the European Union in their 2017 final report - "Study on the review of the list of critical raw materials: Criticality Assessment" [6]. The growing concern about phosphorus future availability and its detrimental environmental impact have driven phosphorus recovery to become crucial. Thus, research on the treatment of phosphorus-containing wastewater is currently focused more on development of technology that can recover phosphorus from the secondary source (like domestic and industrial wastewater) and reuse the recovered P products for agricultural and industrial purposes [7].

Biochar, the carbon-rich residues from pyrolysis or incomplete combustion of biomass, has increasingly been recognized as an efficient and cost-effective sorbent for removal of aqueous organic and inorganic contaminants, such as textile dyes, phenolics, pesticides, polycyclic aromatic hydrocarbons, heavy metals, and metalloids [8-10]. For example, straw derived biochar can effectively remove malachite green, which resists aerobic digestion, due to its reported toxic effects [11]. With acid pretreatment, straw-based biochar was also used as a substitute for activated carbon to remove reactive brilliant blue and rhodamine B [12]. Biochar was recognized as an effective sorbent for heavy metals especially the cationic forms due to the presence of oxygen-containing carboxyl, hydroxyl, and phenolic surface functional groups and high-porous structure [10, 13]. As the surfaces of biochar is predominantly negatively charged, the sorption of anionic forms of pollutants such as arsenates, nitrates or phosphates is relatively low [14, 15]. Therefore, a modification of the biochar structure and surface properties is needed to enhance the affinity for anionic contaminants and, consequently, its environmental benefits [14, 16]. Significantly, the study of the use of biochar to remove phosphates from water has been limited, compared to the study of remediation of other common water pollutants [17], thus we need to fill in the information gap in the research on practical applications of biochar and well-engineered biochar that has been modified for phosphate removal from water.

Rice straw (*Oryza sativa*), left over from rice harvesting, is one of the most abundant lignocellulosic waste materials world-wide [11]. From 0.7 to 1.4 kg of rice straw is produced for each kilogram of milled rice, depending on variety, stubble cutting-height and moisture content during harvest [18]. FAO estimated that about 770 million tonnes of rice was produced in 2018 [19]. Thus, rice straw became available in similar quantities and, consequently, methods for rice straw use and disposal are needed. In Thailand, rice straw was one of the top three unused lignocellulosic agricultural by-products in 2013 [20]. Direct open burning in fields is a common option for disposal, but this causes serious air pollution. Farmers often offer rice straw as a feed for ruminants, but untreated rice straw is not an ideal feed due to the low nutritive value of the highly lignified materials. Hence, effective rice straw consumption strategies that are economically feasible are

badly needed. Here, we show that rice straw can produce biochar that is able to adsorb phosphate from aqueous solutions. This adds value to this agricultural by-product and provides a potential adsorbent for nutrient removal. Further, the spent adsorbent is nutrient-enriched biochar, which can subsequently be applied as fertilizer. We selected an iron modified method to improve the phosphate adsorption, since the method is simpler and more efficient than other treatments such as activation by sulfuric acid and lanthanum [21]. In conclusion, we confirmed the feasibility of using rice straw-derived biochar for aqueous phosphate removal and showed that phosphorus removal capacity can be enhanced by adding iron as the char is produced.

2. Materials and Methods

2.1 Preparation of adsorbent

2.1.1 Biochar production with different pyrolysis temperatures

Rice straw was obtained from a paddy field in Chachoengsao Province (13.69028N, 101.07028E). Prior to pyrolysis, the rice straw was chopped into ~20-30 mm lengths and ground to pass through a 70-mesh (210 μm) sieve. The straw was oven dried at 103-105°C until it reached constant weight. The dried straw was put into a 100 ml ceramic crucible, covered with a lid, and pyrolyzed under limited oxygen conditions in a muffle furnace (Thermolyne Furnace 6000) at 300, 400, 500 and 600°C for 4 h. Once cooled to room temperature, the biochar was stored in sealed sample bags.

2.1.2 Synthesis of Fe-modified biochar

The selected biochar was modified with iron following the method described by Yang *et al.* [21]. Fe(III)-modified biochar was prepared by adding 1 g biochar into 30 ml aqueous solution containing 2.18g $FeCl_3.6H_2O$. The suspension of biochar and Fe solution was stirred vigorously at 150 rpm for 30 min, and this was followed by a dropwise addition of 1 M NaOH solution until the pH reached ~11. The suspension was continuously stirred for 45 min and aged overnight without further stirring. The separated modified biochar samples were washed several times with deionized water and dried at 105°C until they reached constant weight. The preparation of biochar doped with co-precipitation of Fe^{2+}/Fe^{3+} was similar, except that the solution contained 1.17 g $FeSO_4.7H_2O$ and 1.09 g $FeCl_3.6H_2O$.

2.2 Characterization of biochar

For unmodified or virgin rice straw-derived biochar, yield (%) was determined by comparing the weight of the biochar to the weight on a dry basis of the ground rice straw used for pyrolysis. Oxidizable organic carbon content (OC) was determined by the wet oxidation method with potassium dichromate [22]. Loss on Ignition (LOI), Stable Organic Matter (SOM) and Stable Organic Matter Yield Index (SOMYI) were determined and calculated following the methods of Halshejani *et al.* [23]. Specific surface area (SSA) was measured by methylene blue adsorption and calculated following Kaewprasit *et al.* [24]. For unmodified and Fe-modified biochars, the morphological properties of the biochars were determined by scanning electron microscopy (SEM, JEOL, JSM-6355FE). The functional groups on the biochar surface were determined from a Fourier transform infrared spectrum (FTIR, Shimadzu, IRTracer-100) in the 400-4000 cm^{-1} range. The iron contents of modified biochars was examined using X-ray Fluorescence Spectrometry (XRF, Bruker Optic, SRS3400). The pH at point of zero point charge (pH_{pzc}) of the Fe-modified biochars was

measured by adjusting the pH of 50 mL 0.01 mol/l NaCl solution to a value between 3 and 11, and noting the initital pH value (pH_i). Then, 0.15 g of the Fe-modified biochars was added to a conical flask and the flask was shaken in an incubator shaker at 120 rpm for 24 hours. The final pH (pH_f) of the solutions separated by centrifugation was measured, and the pH_{pzc} was found at the point where pH_f - pH_i = 0 from a plot of ΔpH vs pH_i.

2.3 Phosphate removal tests

The phosphorus removal capacity of rice straw-derived biochar and Fe-modified biochars was measured by mixing various amounts of the biochars with 50 mL of 2.5 mg P l^{-1} solution in 125 ml Erlenmeyer flasks at room-temperature. The flasks were then shaken in a mechanical shaker at a constant speed of 150 rpm. At selected time intervals, the flasks were withdrawn and the suspensions were immediately filtered through a 0.45 μm filter. The concentration of remaining phosphorus in the filtrate was determined by the ascorbic acid method [25]. The phosphate removal from aqueous solution (%R) was calculated from:

$$\%R = \frac{(C_o - C_e)}{C_o} \times 100 \quad (1)$$

where C_0 (mg/l) was the initial and C_e (mg/l) was the residual concentration of phosphorus in solution.

3. Results and Discussion

3.1 Rice straw-derived biochar physicochemical properties

Previous research indicated that pyrolysis temperature significantly influences the carbon content of biochar and its surface properties (pore structure, surface area, and capability), which in turn play an important role in the physical or chemical attachment of mineral ions to the biochar structures. Therefore, a pyrolysis temperature that provided a high surface area and yielded stable organic matter (SOM) content of the biochar was determined first. The properties of the biochars produced at different pyrolysis temperatures are shown in Table 1.

From Table 1, the biochar yield decreased with an increase in temperature during slow pyrolysis. Similar trends were also observed by Jiang *et al.* [26] and Wang *et al.* [27], where a decrease in biochar yield was observed with increased pyrolysis temperature between 200ºC and 700ºC. The observed behavior is due to the increase in the rate of dehydration and, in particular, a significant loss of volatile organic matter at higher pyrolysis temperatures, as shown by the decrease of loss on ignition (LOI) of the biochar. In addition, when the temperature during pyrolysis is higher, the oxidizable organic carbon (OC) of the biochar is lower. This reflects an increase in ash content in the biochar at high pyrolysis temperatures, which is consistent with the findings of Halshejani *et al.* [23] and Masto *et al.* [28]. Since the biochar will be exposed to either physical or chemical processes during iron modification, in order to enhance its adsorption capacity for contaminant removal from water and wastewater, the stability of the biochar is critical [16, 29]. The stable organic matter contents (SOM) and the stable organic matter yield index (SOMYI) reflect this characteristic as the importance of both characteristics to the biochar adsorption capacity was stated by Halshejani *et al.* [23] and Masto *et al.* [28]. The SOM of the biochar increased with temperature up to 400ºC, but further increase in temperature yielded lower SOM in the biochar (Table 1). The SOMYI also showed a similar pattern suggesting that biochar produced at 400ºC should be selected

for further study. In addition, pyrolysis temperature affected the biochar surface area, which increased from 66.4 m^2/g to 75.9 m^2/g when pyrolysis temperature was increased from 300°C to 400°C. Maximum specific surface area of rice straw-derived biochar, determined by methylene blue adsorption [24], occurred at 400°C (Table 1). Increase in pyrolysis temperature can cause pore blocking substances to be driven out or thermally cracked, leading to a significant increase in the externally accessible surface area [30]. However, the specific surface area decreased at temperatures above 400°C (Table 1). Previous studies have also reported this and it is attributed to structural ordering and micropore coalescence, resulting in a thermal deactivation of the biochar [31-33]. Since maximum SOMYI and SSA occurred at 400°C, biochar produced at this temperature (BC400) was selected for different levels of iron modification.

Table 1. Properties of rice straw-derived biochar at different pyrolysis temperatures

	Pyrolysis temperature (°C)			
Parameter	**300**	**400**	**500**	**600**
Yield (%)	27.0	22.7	18.6	14.8
Loss on Ignition (LOI, %)	64.6	58.4	47.2	33.6
Oxidizable organic carbon (%)	36.8	19.6	18.0	12.4
Stable Organic Matters (SOM, %)	1.20	24.6	16.2	12.2
Stable Organic Matter Yield Index (SOMYI)	0.3	5.6	3.0	1.8
Specific surface area (m^2/g)[a]	66.4	75.9	48.6	14.9

[a]Calculation method followed Kaewprasit *et al.*[24]

3.2 Fe-modified biochar physicochemical properties

3.2.1 Physical appearance

The ground rice straw samples had a golden brown color (Figure 1a). After pyrolyzing at 400°C for 4 hours, the samples were converted to the blackened biochar (Figure 1b). Small amounts of gray dust were also observed in the biochar, suggesting the presence of some ash. Fe-modified biochars had colors in the red to dark brown range (Figure 1c and 1d), which differed from the biochar without added Fe. The color confirmed that iron was well loaded into the biochar.

Figure 1. Appearance of original input (a) and biochars after pyrolysis (b-d)

3.2.2 Surface structure by SEM

Figure 2 shows SEM images of iron modified biochars compared to the unmodified biochar. The surface of the virgin biochar was smooth, while the surfaces of Fe(III)-modified biochar and Fe(III)+Fe(II) modified biochar were rough, cracked into fragments and had some small particles on their surface.

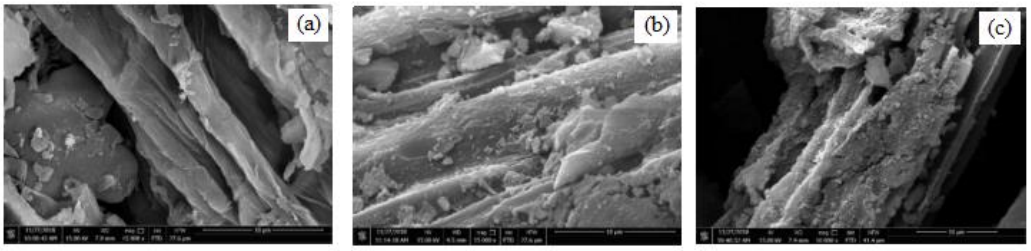

Figure 2. Scanning Electron Micrographs (SEM) of (a) BC400, (b) Fe(III)-modified biochar and (c) Fe(III)+Fe(II)-modified biochar

3.2.3 Functional groups by FT-IR

The FT-IR spectra of the biochar prepared from pyrolyzing rice straw at 400°C and the Fe-modified biochars were captured to determine the various functional groups in the biochars. The presence of several peaks common to all biochars was observed in the spectra of all three samples (Figure 3). The broad peak at ~3420 cm^{-1} and the peak near 1384 cm^{-1} were attributed to -OH stretching vibrations [21, 34]. The peak at ~2920 cm^{-1} corresponded to the aliphatic C-H stretching vibration, while peaks at ~1615 cm^{-1} were assigned to C = O or C = C stretching in aromatic groups [35]. The wide peak at 3420 cm^{-1} in both types of Fe-modified biochars compared with the unmodified biochar is attributed to the use of $FeCl_3$ in the co-precipitation stage, which led to the partial coating of the biochar surface with ferric oxyhydroxide (FeOOH) - also observed by Kulaksiz *et al.* [36]. The intense band at ~1100 cm^{-1} in the unmodified biochar (Figure 3a), which is attributed to C-O vibration [34], was shifted to ~1000 cm^{-1} in the Fe-modified biochars, suggesting that chemical interaction occurred on the modified biochar surface. Yang *et al.* [21] suggested that the band at 1067 cm^{-1} represented Fe-OH, indicating the immobilization of iron on the biochar.

3.2.4 Elemental composition by XRF

XRF analyses were carried out to determine the elemental composition of biochars before and after Fe modification, with results shown in Table 2. The concentration of some minerals, including Si, Ca, Mg and Mn, decreased in the Fe modified biochars compared to those found in unmodified biochar (BC400). These observations were attributed to the dissolution of these minerals under alkaline conditions [37], which could have had a significant impact on the textural properties of biochar, and subsequently on the success on biochar modification process. This assumption was further confirmed by the observed increase in concentration of Fe_2O_3 in both Fe(III)+Fe(II) modified biochar and Fe(III) modified biochar.

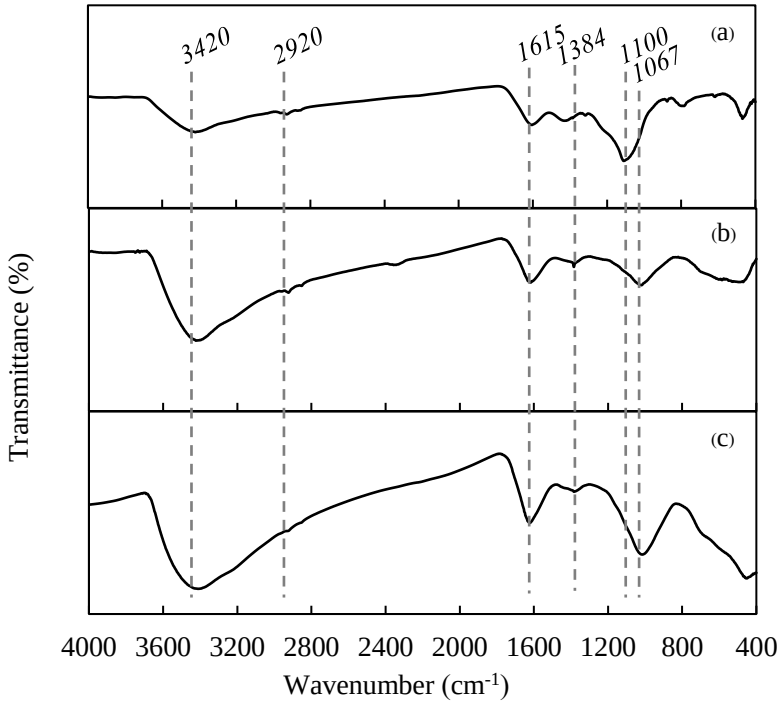

Figure 3. FTIR spectra of (a) BC400, (b) Fe(III) modified biochar and (c) Fe(III)+Fe(II) modified biochar

Table 2. XRF analysis of biochar and Fe-modified biochars

Formula	**BC400**	**Modified biochar**	
		Fe(III)	**Fe(III)/Fe(II)**
CaO	6.58	3.55	3.07
CuO	0.29	0.30	0.28
Cl	11.2	0.53	0.42
Fe_2O_3	0.79	73.0	66.9
K_2O	20.2	n.d.	n.d.
MgO	4.91	1.94	1.98
MnO	0.37	n.d.	n.d.
Na_2O	1.37	1.63	2.22
P_2O_5	2.15	0.43	0.82
SiO_2	49.2	17.0	22.6
SO_3	5.31	0.54	1.11

3.2.5 Point of zero charge (pH_{pzc})

The pH_{pzc} of Fe modified biochars was determined in order to demonstrate the tolerance of the adsorbent towards variation in solution pH [35]. From Figure 4, the pH_{pzc} of Fe(III) modified biochar was approximately 8.0, while the pH_{pzc} of Fe(III)+Fe(II) modified biochar was about 7.6, implying that the Fe-modified biochars would be positively charged when they were applied to treat phosphates in natural water or domestic wastewater (where $pH<pH_{pzc}$), and could effectively remove and recover phosphate owing to the strong electrostatic attraction.

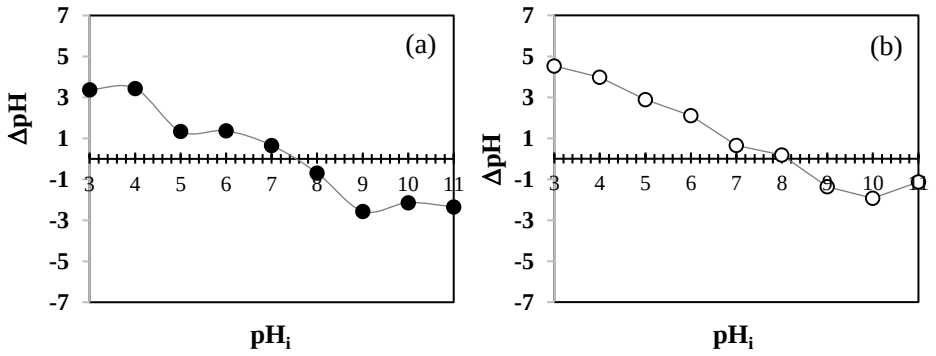

Figure 4. Plots of ΔpH versus initial pH for determination of pH_{pzc} of (a) Fe(III)+Fe(II) modified biochar, and (b) Fe(III) modified biochar

3.3 Phosphate removal

3.3.1 Effect of contact time

Figure 5 shows the phosphorus removal efficiency of unmodified biochar (BC400) and the Fe-modified biochars. It can be seen that phosphate removal efficiency of Fe-modified biochars was higher than BC400. In a 1 h contact time, Fe(III)-modified biochar and Fe(III)+Fe(II)-modified biochar removed more than 50% of phosphorus, suggesting that the adsorption capacity of Fe-modified biochars, for removing phosphate, was rapid in the beginning stages of contact. An increase in phosphorus removal occurred in both types of modified biochar as contact time was extended to 24 h. Phosphate removal efficiencies after 24 hours contact time were 70% for Fe(III)+Fe(II)-modified and 83% for Fe(III)-modified biochar. In the same time, the unmodified biochar (BC400) removed only ~35% of phosphorus. Previous studies reported that the biochar produced from sesame straw exhibits positive phosphate adsorption when pyrolysed at 500 and 700°C [38]. This phenomenon was attributed to the presence of Ca and Mg in the biochar, which chemically react with phosphate through two main mechanisms: precipitation of P through chemical reaction with these metal ions, and surface deposition of P on Mg crystals on biochar surfaces [38-39]. Compared to unmodified biochar, improved phosphate removal efficiency in Fe-modified biochars was attributed to two factors in the iron modification; it changed the surface and the porous structure of the biochar and thus provided more attractive sites for phosphate adsorption [21].

The valence state of iron in the biochars also played important role in phosphate removal. Biochar with Fe^{3+} in alkaline conditions showed higher phosphate removal efficiency than biochar with co-precipitation of Fe^{3+}/Fe^{2+} (Figure 5). The presence of $Fe(OH)_3$ and Fe_2O_3 which should be more prevalent in the Fe(III)-modified biochar compared to Fe(III)+Fe(II) modified biochar

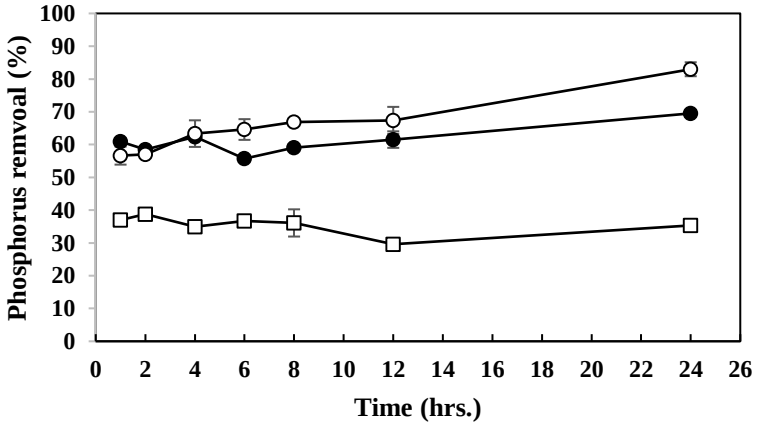

Figure 5. Phosphate removal capacity of (□) BC400, (○) Fe(III) modified biochar and (●) Fe(III)+Fe(II) modified biochar (pH: 7; adsorbent dose: 2g/L; PO_4^{3-}-P: 2.5 mg/l).

explains why the Fe(III) removed phosphate better. Fe(III)'s higher valence state led to a greater affinity for a hard base like PO_4^{3-}, thus reaction between PO_4^{3-} and Fe^{3+} would be more favorable through a combination of electrostatic attraction, surface complexation and anion exchange as reported by Yang *et al.* [21]. The amount of iron in the biochar also played an important role in phosphate removal. XRF analysis (see Table 2) revealed that Fe(III)-modified biochar contained higher iron concentration than Fe(III)+Fe(II)-modified biochar, thus it removed phosphate more efficiently.

3.3.2 Effect of biochar dosage

Adsorbent dosage in water influenced phosphate removal of biochars, especially the Fe-modified biochars (Figure 6). With an increase in dose of Fe(III)-modified biochar from 2 to 16 g/l, phosphate removal efficiency increased to 90%. A similar trend was observed when Fe(III)+Fe(II)-modified biochar was used to treat phosphates in water (Figure 6). This was due to the availability of active sites and increase in surface area at higher dose [23]. On the other hand, increase in dose had no significant effect on phosphate removal in the case of the original biochar, BC400. This further confirmed that iron treatment of these biochars changed the biochar surface properties, resulting in better phosphate removal.

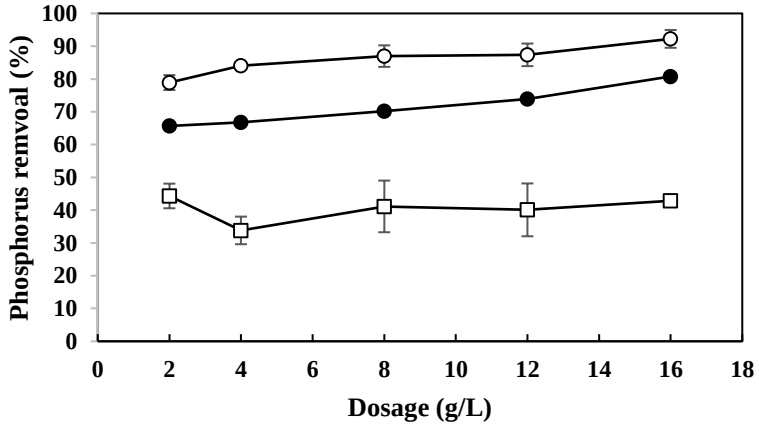

Figure 6. Effect of adsorbent dose on phosphate removal by (□) rice straw-derived biochar, (○) Fe(III) modified biochar and (●) Fe(III)+Fe(II) modified biochar (pH: 7; contact time: 24 h; PO_4-P: 2.5 mg/l).

4. Conclusions

Iron-modified biochar was prepared by pyrolysis of rice straw, followed by coating with iron oxides or hydroxides using two different treatments: direct precipitation of $FeCl_3.6H_2O$ and co-precipitation of $FeCl_3.6H_2O$ and $FeSO_4.7H_2O$. A pyrolysis temperature of 400°C led to the best combination of physicochemical properties related to contaminant sorption (i.e. specific surface area and stable organic matter yield index, SOMYI), and was used as the basis for loading iron onto the biochar surface. Some physicochemical properties (i.e. pH_{pzc}, elemental composition and surface functional groups) of both iron-modified biochars were similar, except Fe(III) loading led to a brownish color of biochar and contained more elemental iron than Fe(II)/Fe(III) combinations. Phosphate sorption assessment showed that the formation of iron hydroxides or oxides on the biochar surface significantly improved phosphate removal ability compared to unmodified biochar. Overall, this study showed that it is possible to turn an abundant agricultural residue, rice straw, effectively and cheaply into a value added product-iron-modified biochar, which efficiently removes phosphorus from water.

5. Acknowledgements

We thank the Department of Chemistry, Faculty of Science, KMITL for financial support for a student's Special Project of KD, NS and PP. Special thanks to John Morris, the author of "Keep it Simple" a guide to English Technical writing and a member of Research Clinic, KMITL Research and Innovation Services (KRIS) for removing unnecessary color and improving the readability of the paper.

References

[1] Kundu, S., Vassanda Coumar, M., Rajendiran, S., Kumar, A. and Subba Rao, A., 2015. Phosphates from detergents and eutrophication of surface water ecosystem in India. *Current Science*, 108(7), 1320-1325.

[2] Thawornchaisit, U., Kongtaweelert, S. and Kasibut, K., 2017. Preparation and evaluation of the alkaline-pretreated and Fe-modified pineapple peel for phosphate removal efficiency. *Proceedings of the International Research Conference on Sustainable Energy, Engineering, Materials and Environment*, Northumbria University, Newcastle Upon Tyne, England, July 26-28, 2017, 217-223.

[3] Duenas, J.F., Alonso, J.R., Rey, A.F. and Ferrer, A.S., 2003. Characterization of phosphorus forms in wastewater treatment plants. *Journal of Hazardous Materials*, 97, 193-205.

[4] Koottatep, T., Chapagain, S.K. and Polprasert, C., 2015. Situation and novel approach for sustainable phosphorus recovery: a case study of Thailand. *Global Environmental Research*, 19, 105-111.

[5] Karthikeyan, K.G., Tshabalala, M.A., Wang, D. and Kalbasi, M., 2004. Solution chemistry effects on orthophosphate adsorption by cationized solid wood residues. *Environmental Science & Technololgy*, 38(3), 904-911.

[6] European Commission, 2017. *Study on the review of the list of critical raw materials* [online] Available at: https://publications.europa.eu/en/publication-detail/-/publication/08fdab5f-9766-11e7-b92d-01aa75ed71a1/language-en. Accessed in April 2019.

[7] Ohtake, H., 2018. *Recovery, reuse of phosphorus from wastewater* [online] Available at: https://www.japantimes.co.jp/news/2018/09/14/national/recovery-reuse-phosphorus-wastewater/#.W_4No-gzbIW. Accessed in April 2019.

[8] Chen, B., Chen, Z. and Lv, S., 2011. A novel magnetic biochar efficiently sorbs organic pollutants and phosphate. *Bioresource Technology*, 102(2), 716-723.

[9] Mohan, D., Sarswat, A., Ok, Y.S. and Pittman, C.U. 2014. Organic and inorganic contaminants removal from water with biochar, a renewable, low cost and sustainable adsorbent – A critical review. *Bioresource Technology*, 160, 191-202.

[10] Ahmad, M., Rajapaksha, A.U., Lim, J.E., Zhang, M., Bolan, N., Mohan, D., Vithanage, M., Lee, S.S. and Ok, Y.S. 2014. Biochar as a sorbent for contaminant management in soil and water: A review. *Chemosphere*, 99, 19-33.

[11] Hameed, B.H. and El-Khaiary, M.I., 2008. Kinetics and equilibrium studies of malachite green adsorption on rice straw-derived char. *Journal of Hazardous Materials*, 153(1-2), 701-708.

[12] Qiu, Y., Zheng, Z., Zhou, Z. and Sheng, G.D., 2009. Effectiveness and mechanisms of dye adsorption on a straw-based biochar. *Bioresource Technology*, 100(21), 5348-5351.

[13] Li, H., Dong, X., da Silva, E.B., de Oliveira, L.M., Chen, Y. and Ma, L.Q., 2017. Mechanisms of metal sorption by biochars: Biochar characteristics and modifications. *Chemosphere*, 178, 466-478.

[14] Saadat, S., Raei, E. and Talebbeydokhti, N., 2018. Enhanced removal of phosphate from aqueous solutions using a modified sludge derived biochar: Comparative study of various modifying cations and RSM based optimization of pyrolysis parameters. *Journal of Environmental Management*, 225, 75-83.

[15] Beesley, L. and Marmiroli, M., 2011. The immobilisation and retention of soluble arsenic, cadmium and zinc by biochar. *Environmental Pollution*, 159(2), 474-480.

[16] Rajapaksha, A.U,. Chen, S.S., Tsang, D.C.W., Zhang, M., Vithanage, M., Mandal, S., Gao, B., Bolan, N.S. and Ok, Y.S., 2016. Engineered/designer biochar for contaminant removal/immobilization from soil and water: Potential and implication of biochar modification. *Chemosphere*, 148, 276-291.

[17] Vikrant, K., Kim, K.-H., Ok, Y.S., Tsang, D.C.W., Tsang, Y.F., Giri, B.S., Tsang, D.C.W., Tsang, Y.F., Giri, B.S. and Singh, R.S., 2018. Engineered/designer biochar for the removal of phosphate in water and wastewater. *Science of the Total Environment*, 616-617, 1242-60.
[18] International Rice Research Insititute, *Rice straw* [online] Available at: http://www.knowledgebank.irri.org/step-by-step-production/postharvest/rice-by-products/rice-straw. Accessed in May 2019.
[19] Food and Agriculture Organization of the United Nations, 2018. *Rice Market Monitor April 2018* [online] Available at: http://www.fao.org/economic/RMM. Accessed in May 2019.
[20] Department of Alternative Energy Department and Efficiency, Ministry of Energy. *Biomass Database Potential in Thailand* [online] Available at: http://biomass.dede.go.th/biomass_web/index.html. Accessed in May 2019.
[21] Yang, Q., Wang, X., Luo, W., Sun, J., Xu, Q., Chen, F., Zhao, J., Wang, S., Yao, F., Wang, D., Li, X. and Zeng, G., 2018. Effectiveness and mechanisms of phosphate adsorption on iron-modified biochars derived from waste activated sludge. *Bioresource Technology*, 247, 537-544.
[22] Land Development Department, 2004. *Manual for Analysis of Soils, Water, Fertilizers, Materials for Soil Improvement and Analysis for Certifying Commodity Standard* (in Thai). 2nd ed. Bangkok: Office of Science for Land Development.
[23] Hafshejani, L.D., Hooshmand, A., Naseri, A.A., Mohammadi, A.S., Abbasi, F. and Bhatnagar, A., 2016. Removal of nitrate from aqueous solution by modified sugarcane bagasse biochar. *Ecological Engineering*, 95, 101-111.
[24] Kaewprasit, C., Hequet, E.F., Abidi, N. and Gourlot, J.-P., 1998. Application of methylene blue adsorption to cotton fiber specific surface area measurement: Part I. Methodology. *Journal of Cotton Science*, 2(4), 164-173.
[25] American Public Health Association, American Water Works Association, Water Environment Federation. 2012. *Standard Methods for the Examination of Water and Wastewater*. 22nd ed. Washington, DC: APHA-AWWA-WEF.
[26] Jiang, J., Peng, Y., Yuan, M., Hong, Z., Wang, D. and Xu, R., 2015. Rice straw-derived biochar properties and functions as Cu(II) and cyromazine sorbents as influenced by pyrolysis temperature. *Pedosphere*, 25(5), 781-789.
[27] Wang, H., Chu, Y., Fang, C., Huang, F., Song, Y. and Xue, X., 2017. Sorption of tetracycline on biochar derived from rice straw under different temperatures. *PLoS One*, 12(8), e0182776.
[28] Masto, R.E., Kumar, S., Rout, T.K., Sarkar, P., George, J. and Ram, L.C., 2013. Biochar from water hyacinth (*Eichornia crassipes*) and its impact on soil biological activity. *Catena*, 111, 64-71.
[29] Ahmed, M.B., Zhou, J.L., Ngo, H.H., Guo, W. and Chen, M., 2016. Progress in the preparation and application of modified biochar for improved contaminant removal from water and wastewater. *Bioresource Technology*, 214, 836-851.
[30] Rafiq, M.K., Bachmann, R.T., Rafiq, M.T., Shang, Z., Joseph, S. and Long, R., 2016. Influence of pyrolysis temperature on physico-chemical properties of corn stover (*Zea mays* L.) biochar and feasibility for carbon capture and energy balance. *PLoS One*, 11(6), e0156894.
[31] Angın, D. and Şensöz, S., 2014. Effect of pyrolysis temperature on chemical and surface properties of biochar of Rapeseed (*Brassica napus* L.). *International Journal of Phytoremediation*, 16(7-8), 684-693.
[32] Angın, D., 2013. Effect of pyrolysis temperature and heating rate on biochar obtained from pyrolysis of safflower seed press cake. *Bioresource Technology*, 128, 593-597.
[33] González, J.F., Ramiro, A., González-García, C.M., Gañán, J., Encinar, J.M., Sabio, E. and Rubiales, J. 2005. Pyrolysis of almond shells. *Energy Applications of Fractions. Industrial & Engineering Chemistry Research*, 44, 3003-3012.

[34] Liao, T., Li, T., Su, X., Yu, X., Song, H., Zhu, Y. and Zhang, Y., 2018. $La(OH)_3$-modified magnetic pineapple biochar as novel adsorbents for efficient phosphate removal. *Bioresource Technology*, 263, 207-213.

[35] Komnitsas, K. A. and Zaharaki, D., 2016. Morphology of modified biochar and its potential for phenol removal from aqueous solutions. *Frontiers in Environmental Science*, 4(26), 1-11. doi:10.3389/fenvs.2016.00026.

[36] Kulaksiz, E., Gözmen, B., Kayan, B. and Kalderis, D., 2017. Adsorption of malachite green on Fe-modified biochar: influencing factors and process optimization. *Desalination and Water Treatment*, 74, 383-394.

[37] Tang, Q., Shi, C., Shi, W., Huang, X., Ye, Y., Jiang, W., Kang, J., Liu, D.,Ren, Y. and Li, D., 2019. Preferable phosphate removal by nano-La(III) hydroxides modified mesoporous rice husk biochars: Role of the host pore structure and point of zero charge. *Science of the Total Environment*, 662, 511-520.

[38] Yin, Q., Zhang, B., Wang, R., and Zhao, Z., 2018. Phosphate and ammonium adsorption of sesame straw biochars produced at different pyrolysis temperatures. *Environmental Science & Pollution Research*, 25, 4320-4329.

[39] Yao, Y., Gao, B., Chen, J. and Yang, L., 2013. Engineered biochar reclaiming phosphate from aqueous solutions: Mechanisms and potential application as a slow- release fertilizer. *Environmental Science & Technology*, 47(15), 8700-8708.

Release of Various Elements from Organic Fertilizers Incubated in Organic and Non-organic Paddy Soils at Various Time Periods

Patcharin Surin, Phasini Supsuan and Sukunya Yampracha*

Department of Plant Production Technology, Faculty of Agricultural Technology, King Mongkut's Institute of Technology Ladkrabang, Bangkok, Thailand

Received: 2 August 2019, Revised: 15 August 2019, Accepted: 21 August 2019

Abstract

Organic fertilizers often contain numerous elements beside nitrogen (N) such as phosphorus (P), potassium (K), calcium (Ca), magnesium (Mg) and sodium (Na). In general, the application rates of organic fertilizer are based on N requirement which could result in extra amount of other elements i.e. P and Na which could negatively impact on environment. This study aimed to investigate the release of P, K, Ca, Mg, and Na using a batch technique from three organic fertilizers (e.g. cow manure, compost and sunn hemp) incubated in two paddy soils at various time periods (e.g. 0, 3, 5, 7, 14, 21, 28, 42, 56, 70, 98 and 120 days). A 2×4 factorial in completely randomized experimental design with three replications was employed. A factor A was type of paddy field (an organic paddy field (SO), and non-organic paddy field (SC)) and a factor B was four different organic fertilizers application type (control, cow manure compost and sunn hemp). Soil samples were collected to analyze soil pH, electrical conductivity, available P (Bray II), exchangeable K, Ca, and Mg and extractable Na at the end of each incubation time period. Results showed that the incubation time period did not play a role on the release of P, K, Ca, Mg and Na in soils. Release of P, K, Ca, Mg, and Na in SC was higher than SO. Release of P, K, and Na were highest in cow manure, while compost gave higher release of Ca and Mg. Electrical conductivity did not exceed safety levels with all treatments less than 0.50 mS/cm.

Keywords: organic fertilizer, phosphorus, potassium, calcium, magnesium, sodium
DOI 10.14456/cast.2019.23

1. Introduction

Organic fertilizer is sustained source of nutrients due to slow release during decomposition of plant materials and/or animal manures which often contains several elements. Increasing soil organic matter, improving soil fertility, and other essential plant nutrients can improve crop productivity [1]. However, organic fertilizer contains low levels of nitrogen (N) and accumulates some nutrients of essential and non-essential nutrients in soil [2]. The other essential plant nutrients in organic fertilizer are phosphorus (P), potassium (K), calcium (Ca) and magnesium (Mg) as well as non-essential nutrients such as sodium [3]. Moreover, long-term organic fertilizer applications may result in calcium, magnesium and sodium accumulation in paddy fields [4]. Phosphorus, potassium, calcium and magnesium are essential nutrients for rice growth. Rice acquires these

*Corresponding author: Tel.: +6602-329-8511
E-mail: sukunya.ya@kmitl.ac.th

nutrients from both chemical and organic fertilizers [5]. In general, the application rates of organic fertilizer for rice plants are based on nitrogen requirements. Therefore, these elements can also accumulate in soils along with organic fertilizers application.

Accumulation of total phosphorus may benefit soils by decreasing the toxicity of aluminum, iron and manganese through phosphorus fixation [6]. However, phosphorus can be easily lost in paddy soil by runoff and transportation into water sources, thereby promoting eutrophication phenomena. High soil organic matter or sandy soil enhances high phosphorus leaching [7]. In addition, available phosphorus is a sensitive element and shows a positive correlation coefficient with soil pH. Phosphorus develops higher availability in submerged soils which are affected by iron reduction [8]. Historically, research has focused on the importance of inorganic phosphorus for plant nutrition. However, organic phosphorus usually accounts for 20-50% of the total phosphorus and mineralization of organic phosphorus to inorganic available forms plays an important role in soil phosphorus storage [9]. Accumulation of potassium, calcium, magnesium, and sodium are not affected by reduction conditions during paddy soil submergence but these sensitive elements determine soil electrical conductivity (EC). Organic fertilizer application increases soluble and exchangeable forms of Ca, Mg, K and Na, with higher release of soluble K and Na than exchangeable K and Na. However, release of exchangeable Ca and Mg is higher than soluble Ca and Mg [10]. Moreover, high accumulation of these nutrients may induce deficiencies of other nutrients such as high soil phosphorus may induce zinc deficiency in paddy soil [11]. In addition, if a plant uptakes potassium, this can induce calcium and magnesium deficiency with an antagonistic effect on the uptake of calcium and magnesium [12].

The release nutrients rate is depending on the component of the organic fertilizer [13]. Release of phosphorus, potassium, calcium, and magnesium is beneficial for rice growth. Continuous applications of organic fertilizer may induce accumulation of these elements while phosphorus and sodium can adversely impact on the environment. Manure applications might induce the risk of phosphorus, potassium and sodium loss to the environment [14].

Applications of organic fertilizers may improve all soil properties but continuous applications of the same organic fertilizer type may induce a negative effect. Accumulation of phosphorus, potassium, calcium, magnesium and sodium in the soil from fertilizer application adversely affects crop growth, the economy and the environment. Therefore, the purpose of this study was to investigate the release of phosphorus, potassium, calcium, magnesium, and sodium from different types of organic fertilizers in two different management paddy soils at various time periods.

2. Materials and Methods

2.1 Soil sampling

Two soil samples were collected from two rice fields as two paddy soils from an organic rice field by applying organic fertilizer more than 10 years (SO) and from a nearby rice field which used only chemical fertilizer (SC) in Nong Chok district, Bangkok. The soils were classified into Bangkok soil series (very-fine, smectitic, nonacid, isohyperthermic Vertic Endoaquepts). Each sample was collected at 0-15 cm depth, air-dried and passed through a 2-mm sieve prior to soil properties analysis.

Soil pH was determined at 1:1 ratio of soil to deionized water. Electrical conductivity (EC) was determined at 1:5 ratio of soil to deionized water. Soil pH and electrical conductivity were measured using a pH meter and an EC meter, respectively [15]. Soil phosphorus solution was extracted using 0.01M calcium chloride ($CaCl_2$) at 1:5 ratio of soil to solution, shaken for 15 min

and filtered through filter paper No. 42 [16]. Water extractable phosphorus was extricated using deionized water at 1:10 ratio of soil to water and shaken for 1 h [17]. Concentration of water extractable phosphorus was measured using an inductively coupled plasma optical emission spectrometer (ICP-OES). Available phosphorus was extracted using Bray II at 1:10 ratio of soil to solution. Phosphorus concentration was measured using the molybdenum blue method and determined using a spectrophotometer at wavelength 882 nm [18]. Total phosphorus, potassium, calcium and magnesium were digested with nitric acid (HNO_3): perchloric acid ($HClO_4$) at 2:1 ratio. Concentration of total phosphorus was measured using an ICP-OES [19]. Exchangeable K, Ca, Mg and Na were extracted using 1M ammonium acetate pH 7.0 and measured by an ICP-OES [20].

2.2 Organic fertilizer

Manure, compost and green manure are some of the major sources of N fertilizer for organic rice cultivation in Thailand [21]. In the study, three organic fertilizers were used including cow manure (CM), compost (CP) from a farmer in Nong Chok district, Bangkok, and sunn hemp (SH) from an extension plot at the Faculty of Agricultural Technology, King Mongkut's Institute of Technology Ladkrabang (KMITL), Bangkok, Thailand. Compost was prepared from the decomposition of cow manure and rice straw at a ratio of 1:3 by weight. Each organic fertilizer was ground and passed through a 2-mm sieve prior to analysis. The pH and electrical conductivity were determined at 1:5 ratio of organic fertilizer to deionized water. Concentration of total nitrogen was measured using dry combustion [22]. Total diphosphorus pentoxide (P_2O_5), total potassium oxide (K_2O), total Ca, total Mg and total Na were measured using dry ashing method and filtered through filter paper No. 5. Water extractable of P, K, Ca, Mg and Na were extracted using deionized water at 1:10 ratio of soil to solution. Each sample was shaken for 1 h and filtered through filter paper No. 5 [17]. Concentrations of total and water extractable elements were measured using an ICP-OES.

2.3 Experimental design and incubation study

Batch incubation experiments were conducted in an incubator with a 2×4 factorial completely in randomized design with three replications. Factor A was two paddy soils from an organic rice field (SO) and a nearby rice field which used only chemical fertilizer (SC). Factor B was four different organic fertilizers consisting of control, cow manure, compost, and sunn hemp. The organic fertilizers were applied at the rate of 300 mg N/kg (based on total N in organic fertilizers) [14]. Soil with and without fertilizer was flooded with 200 ml of deionized water and incubated at 30°C for 120 days according to the rice growth cultivation. Other nutrient contents of organic fertilizers applied to meet nitrogen at the rate of 300 mg N/kg were shown in Table 1.

The release nutrients were released at the earliest stage of incubation [13]. Samples were collected at 0, 3, 5, 7, 14, 21, 28, 42, 56, 70, 98, and 120 days after incubation for analysis of soil pH, electrical conductivity, available P (Bray II), exchangeable K, Ca, Mg and Na extracted using 1M ammonium acetate pH 7.0 and measured by an ICP-OES [20].

2.4 Statistical analyses

All data were analyzed by analysis of variance (ANOVA) using a statistical software package. Mean comparison was analyzed using Duncan's multiple range test (DMRT) at a significant level of 95%.

Table 1. Nutrient content of organic fertilizers applied to meet nitrogen at the rate of 300 mg N/kg.

Organic fertilizer	Cow manure	Compost	Sunn hemp
Total nitrogen (mg/kg)	300.00	300.00	300.00
Total phosphorus (mg/kg)	480.24	230.68	252.48
Total potassium (mg/kg)	2,839.00	464.98	1,589.00
Total calcium (mg/kg)	2,346.00	709.00	753.00
Total magnesium (mg/kg)	481.95	303.76	517.65
Total sodium (mg/kg)	197.64	73.15	259.96

3. Results and Discussion

3.1 Soil and organic fertilizer properties before incubation

Physical and chemical properties of SO and SC were analysed as shown in Table 2. Both soils were clayey with an acidic reaction and soil pH at 6.10 and 5.30 for SC and SO, respectively (Table 2). Electrical conductivity (EC) of both soils did not exceed the safety level for rice growth (<2 mS/cm), while available phosphorus and exchangeable potassium, calcium and magnesium contents were high and adequate for rice growth. Exchangeable sodium of SC was higher than SO; however, organic matter and total nitrogen contents of both soils were not significantly different.

Organic fertilizer properties were presented in Table 3. The pH values of the three organic fertilizers as cow manure, compost, and sunn hemp were moderately alkaline (8.2), slightly acid (6.3) and strongly acidic (5.1), respectively. Electrical conductivities (EC) of cow manure and sunn hemp were higher than the regulations of the Department of Agriculture of Thailand (<3.5 mS/cm) [23]. Water soluble P, Ca, Mg and Na were highest in sunn hemp, while water soluble K was highest in cow manure.

3.2 Change in soil pH and electrical conductivity (EC)

Results showed that the pH of each soil at initial was significantly different (Figure 1). The initial soil pH of both soils was acidic, with SC higher than SO. The two amended soils with cow manure had the highest pH followed by soils amended with compost. The pH of SO amended with cow manure at 0 day highest with 5.79 value, followed by SO with compost and sunn hemp at 5.65 and 5.52, respectively. The pH of SC amended with cow manure at 0 day was highest with 6.48, followed by SC with compost and sunn hemp at 6.04 and 5.78, respectively. Soil pH of all treatments increased rapidly to neutral within 3 days of incubation, with a slightly increase from 3-14 days after incubation and then became steady at neutral pH after 14 days of incubation. Soil pH of all treatments at 120 days after incubation showed no significant difference. This indicated that soil and organic fertilizer types did not affect soil pH changes under submergence. Soil pH of amended soil with organic fertilizer become neutral after 14 days as influenced by the reduction reaction [24]. It might be noticeable that the soil pH increased rapidly at the initial of flooding resulted by high organic carbon in soil and organic fertilizer [25].

Table 2. Soil properties before incubation.

Soil properties	Organic paddy field (SO)	Non-organic paddy field (SC)
pH (1:1 soil: water)	5.30	6.10
Electrical conductivity (1:5 soil: water) (mS/cm)	0.23	0.40
Soil texture	Clay	Clay
Sand (g/kg)	259.60	299.60
Silt (g/kg)	247.20	227.20
Clay (g/kg)	493.20	473.20
Organic matter (g/kg)	45.60	45.50
Total carbon (g/kg)	26.45	26.38
Total nitrogen (g/kg)	2.51	2.25
Total phosphorus (g/kg)	0.18	0.26
Total potassium (g/kg)	7.98	6.88
Total calcium (g/kg)	2.57	3.05
Total magnesium (g/kg)	3.83	3.08
Available phosphorus Bray II (mg/kg)	35.47	63.85
Available phosphorus Olsen (mg/kg)	8.96	15.43
Water extractable phosphorus (mg/kg)	0.28	0.24
Soil solution phosphorus ($CaCl_2$-P) (mg/kg)	0.68	0.71
Exchangeable potassium (mg/kg)	251.53	130.65
Exchangeable calcium (mg/kg)	2,343	1,838
Exchangeable magnesium (mg/kg)	661.99	226.32
Extractable sodium (mg/kg)	37.14	89.99
C/N ratio	10.54	11.71
Cation exchange capacity (cmol(+)/kg)	26.85	30.33

Table 3. Chemical properties of three organic fertilizer used in this study.

Organic fertilizer properties	Cow manure	Compost	Sunn hemp
pH (1:5 organic fertilizer: water)	8.20	6.30	5.10
Electrical Conductivity (1:5 organic fertilizer: water) (mS/cm)	10.48	2.94	10.23
Total nitrogen (g/kg)	7.80	19.40	23.20
Total P_2O_5 (g/kg)	11.00	5.28	5.78
Total K_2O (g/kg)	65.02	10.65	36.40
Total calcium (g/kg)	23.46	7.09	7.53
Total magnesium (g/kg)	4.82	3.04	5.18
Total sodium (g/kg)	1.98	0.73	2.60
Water soluble phosphorus (mg/kg)	32.61	13.80	77.57
Water soluble potassium (mg/kg)	2,139.00	345.17	1,491.00
Water soluble calcium (mg/kg)	35.64	121.05	200.63
Water soluble magnesium (mg/kg)	17.92	126.50	325.92
Water soluble sodium (mg/kg)	305.40	65.56	361.92
C:N ratio	15.76	13.44	18.66

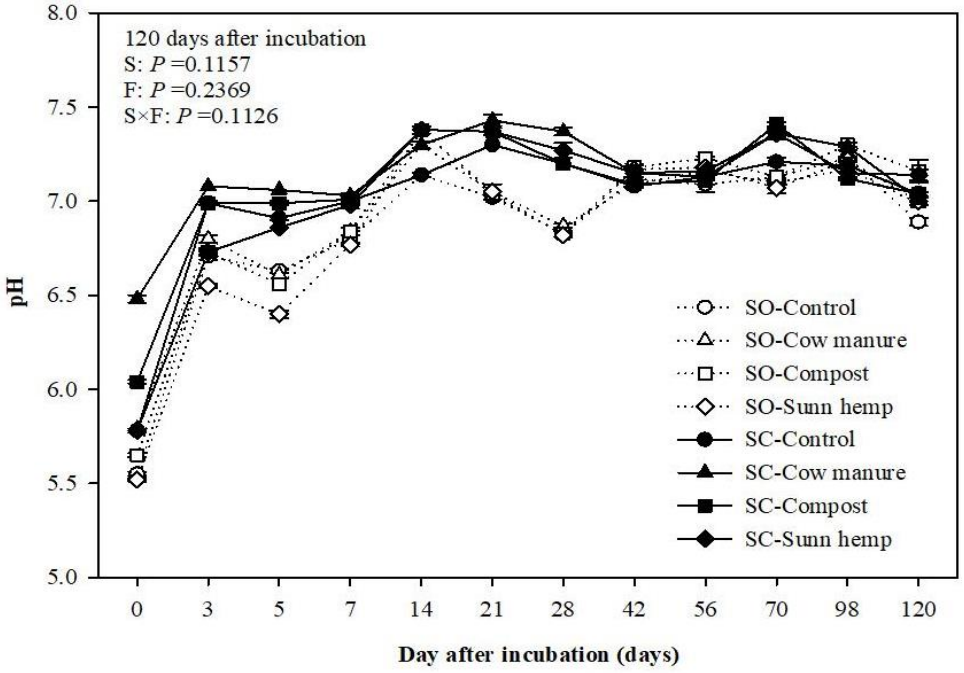

Figure 1. Changes of soil pH during incubation. S = Soil, F = Fertilizer, Error bar = Standard error of mean (SE), *P*-value = Significant at 0.01 and 0.05 level.

Soil electrical conductivity was highest at 3 days after incubation before decreasing dramatically and reaching steady state after 5 days of incubation, with a gradual decrease until the end of incubation (Figure 2). Results showed that EC of all treatments significantly differed during the incubation period. The electrical conductivity of SC amended with cow manure at 120 days was highest at 0.37 mS/cm, followed by SC with compost and sunn hemp at 0.24 and 0.22 mS/cm, respectively. The electrical conductivity of SC soil was higher than SO, while the application of cow manure significantly increased EC to higher than other organic manure. Meanwhile, the application of sunn hemp showed no significant difference with the control (Figure 2), possibly due to the high EC of cow manure to meet nitrogen rate which induced high quantities of cations. Electrical conductivity in all treatments did not exceed the safety level at the end of incubation (less than 0.50 mS/cm) [26].

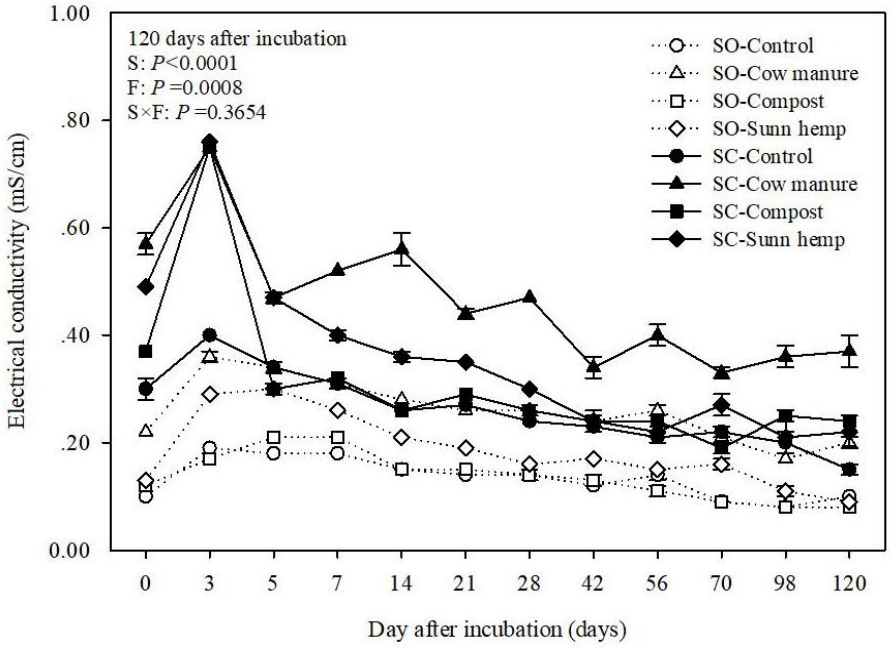

Figure 2. Changes of electrical conductivity (EC) during incubation. S = Soil, F = Fertilizer, Error bar = Standard error of mean (SE), *P*-value = Significant at 0.01 and 0.05 level.

3.3 Release of phosphorus

A release of phosphorus from organic fertilizers was calculated from the difference of available phosphorus (Bray II) in control and soil amended with the three organic fertilizers. Results showed that phosphorus release after incubation was higher for SC than SO. The SC with cow manure at 0 day released the highest phosphorus (14.12%), followed by SC with cow manure at 120 days (12.35%) (Figure 3). After incubation at 120 days, each soil and organic fertilizer type was significantly different (Figure 3). The amount of phosphorus in solution and available P was analysed. In both paddy soils, the highest amount of phosphorus in solution was found at the 120 days of incubation period amended with cow manure (0.28 and 0.34 mg/l in SO and SC,

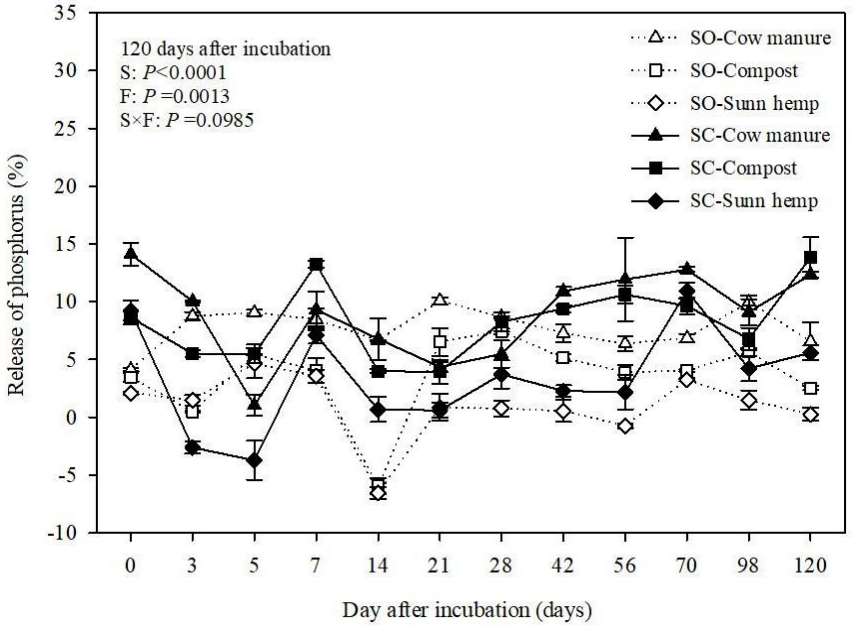

Figure 3. Changes of phosphorus release during incubation. S = Soil, F = Fertilizer, Error bar = Standard error of mean (SE), *P*-value = Significant at 0.01 and 0.05 level.

respectively, data not shown). Phosphorus in solution of both soils with cow manure was higher than the Department of Pollution Control of Thailand regulations (<0.04 mg/L) [27]. Meanwhile, available phosphorus (Bray II) at 120 days after incubation of both soils amended with cow manure had the highest contents at 120.09 and 229.14 mg/kg for SO and SC, respectively. Available phosphorus of both soils amended with cow manure was higher than the critical value of phosphorus leaching risk at 43.85 mg/kg [7]. It might be due to high amount of the total phosphorus in cow manure (Table 2). These results showed that the total phosphorus amount is an important role in the release of phosphorus in submerged soil. This indicated that the amount of P release from paddy soils amended with cow manure could be potentially risk to the environment [28].

3.4 Release of potassium, calcium and magnesium

A release of potassium, calcium, and sodium from organic fertilizers was calculated from the difference of exchangeable potassium, calcium and magnesium in control and soil amended with the three organic fertilizers. Both soils amended with cow manure released the highest extractable potassium at 17.49 and 28.18% in SO and SC, respectively (Figure 4). Release of extractable Ca was 26.54% and 33.80% in SO amended with sunn hemp and SC amended with compost, respectively (Figure 5) while release of Mg in SO was slightly higher than SC, with little difference between the three organic fertilizers at 12.88-13.13% (Figure 6).

At the end of the incubation period, soil and organic fertilizer type strongly affected the release of K, while soil type influenced Ca and Mg release more than organic fertilizer, possibly due to high K content of cow manure. However, the repeating large amounts of manure build up increased high amounts of exchangeable Ca and Mg and decreased exchangeable K in soil [3].

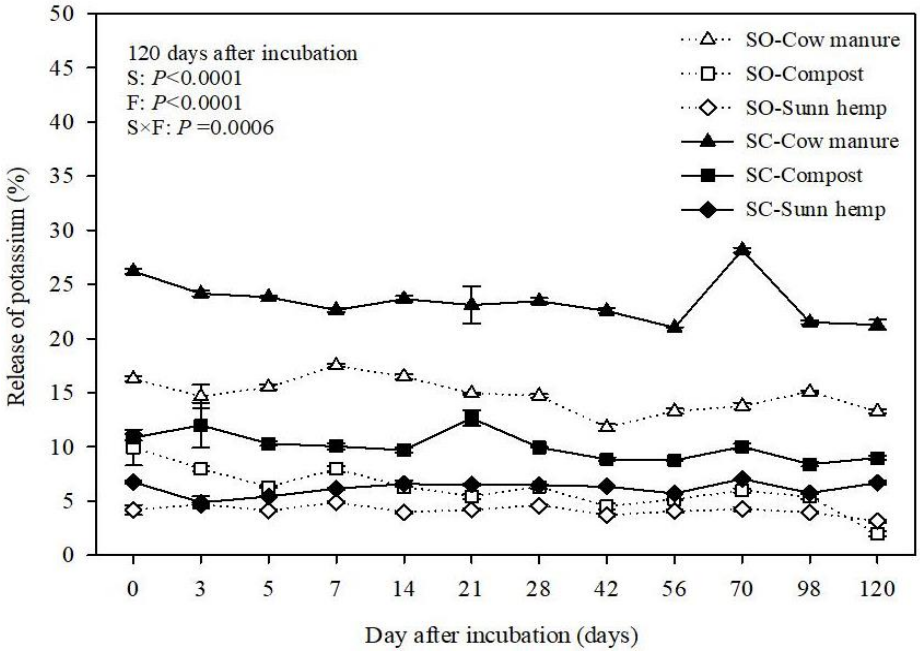

Figure 4. Changes of potassium release during incubation. S = Soil, F = Fertilizer, Error bar = Standard error of mean (SE), *P*-value = Significant at 0.01 and 0.05 level.

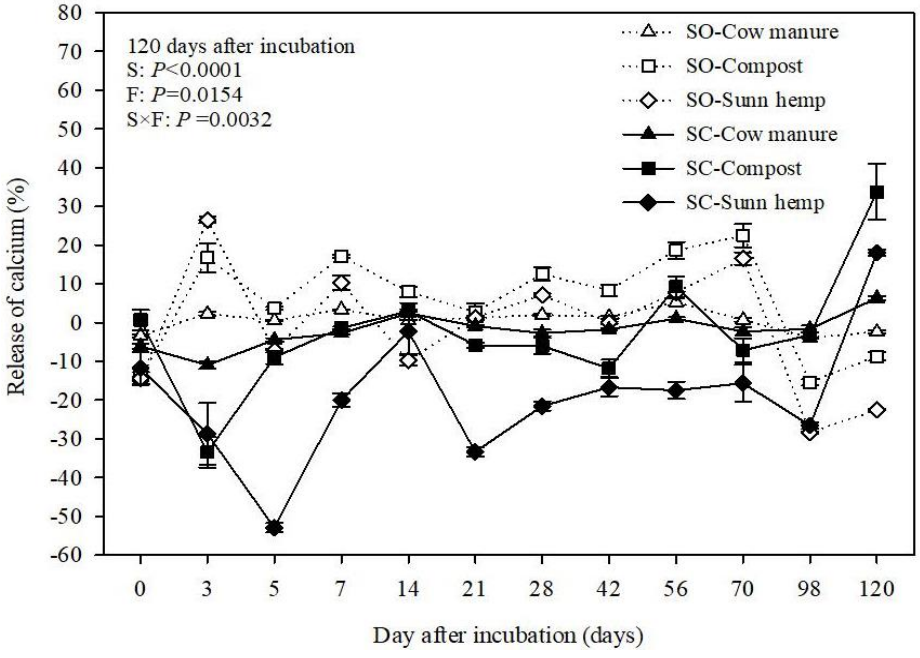

Figure 5. Changes of calcium release during incubation. S = Soil, F = Fertilizer, Error bar = Standard error of mean (SE), *P*-value = Significant at 0.01 and 0.05 level.

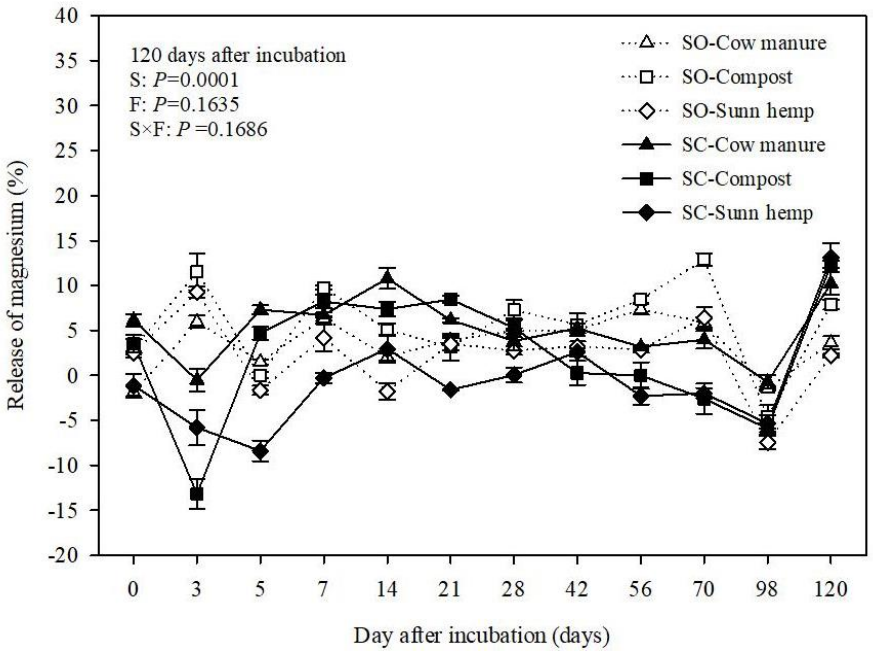

Figure 6. Changes of magnesium release during incubation. S = Soil, F = Fertilizer, Error bar = Standard error of mean (SE), *P*-value = Significant at 0.01 and 0.05 level.

3.5 Release of sodium

A release of sodium from organic fertilizers was calculated from the difference of extractable sodium in control and soil amended with the three organic fertilizers. Results indicated that sodium release after incubation of both soils showed no significant difference. The SO amended with cow manure released the highest sodium at 31.12%, 70 days while the SC amended with cow manure had the highest sodium at 42.19% at 0 day (Figure 7). After incubation at 120 days, sodium release of each soil and organic fertilizers type was significantly different. Sodium is not an essential nutrient for rice growth. Soil exchangeable Na increases when a large amount of manure is applied [3]. Sodium in solution at 120 days after incubation for both soils amended with cow manure was highest at 27.17 and 137.03 mg/l in SO and SC, respectively (data not shown). Meanwhile, exchangeable sodium at 120 days after incubation of both soils amended with cow manure was highest at 146.50 and 189.81 mg/kg for SO and SC, respectively.

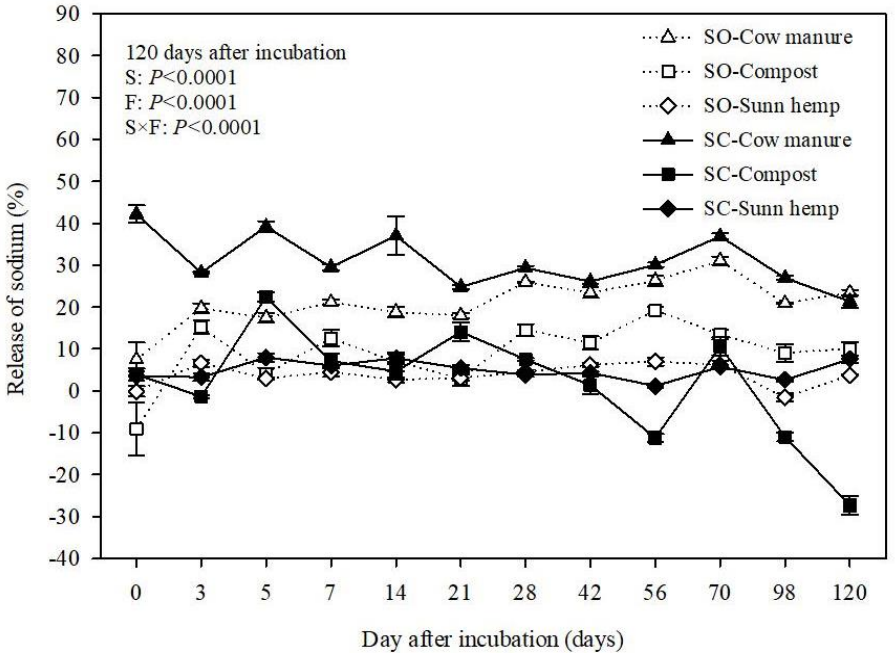

Figure 7. Changes of sodium release during incubation. S = Soil, F = Fertilizer, Error bar = Standard error of mean (SE), *P*-value = Significant at 0.01 and 0.05 level.

4. Conclusions

This study showed that the incubation period did not play a role on the release of phosphorus, potassium, calcium, magnesium, and sodium in soil. Release of phosphorus, potassium, calcium, magnesium and sodium in non-organic paddy soil was higher than organic paddy soil. It was found that the release of phosphorus, potassium, and sodium was higher in both soils amended with cow manure. Phosphorus in solution of both soils with cow manure was higher than the Department of Pollution Control of Thailand regulations (<0.04 mg/L). The available phosphorus (Bray II) was also higher than the critical value of phosphorus leaching risk at 43.85 mg/kg. The release of calcium and magnesium was higher in both soils amended with compost and sunn hemp. Electrical conductivity in all treatments did not exceed the safety level at less than 0.50 mS/cm. Soil and organic fertilizer types are important factors which have an effect on the release of phosphorus and sodium.

5. Acknowledgements

This study was supported by the Graduate Research Fund from the Faculty of Agricultural Technology, King Mongkut's Institute of Technology Ladkrabang, Thailand (Project number 2562-02-04-016).

References

[1] Singh, P.R., 2012. *Organic Fertilizers: Types, Production and Environmental Impact*. New York: Nova Science Inc.

[2] Kokoasse, K.A. and Desmond, M., 2016. Organic Fertilizers in Alabama: Composition, Transformations, and Crop Response in Selected Soils of the Southeast United States. In M. L. Larramendy and S. Soloneski, eds. *Organic Fertilizers from Basic Concepts to Applied Outcomes,* Rijeka: IntechOpen, pp. 25-50.

[3] Meek, B., Graham, L. and Donovan, T., 1982. Long-term effects of manure on soil nitrogen, phosphorus, potassium sodium, organic matter, and water infiltration rate. *Soil Science Society of America Journal*, 46, 1014-1019.

[4] Yan, X., Wei, Z., Hong, Q., Lu, Z. and Wu, J., 2017. Phosphorus fraction and sorption charateristics in a subtropical paddy soil as influenced by fertilizer sources. *Journal of Geoderma*, 295, 80-85.

[5] Xin, X., Qin, S., Zhang, J., Zhu, A., Yang, W. and Zhang, X., 2017. Yield, Phosphorus use efficiency and balance response to substituting long-term chemical fertilizer use with organic manure in a wheat-maize system. *Journal of Field Crops Research*, 208, 27-33.

[6] Surin, P., Pronkanung, S., Lachitavong, K. and Yampracha, S., 2018. Effect of limestone and drainage on ameliorate acidity, salinity and toxicity of aluminum, iron and manganese in acid sulfate soil. *King Mongkut's Agricultural Journal*, 36 (supplement), 45-53.

[7] Pibumrung, P., 2015. Phosphorus and Phosphorus leaching loss from paddy field in Phra Nakhon Si Ayutthaya. *Khon Kaen Agricultural Journal*, 43 (supplement), 951-955.

[8] Wanna, S., Supaphol, S., Luanmanee, S. and Anusontpornperm, S., 2016. Involving bacteria to inorganic substance changes in an acid sulfate soil (Rangsit soil series). *Khon Kaen Agricultural Journal*, 44, 19-28.

[9] Dai, L., Tan, F., Wu, B., He, M., Wang, W., Tang, X., Hu, Q. and Zhang, M., 2015. Immobilization of phosphorus in cow manure during hydrothermal carbonization. *Journal of Environmental Management,* 157, 49-53.

[10] Cees, S. and Wim, V., 2009. *Plant Nutrition of Greenhouse Crops*. London: Springer Dordrecht Heidelberg., pp. 430.

[11] Yampracha, S., 2011. *Soil Chemical*. Department of Plant Production Technology. Faculty of Agricultural Technology. King Mongkut's Institute of Technology Ladkrabang, Bangkok.

[12] Thawinthung, N., 2016. *Soil and Plant Nutrient Management*. Department of Plant Production Technology. Faculty of Agricultural Technology. King Mongkut's Institute of Technology Ladkrabang, Bangkok.

[13] Organically done, 2019. *Nutrient Availability and ReleaseTtime*. [online] Available at: https://organicallydone.com/nutrient-availability-and-release-time.

[14] Fortune, S., Lu, J., Addiscott, T.M. and Brookes, P.C., 2005. Assessment of phosphorus leaching losses from arable land. *Plant and Soil*, 269, 99-108.

[15] Richards, L. A., 1954. *Diagnosis and Improvement of Saline and Alkali Soil*. *Handbook 60*. Washington, D. C. : USDA Agriculture.

[16] Richard, M.D., Sokrat, S., Androw, S. and Emmanuel, F., 2001. The use of isotopic exchange kinetice to assess phosphorus availability in overland flow and subsurface drainage waters. *Soil Science*, 166, 365-373.

[17] Pizzeghello, D., Berti, A., Nardi, S. and Morari, F., 2016. Relationship between soil test phosphorus and phosphorus release to solution in three soil after long-term mineral and manure application. *Agriculture, Ecosystems and Environment*, 233, 214-223.

[18] Bray, R. H. and Kurtz, L. T., 1945. Determination of total organic and available forms of phosphorus in soil. *Soil Science*, 59, 39-45.

[19] Yampracha, S., 2013. *Soil and Plant Analysis*. Department of Plant Production Technology. Faculty of Agricultural Technology. King Mongkut's Institute of Technology Ladkrabang, Bangkok.
[20] Soil Chemical Research Center, 2001. *Soil and Plant Analysis Manual*. Bangkok : Soil Science. Department of Agriculture.
[21] Supsuan, P., Surin, P. and Yampracha, S., 2018. Effects of organic fertilizer application on the transformation of nitrogen in paddy soil. *International Journal of Agricultural Technology*, 14(7), 1999-2014.
[22] LECO Corporation, 2016. *Operation In: Trumac CNS/ NS Carbon/ Nitrogen/ Sulfur Determinators Instruction Manual*. U.S : LECO Europe B.V., pp. 1-56.
[23] Jirasuthad, D., 2014. *Organic Fertilizer Regulations.* Bangkok : Department of Agricultural of Thailand.
[24] Kyuma, K., 2004. *Paddy Soil Science*. Kyoto: Kyoto University Press and Trans Pacific Press, pp. 280.
[25] Attanandana, T., 2007. Basic of chemical reaction in paddy soils. In: *Paddy Soil Science*, Bangkok : Department of Soil Science, Kasetsart University, pp. 29-46.
[26] Arunnin, S., 1996. *Alkaline Soil in Thailand*. Bangkok : Department of Land Development. pp. 37.
[27] Department of Pollution Control of Thailand, 2010. *Water Quality Regulations*. [online] Available at: http://www.pcd.go.th/info_serv/reg_std_water04.html
[28] Li, L., Liang. X., Ye, Y., Zhao, Y., Zhang, Y., Jin, Y., Yuan, J. and Chen, Y., 2014. Effects of repeated swine manure applications on legacy phosphorus and phosphomonoesterase activities in a paddy soil. *Biological Fertilizer Soils*, 51, 167-181.

The Effect of Exogenous Spermidine and Wood Vinegar on Growth and Physiology of Rice (*Oryza sativa* L.) cv. RD6 under Salt Stress

Anuchat Srisompan* and Piyada Theerakulpisut

Salt-tolerant Rice Research Group, Department of Biology, Faculty of Science, Khon Kaen University, Khon Kaen, Thailand

Received: 9 August 2019, Revised: 20 August 2019, Accepted: 29 August 2019

Abstract

Rice cv. RD6 is one of the most important crops for Thailand particularly for people and farmers in the northeastern part of the country. Saline soil in the northeastern part of Thailand is an important problem that causes low yield of rice. Treatment of plants with some plant growth regulators (PGR) such as polyamine or bio-stimulants, for example wood vinegar (WV), can induce physiological response so that plants become more tolerant to abiotic stresses including salinity. The objective of this study was to investigate the effects of spermidine (Spd) and WV on increasing tolerance of rice seedlings in saline soil under greenhouse condition. Rice seedlings were grown for 30 days in pots containing 5 kg soil. The plants were then sprayed with distilled water (control), WV (1:500), Spd (0.05, 0.1 and 0.5 mM) and mixture between WV (1:500) and Spd (0.05, 0.1 and 0.5 mM) for 5 days and then exposed to salt stress (150 mM NaCl) for 14 days. The result indicated that salt stress decreased net photosynthesis rate, maximal quantum yield of PSII photochemistry (F_v/F_m), but increased membrane damage as indicated by increase in electrolyte leakage (EL). Under salt stress, spraying with WV (1:500) and 0.1 mM Spd (with or without WV) tended to increase shoot and root growth, respectively. Spraying with 0.05 mM Spd and 0.5 mM Spd significantly reduced EL and increased F_v/F_m, respectively. The most effective solutions to promote shoot growth, root growth, reduce membrane damage and improve photochemical function of PSII were WV (1:500), 0.1 mM Spd, 0.05 mM Spd and 0.5 mM Spd, respectively.

Keywords: spermidine, wood vinegar, salt stress, photosynthesis, photosystem II, electrolyte leakage, glutinous rice
DOI 10.14456/cast.2019.24

1. Introduction

Rice is one of the main crops of Thailand and especialy in the northeastern part of the country. Saline soil is an important problem in the northeastern part of Thailand that causes low yield of rice [1]. Rice cv. RD6 is moderately sensitive to salinity [2]. Saline soil is also one of the most important factors in reducing yields of other crop species in many countries of the world.

*Corresponding author: Tel.: 094-3848530
E-mail: anuchatbank@gmail.com

The problem of salinity is intensified because agricultural areas affected by salinity tend to increase. Global warming, deforestation, salt making and irrigation systems will greatly increase areas of salt-affected soils. For all over the world, 45 million hectares of irrigated land have been damaged by salt [3]. There are around 19.7 million rais or 3.2 million hectares of saline soils in Thailand, of which 17.8 million rais are found in the northeastern region. Spreading of salinity in northeast of Thailand has been caused by both nature and human activities. The natural causes of soil salinity included decay of salt rock at 1-2 m deep and evaporation of groundwater which brings salt to the surface. Human causes in the last 50 years included salt mining, deforestation and building irrigation systems and water resources on saline soils [1].

Salinity induced morphological and physiological changes including a reduction in the dry weight of leaves and roots, leaf area, root length, root volume, average root diameter, total chlorophyll, chlorophyll a, chlorophyll b, carotenoids, net photosynthesis and stomatal conductance and increasing in proline and MDA content [4-6]. In addition, salinity caused ion imbalance in plants as shown by higher Na^+ and Cl^- contents and lower K^+, Ca^{2+} and Mg^{2+} concentrations [4, 6-8]. These imbalances of the cellular ions result in ion toxicity, osmotic stress and production of reactive oxygen species (ROS) including superoxide anions, hydrogen peroxide and hydroxyl radicals. Salt-tolerant plants can regulate ion and water movements more efficiently than salt-sensitive plants and have a better antioxidant system for effective removal of ROS [9, 10]. These antioxidant systems include antioxidant enzymes for example superoxide dismutase, catalase, glutathione peroxidase and peroxidases and enzymes of ascorbate-glutathione cycle including ascorbate peroxidase and glutathione reductase. These antioxidant enzymes will help to decrease salt stress effect from oxidation processes of biomolecules [11].

Polyamine is one of plant growth regulators consisting of putrescine (Put), spermidine (Spd) and spermine (Spm) which can alleviate the effects of abiotic stresses on plants. Exogenous Spd has been reported to improve plant tolerance to abiotic stresses including salinity [12]. Spraying with Spd on rice leaves could also alleviate oxidative stress on rice [13]. Moreover, diluted wood vinegar (WV) could promote growth under salt stress of rice seedlings [14]. The objective of this study was to examine the effect of two plant growth regulators including Spd and WV on alleviation of salt-stress damages in rice under salt stress.

2. Materials and Methods

2.1 Plant materials and treatment

Seeds of rice cv. RD6 were obtained from Khon Kaen Rice Research Center, Department of Rice, Thailand. The experiment was performed in a greenhouse at the Department of Biology, Faculty of Science, Khon Kaen University. Seeds were surface-sterilized with 15% sodium hyperchlorite for 15 min, then rinsed 5 times with distilled water. The seeds were germinated in dark conditions for 3 days. Seedlings were then planted in pots containing 5 kg of dry soil from paddy field. The soil was loamy sand comprising 0.55% organic matter, 0.045% Nitrogen, 0.32 mg kg^{-1} Phosphorous, 25.21 mg kg^{-1} Potassium, 68.70 mg kg^{-1} Sodium and 11.50 mg kg^{-1} Chlorine, having a slightly alkaline pH at 6.55 and electrical conductivity at 0.045 dS m^{-1}. When rice seedlings were 30 days old, they were subjected to 8 spraying treatments as follows: distilled water (control), diluted wood vinegar (WV) (1:500), Spd solutions (0.05, 0.1, 0.5 mM) and mixture between WV (1:500) and Spd solutions (0.05, 0.1, 0.5 mM) using 50 ml of solutions per pot during 17.00-18.00 for 5 days. The dilution of WV and concentrations of Spd used were based on previous studies [14, 15]. Afterwards, salt stress was imposed by watering with 100 mM NaCl solution (salt-stressed group) for 3 days. Then, NaCl concentration was increased to 150 mM. Another set of plants also received

8 spraying treatments but continued to be fed with regular watering (non-stressed group). Experimental design was completely randomized with five pots for each spraying treatment and each pot contained 12 plants.

2.2 Measurement of plant growth

Growth data and leaf physiological parameters were collected at 14 days after adding sodium chloride. Plant growth parameters measured included shoot fresh weight, shoot dry weight, root fresh weight, root dry weight, shoot length and root length. For dry weight measurement, all samples were dried in hot air oven at 70 °C for 72 h.

2.3 Measurement of physiology

Physiological measurements included net photosynthetic rate (P_N) by using an infra-red gas analyzer (LI-COR 6400XT portable photosynthesis system, LI-COR, Lincoln, Nebraska, USA) using the following conditions; light intensity at 1,500 µmol (photon) m^{-2} s^{-1}, chamber temperature at 30 °C and CO_2 concentration at 400 µl l^{-1}, chlorophyll fluorescence parameters by chlorophyll fluorometer (HandyPEA, Hansatech Instruments), relative water content (RWC) by using the following formula RWC=(FW-DW)/(TW-DW) × 100, where FW, DW and TW was initial fresh weight, dry weight and fully turgid weight, respectively. Membrane stability was determined by measuring electrolyte leakage percentage (EL) by cutting fresh leaves sample into 1 cm^2, placing 6 pieces in closed vials containing 10 ml of deionized distilled water, incubating at 25 °C for 24 h in the dark and measure electrical conductivity (EL1). Then, the vials containing leaf pieces were boiled (100 °C) for 15 min and left to cool down to room temperature, electrical conductivity of the solution was measured to obtain EL2. EL (%) was estimated as: (EL1/EL2) × 100.

2.4 Statistical analysis

SPSS ver. 23 was used for statistical analysis. Data were presented as means ± SE. Significant difference among the treatment means was determined by Duncan's multiple range test (DMRT) ($p \leq 0.05$). Each treatment had five replications and this experiment was designed by using completely randomized design (CRD).

3. Results and Discussion

As shown in Table 1, plants exposed to salt stress for 14 days did not show significant reduction in growth parameters compared with those of the non-stress plants. Among the non-stressed groups, only plants sprayed with 0.5 mM Spd+WV had significantly higher growth (shoot and root fresh weight, FW and shoot dry weight, DW) than the control plants sprayed with H_2O. The solution 0.5 mM Spd+WV induced the highest shoot FW (7.63 g $plant^{-1}$) and root FW (8.28 g $plant^{-1}$) which were 45.33 and 53.90% increase from the plants sprayed with H_2O. In addition, plants sprayed with diluted WV (1:500) had significantly higher shoot DW (1.64 g $plant^{-1}$) than that of the control (1.17 g $plant^{-1}$). For the plants exposed to NaCl stress, most spraying treatments tended to increase growth (fresh and dry weights) compared with plants sprayed with H_2O but the differences were not statistically significant. It is noted that, among salt-stress groups, spraying with diluted WV resulted in highest shoot FW (7.32 g $plant^{-1}$) and shoot DW (1.73 g $plant^{-1}$) (although not significantly different from the plants sprayed with water). WV was the most effective solution that induced the

highest shoot growth (both FW and DW) for NaCl-treated plants. For root growth, highest FW was recorded for 0.1 mM Spd, and highest DW for 0.05 mM Spd. Similar with Shunkao and Theerakulpisut [16] suggested that foliar spraying with Spd could alleviate salt-stress effects and enhance growth of rice cv. KDML105. Chunthaburee *et al*. [15] also reported that Spd priming improved growth of rice seedling when plants were exposed to salt stress. Moreover, Theerakulpisut *et al*. [14] demonstrated that seed priming with wood vinegar could also alleviate the effect of salt stress on growth in rice cv. KDML105.

Salinity stress damaged plant membranes as indicated by dramatic increase in electrolyte leakage from 6.3-16.3% in the non-stressed group to 48.1-75.7 % in the salt-stressed group (Figure 1 A). Under non-stressed condition, spraying with Spd and WV demonstrated no significant difference as compared with water spraying. Under salt stress condition, spraying with 0.05 mM Spd was able to significantly decrease EL from 75.7 % (sprayed with H_2O) to 48.1%. Similar findings by Shunkao and Theerakulpisut [16] showed that foliar spray with Spd also reduced membrane damage in leaves of salt-stressed rice cv. KDML105.

Salinity caused osmotic effects and salt-stressed plants had lower RWC than non-stressed plants (Figure 1B). Plants treated with salts had lower RWC than non-stressed ones. However, for both non-stressed and salt-stressed conditions, RWC of plants sprayed with all Spd and WV treatments did not differ significantly from that of the controls (sprayed with water). Our results are in agreement with Bassiouny and Bekheta [17] who reported that salt stress decreased the RWC of wheat.

Table 1. Effect of foliar spraying with wood vinegar (WV), spermidine (Spd) and mixture of both, on growth of rice plants after exposure to sodium chloride (150 mM NaCl) for 14 days.

Treatment	Lengths (cm)		Fresh weights (FW) (g plant^{-1})		Dry weights (DW) (g plant^{-1})	
	Shoot	Root	Shoot	Root	Shoot	Root
Non-stressed (H_2O)						
H_2O	69.6abc	21.0a	5.25bc	5.38bcd	1.17cd	0.80abc
WV (1:500)	71.6a	24.9a	7.42ab	8.08ab	1.64ab	1.11a
0.05 mM Spd	66.1abc	24.2a	5.99abc	7.14abcd	1.31abcd	0.96ab
0.1 mM Spd	70.7ab	26.5a	6.92abc	7.60abc	1.48abcd	0.96ab
0.5 mM Spd	68.3abc	26.3a	5.59abc	6.20abcd	1.24bcd	0.86abc
0.05 mM Spd+WV	68.4abc	22.1a	4.85c	5.51bcd	1.08c	0.72bc
0.1 mM Spd+WV	71.6a	26.0a	6.96abc	7.82abc	1.60abc	1.09a
0.5 mM Spd+WV	71.4a	24.7a	7.63a	8.28a	1.69ab	1.09a
Salt-stressed (NaCl)						
H_2O	67.6abc	21.6a	5.60abc	4.55c	1.28abcd	0.52c
WV (1:500)	66.7abc	21.3a	7.32ab	5.52bcd	1.73a	0.65bc
0.05 mM Spd	64.8bc	24.6a	6.47abc	6.36abcd	1.43abcd	0.71bc
0.1 mM Spd	64.2c	26.0a	6.51abc	6.58abcd	1.36abcd	0.65bc
0.5 mM Spd	65.9abc	25.9a	5.45abc	5.92abcd	1.29abcd	0.58c
0.05 mM Spd+WV	64.9bc	24.8a	6.20abc	6.12abcd	1.39abcd	0.63bc
0.1 mM Spd+WV	66.3abc	25.7a	6.08abc	5.96abcd	1.31abcd	0.84abc
0.5 mM Spd+WV	66.5abc	22.5a	7.16ab	5.29bc	1.58abc	0.68bc

*Means in the same column sharing same alphabets were not significantly different at P≤0.05

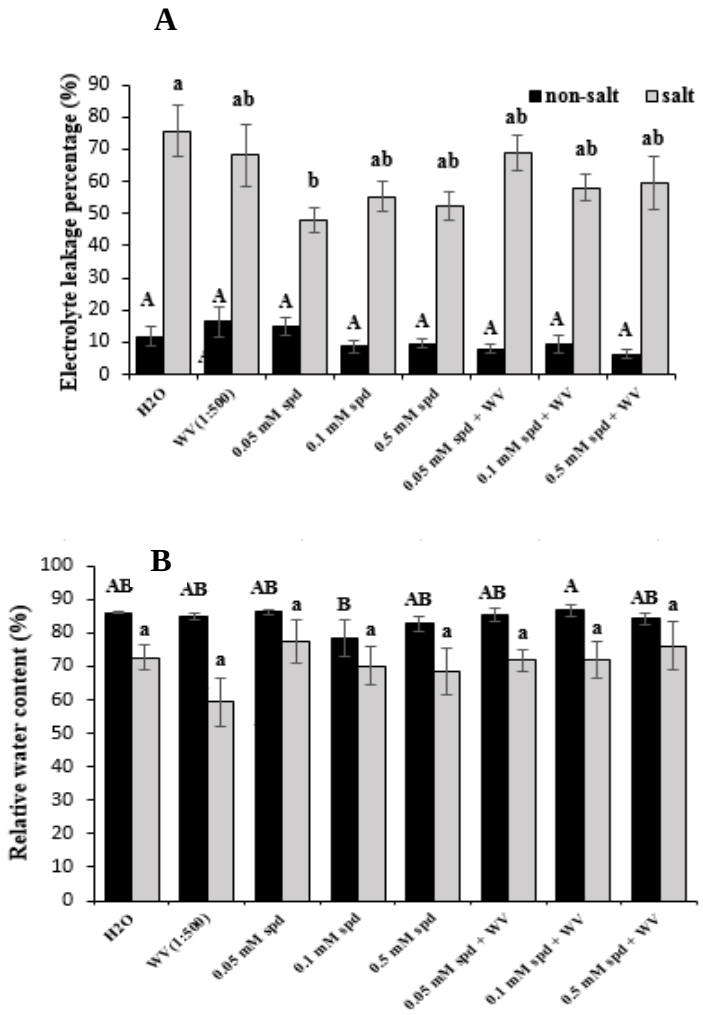

Figure 1. Effect of spraying with spermidine and wood vinegar on electrolyte leakage percentage (A) and relative water content (B) after giving sodium chloride (150 mM NaCl) for 14 days. [mean±SE, means sharing same alphabets (uppercase, non-saline condition; lowercase, saline condition) were not significantly different at P≤0.05].

Salt stress decreases photosynthesis of crops by inducing stomatal closure and hence reducing CO_2 diffusion or by alteration of photosynthetic metabolism as a result of ion toxicity [18]. Salt treatment could reduce photosynthesis in *Populus euphratica* [19], *Citrus reshni* [20] and *Oryza sativa* [21]. In this study, net photosynthesis rates under non-stressed conditions ranged from 22.1 to 25.1 µmol CO_2 m^{-2} s^{-1} while those of the stressed plants reduced from 7.5 to 11.6 µmol CO_2 m^{-2} s^{-1}. Spraying with 0.1 mM Spd+WV, 0.5 mM Spd+WV and 0.5 mM Spd could alleviate effects of salt stress on photosynthesis by causing 36.5, 28.2 and 28.2%, respectively increase (although non-significantly different) in net photosynthesis rates compared with water spraying. In non-stressed condition, spraying with 0.05 mM Spd+WV, 0.1 mM Spd+WV and 0.5 mM Spd+WV can cause non-significant increase in net photosynthesis rates (9.6%, 5.2% and 4.8%, respectively)

compared with water spraying (Figure 2A). Similar to Anjum [22], adding 0.5 mM Spd to the NaCl nutrient solution could significantly increase net photosynthesis rate of Troyer citrange stressed with 75 mM NaCl. In addition, foliar spraying with 0.5 mM Spd could increase net photosynthesis rate of rice cv. Pokkali under salt stress [16].

Salt stress affected function of chloroplast photosystems by reducing maximal quantum yield of PSII photochemistry (Fv/Fm) [23]. Similar to this study, salt stress reduced Fv/Fm of plants sprayed with H_2O (from 0.827 to 0.812) and spraying with 0.5 mM Spd significantly increase Fv/Fm of salt-stressed plants to 0.821 (Figure 2B). The remaining spraying treatments also increased Fv/Fm without any significantly difference from water spraying.

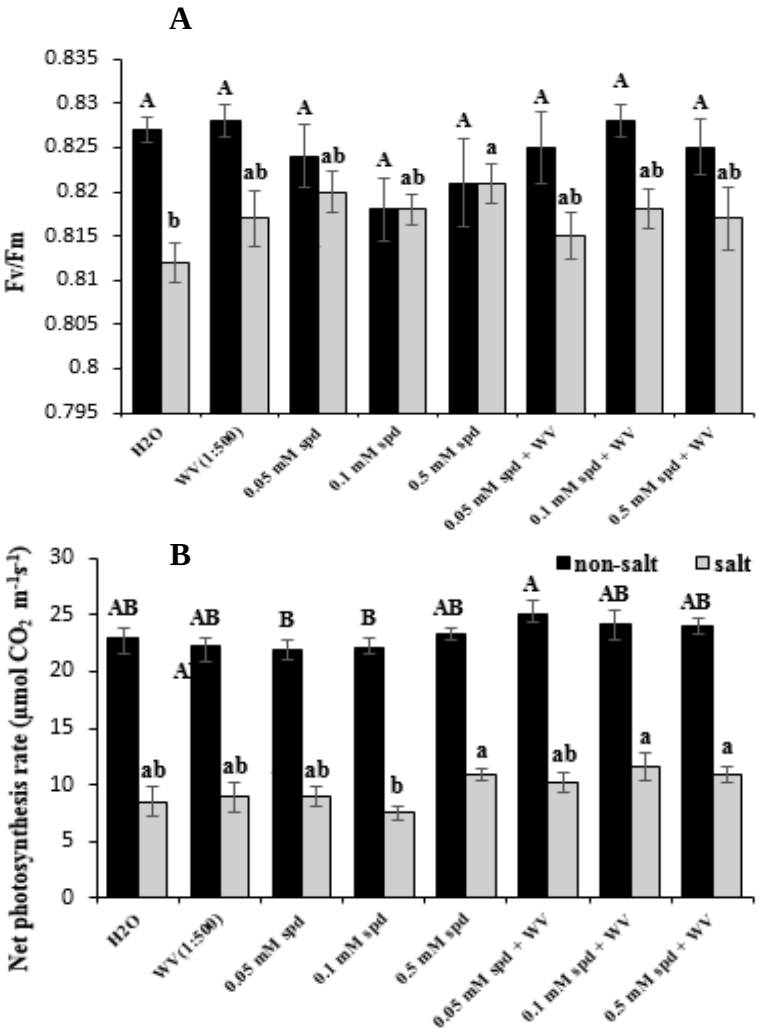

Figure 2. Effect of spraying with spermidine and wood vinegar on net photosynthesis rate (A) and Fv/Fm (B) after giving sodium chloride (150 mM NaCl) for 14 days. [mean±SE, means sharing same alphabets (uppercase, non-saline condition; lowercase, saline condition) were not significantly different at P≤0.05].

4. Conclusions

Under salt stress, foliar spraying with diluted WV tended to promote shoot growth of rice cv. RD6 while spraying with 0.1 mM Spd (with or without WV) had a tendency to increase root growth. The physiological characteristics showed that salt stress increased EL, and reduced RWC, P_N and F_v/F_m. Foliar spraying with 0.05 mM Spd and 0.5 mM Spd alleviated adverse effects of salt stress by reducing EL and increasing Fv/Fm, respectively. For practical application, the effectiveness of Spd and WV on alleviation of salt stress in rice should be further explored in the field condition.

5. Acknowledgements

This study was supported by Science Achievement Scholarship of Thailand (SAST) and Salt-tolerant Rice Research Group, Department of Biology, Faculty of Science, Khon Kaen University.

References

[1] Topark-Ngam, B., 2006. *Saline Soils in Northeast Thailand.* 1st ed. Khon Kaen: Khon Kaen Printing Co., Ltd. [In Thai]

[2] Kanawapee, N., Sanitchon, J., Lontom, W. and Threerakulpisut, P., 2012. Evaluation of salt tolerance at the seedling stage in rice genotypes by growth performance, ion accumulation, proline and chlorophyll content. *Plant and Soil,* 358, 235-249.

[3] Land Development Department, 2016. *Farmer's Guide to Northeastern Saline Management*. Ministry of Agriculture and Cooperatives : Bangkok.

[4] Estaji, A., Roosta, H.R., Rezaei, S.A., Hosseini, S.S. and Niknam, N., 2018. Morphological, physiological and phytochemical response of different *Satureja hortensis* L. accessions to salinity in a greenhouse experiment. *Journal of Applied Research on Medicinal and Aromatic,* 10, 25-33.

[5] Munns, R. and Tester, M., 2008. Mechanisms of salinity tolerance. *Annual Review of Plant Biology,* 59, 651-681.

[6] Zhang, L., Ma, H., Chen, T., Pen, J., Yu, S. and Zhao, X., 2014. Morphological and physiological responses of cotton (*Gossypium hirsutum* L.) plants to salinity. *PLoSONE,* 9(11): e112807.

[7] Farhoudi, R., Modhej, A. and Afrous, A., 2015. Effect of salt stress on physiological and Morphological parameters of rapeseed. *Journal of Scientific Research and Development,* 2(5), 111-117.

[8] Ramezani, E., Sepanlou, M.G. and Badi, H.A.N., 2011. The effect of salinity on the growth, morphology and physiology of *Echium amoenum* Fisch. & Mey. *African Journal of Biotechnology,* 10(44), 8765-8773.

[9] Ashraf, M., 2009. Biotechnological approach of improving plant salt tolerance using antioxidants as markers. *Biotechnology Advances,* 27, 84-93.

[10] Foyer, C.H. and Halliwell, B., 2000. Oxygen processing in photosynthesis: regulation and signaling. *New Phytologist,* 146(3), 359-388.

[11] Theerakulpisut, P., 2016. *Physiology of Plants under Salt Stress*. Khon Kaen: Khon Kaen Printing Co., Ltd. Khon Kaen University. pp. 73-140. [In Thai]

[12] Chen, D., Shao, Q., Yin, L., Younis, A. and Zheng, B., 2018. Polyamine function in plants: Metabolism, regulation on development, and roles in abiotic stress responses. *Frontiers in Plant Science,* 1945 (9), 1-13.

[13] Liu, M., Chu, M., Ding, Y., Wang, S., Liu, Z., Tang, S., Ding, C. and Li, G., 2015. Exogenous spermidine alleviates oxidative damage and reduce yield loss in rice submerged at tillering stage. *Frontiers in Plant Science* 919(1), 1-11.

[14] Theerakulpisut, P., Kanawapee, N. and Panwong, B., 2016. Seed Priming Alleviated Salt Stress Effects on Rice Seedlings by Improving Na^+/K^+ and Maintaining Membrane Integrity. *International Journal of Plant Biology*, 6402(7), 53-58.

[15] Chunthaburee, S., Sanitchon, J., Pattanagul, W. and Theerakulpisut, P., 2014. Alleviation of salt stress in seedlings of black glutinous rice by seed priming with spermidine and gibberellic acid. *Notulae Botanicae Horti Agrobotanici Cluj-Napoca*, 42, 405-413.

[16] Shunkao, S. and Theerakulpisut, P., 2019. Effects of salinity on photosynthesis and growth of rice and alleviation of salt-stress by exogenous spermidine. *Khon Kaen Agriculture Journal*, 47(1), 1-6.

[17] Bassiouny, H.M.S. and Bekheta, M.A., 2005. Effect of salt stress on relative water content, lipid peroxidation, polyamines, amino acids and ethylene of two wheat cultivars. *International Journal of Agriculture & Biology*, 3(7), 363-368.

[18] Chaves, M.M., Flexas, J. and Pinheiro., 2009. Photosynthesis under drought and salt stress: Regulation mechanisms from whole plant to cell. *Annals of Botany*, 103, 551-560.

[19] Ma, H.C., Fung, L., Wang, S.S., Altman, A. and Hüttermann, A., 1997. Photosynthetic response of *Populus euphratica* to salt stress. *Forest Ecology and Management*, 93, 55-61.

[20] Anjum, M.A., 2010. Response of Cleopatra mandarin seedlings to a polyamine biosynthesis inhibitor under salt stress. *Acta Physiologiae Plantarum*, 32, 951-959.

[21] Nounjan, N., Chansongkrow, P., Charoensawan, V., Siangliw, J.L., Toojinda, T., Chadchawan, S. and Theerakulpisut, P., 2018. High performance of photosynthesis and osmotic adjustment are associated with salt tolerance ability in rice carrying drought tolerance QTL: Physiological and co-expression network analysis. *Frontiers in Plant Science*, 9, 1135.

[22] Anjum, M.A., 2011. Effect of exogenously applied spermidine on growth and physiology of citrus rootstock Troyer citrange under saline conditions. *Turkish Journal of Agriculture and Forestry*, 35, 43-53.

[23] Demetriou, G., Neonaki, C., Navakoudis, E. and Kotzabasis, K., 2007. Salt stress impact on the molecular structure and function of the photosynthetic apparatus -The protective role of polyamines. *Biochimica et Biophysica Acta*, 1767, 272-280.

Responses of Landrace Rice to Organic Fertilizer for Physiological Traits, Grain Yield and Total Phenolic Content

Nattareeporn Rodnuch, Sitthichai Phongsri and Chorkaew Aninbon*

Department of Plant Production Technology, Faculty of AgriculturalTechnology, King Mongkut's Institute of Technology Ladkrabang, Bangkok, Thailand

Received: 2 August 2019, Revised: 28 August 2019, Accepted: 30 August 2019

Abstract

Organic fertilizers are used as a main source of plant nutrients in organic food production. A better understanding on the responses for the physiological traits of rice to the application of organic fertilizers is essential for organic rice production. The aim of this study was to determine the effect of organic fertilizer on physiological traits, yield components and total phenolic content of two landrace rice varieties, i.e Leam Phu and Hom Dong. A 2×3 factorial experiment in randomized complete block design with three replications was undertaken under field condition during July 2018 to December 2018. Two rice varieties were assigned as factor A and three fertilizers were assigned as factor B. Data were collected for crop growth rate (CGR) at tillering to panicle initiation stage. Leaf area index (LAI) was collected at 60, 90 and 120 days after transplanting (DAT). Agronomic traits including number of tiller per plant, plant height, number of panicle per plant, one thousand seed weight, grain yield and total phenolic content were collected at appropriate times. Fertilizers showed significantly different effect on CGR and LAI. Although chemical fertilizer gave the highest grain yield (2,572.6 kg/ha), it was not significantly higher than organic fertilizer (2,100 kg/ha). Leam Phu gave higher total phenolic content than Hom Dong at all fertilizers applied without significant difference.

Keywords: fertilizer types, crop growth rate, polyphenol, yield components
DOI 10.14456/cast.2019.25

1. Introduction

Rice is an important staple food crop of the world and it is source of carbohydrate and protein. Rice is also rich in many important phytochemicals including flavonoids, niacin, riboflavin and phenolic compounds [1]. Phenolic compounds with strong antioxidant activity are the secondary metabolites found in many plant species. Daily consumption of 500-1,000 mg of phenolic compounds can reduce the risk of heart disease, have anti-cancer and anti-inflammatory effects, and reduce blood cholesterol [2].

Rice productivity has increased continually due largely to the use of high yielding varieties and the application of chemical fertilizers. The application of chemical fertilizers is more important means for yield increase of rice [3]. However, the application of chemical fertilizers at high rates and for long term in recent years causes a serious concern about the harmful effects on soil and environment [4]. Therefore, the application of fertilizers from organic sources might help reduce the application of chemical fertilizers.

*Corresponding author: E-mail: chorkaew.an@kmitl.ac.th

Previous studies have been reported on the effects of organic fertilizers on phytochemical traits of many crops. In pepper, application of organic manures represented a suitable alternative means for food production with nutraceutical quality [5]. Organic fertilizer was also found to increase phenolic compounds and antioxidant activity in tomato [6]. Total phenolic content was found to be lower in rice treated with control and organic fertilizer than rice treated with inorganic fertilizer [7]. Phenolic compound in japonica rice grown under organic and conventional farming systems showed the same total phenolic content but the antioxidant capacity (DPPH) was significantly higher in organic farming treatment [8].

The effects of organic fertilizers on phenolic compounds are still not conclusive. The effects seemed to be dependent on plant species and genotype. The responses to organic fertilizer in rice on physiological traits, grain yield and phenolic content have not been clearly studied in indigenous rice, which might be different from high yielding varieties. The objective of this study was to determine the effects of organic fertilizer on physiological traits, grain yield, yield components and total phenolic content in rice. The information will be used for planning organic rice production in the future.

2. Materials and Methods

2.1 Location and experimental design

A 2×3 factorial experiment was undertaken under field condition to study the effects of organic fertilizer on growth, yield and phenolic content of two indigenous rice varieties. Two rice varieties which was representative of rice with black and white pericarp including Leam Phu and Hom Dong were assigned as factor A. Leam Phu is a black sticky landrace rice in Thailand. Hom Dong is a fragrant landrace variety with white pericarp. Three fertilizer applications consisting of no fertilizer (NO), chemical fertilizer (CF) and organic fertilizer (OF) were assigned as factor B. and the six treatment combinations were arranged in a randomized complete block design with three replications at the Research Station of Plant Production Technology Department, Faculty of Agricultutal Technology, King Mongkut's Institute of Technology Ladkrabang, Bangkok, Thailand. The organic fertilizer used in this study was well-decomposed livestock manure and pH, EC, organic matter, total N, total P and total K were 8.3, 27.3 dS/m, 44.3%, 1.85%, 1.15% and 1.89%, respectively. The chemical fertilizers consisted of N-P-K (16-20-0 and 46-0-0).

2.2 Experimental details and crop management

Two rice varieties were planted for 25 days and the seedlings were transplanted at the rate of one plant per hill and a spacing of 25 cm between plants and 25 cm between rows in a plot size of 1.5×1.5 m. The rice bunds with 1 m in width were constructed as the alleys between blocks. The water level was maintained at 5 cm above the soil surface throughout the experiment. Chemical fertilizer with 16-20-0 of N-P-K at the rate of 156.25 kg/ha was applied at 15 days after transplanting (DAT) and chemical fertilizer (46-0-0) at the rate of 156.25 kg/ha was pre-heading stage. Organic fertilizer at the rate of 2,000 kg/rai (12,500 kg/ha) was applied at 15 DAT and pre-heading stage. Therefore, total chemical fertilizer applied to the crop was 312.50 kg/ha and total organic fertilizer was 25,000 kg/ha. Pesticide and herbicide were applied as needed.

2.3 Data collection

1) Physiological traits: Leaf Area Index (LAI) was recorded at 60, 90 and 120 days after transplanting. LAI was calculated as a formula;

$$LAI = \text{leaf area } (cm^3)/\text{ground area (GA)}.$$

Crop growth rate (CGR) was recorded at tillering to panicle initiation stages. Two plants from each plot were cut into small pieces and oven-dried at 80 °C for 72 h or until the weight was constant. Crop growth rate ($g\ m^{-2}\ day^{-1}$) during tillering to panicle initiation stages was calculated by using the formula;

$$CGR = W2\text{-}W1/T2\text{-}T1,$$

where W2 = plant dry weight at panicle initiation stage and W1 = plant dry weight at tillering stage, T1 = Time unit at first harvest, T2 = Time unit at next harvest.

2) Yield components: At flowering stage, five plants of each subplot were randomly chosen and the data were recorded for plant height in the field. The same plants in each plot were also used for recording number of tillers per plant and number of panicles per plant. Seed yield was measured at harvest time (120 DAT). The seeds were sundried at approximately 13% moisture content and weighed. One thousand seed were randomly chosen and weighted to determine 1000-seed weight.

3) Total phenolic content: Husked rice (with husk removal) was ground using a grinding machine and subsample of 2 g for each plot was used for extraction of phenolic compounds. The ground rice powder was then extracted in 10 ml of methanol for 24 h at room temperature, filtered through a 0.45 μm of nylon membrane filter and stored at 4 °C for further analysis.

Total phenolic content was determined by Folin-Ciocalteu's assay [9]. The crude extract (50 μl) was diluted to 3.0 ml with distilled water. Folin-Ciocalteu reagent at the concentration of 250 μl was added to the sample and stirred thoroughly. The sample was further added with 20% sodium carbonate solution at the volume of 750 μl and the mixture was allowed to stand for 2 h. The mixture solution was measured at 765 nm using a Thermo Spectrophotometer. The phenolic content was demonstrated as Gallic acid equivalent (mg GAE/100 g dry weight of rice seed).

2.4 Data analysis

Data were analyzed statistically according to a factorial experiment in a randomized complete block design using STATISTIX 8 [10]. Least significance difference (LSD) was used to compare means [11]. The correlations between grain yield and LAI and total phenolic content were analyzed using regression method.

3. Results and Discussion

3.1 Physiological traits

Varieties were not significantly different for CGR at tillering to panicle initial stage whereas fertilizers were significantly different ($P \leq 0.01$) (Table 1). Chemical fertilizer produced the highest

Table 1. Crop growth rate (CGR) during tillering to panicle initiation stage and leaf area index (LAI) at 60, 90 and 120 days after transplanting (DAT) of two landrace rice varieties treated with different fertilizer applications.

Treatment	CGR ($g\ day^{-1}cm^{-1}$)	LAI at 60 DAT	LAI at 90 DAT	LAI at 120 DAT
Variety (V)				
Leam Phu (LP)	26.39	1.79[b]	6.57[a]	6.88
Hom Dong (HD)	24.47	2.35[a]	5.46[b]	4.28
Fertilizer (F)				
Chemical fertilizer (CF)	37.46[a]	0.98[b]	8.42[a]	9.20
Organic Fertilizer (OF)	22.20[a]	4.23[a]	5.95[b]	5.36
Non-fertilizer (NF)	16.63[b]	1.00[b]	3.76[c]	1.88
Variety × Fertilizer				
LP × CF	36.29	0.93	8.93	12.18[a]
LP × OF	21.85	3.74	7.34	5.80[b]
LP × NF	15.28	0.67	3.41	2.04[c]
HD × CF	38.63	1.01	7.91	5.80[b]
HD × OF	22.54	4.71	4.54	4.92[b]
HD × NF	17.99	1.33	3.92	1.71[c]
F – Test				
V	ns	*	**	**
F	**	**	*	**
V × F	ns	ns	ns	*
C.V. (%)	8.72	13.10	17.52	24.80

Means in the same column followed by the same letter were not significantly different at $P \leq 0.05$ by LSD.
ns, * and ** = non-significant, significant at $P \leq 0.05$ and significant at $P \leq 0.01$, respectively.

CGR of 37.46 g $day^{-1}cm^{-1}$ followed by organic fertilizer (22.20 g $day^{-1}cm^{-1}$) whereas control (non-fertilizer) control showed significantly lowest CGR. The interaction between rice variety and fertilizer was not significant.

CGR is a simple and important index for evaluating agricultural productivity based on the rate of dry matter production. In this study, fertilizer types were significantly different for CGR. According to Reddy and Reddi [12], application of nitrogen significantly affected CGR but it did not significantly affect plant height of rice. In this study, both chemical and organic fertilizers could increase GGR. Higher GCR for these treatments would be possibly due to higher tillers and higher vegetative growth. According to Hasanuzzaman *et al*. [13], wetland rice treated with poultry manure had the highest crop growth rate (CGR) and relative growth rate (RGR) because of the higher number of tillers per plant. The interaction between rice variety and fertilizer was not significant, indicating that the indigenous rice varieties responses to fertilizer application in a similar pattern.

The differences between rice varieties were significant for LAI at all growth stages (Table 1). At final harvest (120 DAT), Leam Phu had higher LAI than Hom Dong. The results indicated that Leam Phu had slower leaf senescence than did Hom Dong. Organic fertilizer produced the highest LAI at 60 DAT whereas chemical fertilizer produced the highest LAI at 120 DAT. The interaction between rice variety and fertilizer for LAI was significant at 120 DAT but not at 60 and 90 DAT. It was shown that Leam Phu treated with chemical fertilizer gave the highest LAI of 12.18

with significant difference. The results were similar to earlier report by Ko *et al*. [14] who reported that LAI in rice had the highest under inorganic fertilizer treatment. Kumar *et al*. [15] also reported that chemical fertilizer influence LAI by increasing leaf size and tiller number.

3.2 Growth and yield components

Rice varieties and fertilizers were not significantly different for plant height and the interaction between rice variety and fertilizer was not significant (Table 2). The lack of variation for plant height would possibly due to the fact that both rice varieties are indigenous varieties with tall type.

Rice varieties were not significantly different for tiller number but fertilizers was significantly different for this trait. Chemical fertilizer had the highest tillers (9.23) followed by organic fertilizer (8.06) whereas non-fertilizer had the lowest tillers (5.78). There is no significant difference on the interaction between rice variety and fertilizer which indicated that rice varieties responded to fertilizers in the similar fashion.

Rice varieties were not significantly different for number of seeds per panicle but fertilizers was significantly different for this trait. Chemical fertilizer produced the highest the number of seeds per panicle (326.13 seeds) followed by organic fertilizer (291.73 seeds) and non-fertilizer (234.03 seeds), respectively. The non significant interaction between rice variety and fertilizer indicated that the responses of rice varieties were similar.

Varieties and fertilizers were significantly different for 1,000 seed weight but the interaction between variety and fertilizer was not significant (Table 2). Hom Dong had large seeds (28.72 g) than did Leam Pua (20.71 g). Chemical fertilizer and organic fertilizer produced higher 1,000 seed weight than did non-fertilizer control. The non significant interaction between rice variety and fertilizer showed that rice varieties responded similarly for this trait.

Rice varieties were not significantly different for grain yield but the differences among fertilizers were significant. Chemical fertilizer had the highest grain yield per hectare (2,572.6 kg/ha) followed by organic fertilizer (2,100.4 kg/ha) and no fertilizer control (1,711.0 kg/ha), respectively.

The results were similar to those reported in previous studies. Sudarsono *et al*. [16] found that application of cattle manure increased plant height, number of tillers per plant and grain yield. However, the application of organic fertilizer was still lower than the application of chemical fertilizer for these traits. Non-significant interaction between rice variety and fertilizer also indicated the similar responses of rice varieties for grain yield.

3.3 Phenolic content

Significant difference between rice varieties was observed for phenolic content and Leam Phu gave higher phenolic content than Hom Dong (Figure 1). Fertilizers were not significantly different for phenolic content and the interaction between rice variety and fertilizer was not significant.

Phenolic compounds are known to have antioxidant activity. In this study, fertilizers were not significantly different for phenolic content. The results were in agreement with those reported in previous studies. Kessarwani *et al*. [8] found that rice crops grown under organic and conventional faming systems were not significantly different for phenolic content. In many plant species such as raspberry [17], pepper [5] and tomatoes [6], organic management increased total phenolic content better than did conventional management. The results indicated that plant species respond differently to organic fertilizer for phenolic content.

In this study, Leam Phu had total phenolic contents four times higher than did Hom Dong (Figure 1). This is because Leam Phu is black rice and Hom Dong is normal white rice. Muntana

Table 2. Plant height (cm), number of tillers per plant (Till./Plant), number of seeds per panicle (Seed/Pa), 1,000 seed weight (1,000 SW) and grain yield of two landrace rice varieties treated with different fertilizer applications.

Sources of variation	Height (cm)	Till./Plant	Seed/Pa (seeds)	1,000 SW (g)	Grain yield (kg/ha)
Variety (V)					
Leum Pua (LP)	164.71	7.51	290.56	20.71[b]	1,880.5
Hom Dong (HD)	186.74	7.87	277.38	28.72[a]	2,376.1
Fertilizer (F)					
Chemical fertilizer (CF)	179.05	9.23[a]	326.13[a]	25.27[a]	2,572.6[a]
Organic Fertilizer (OF)	182.00	8.06[a]	291.73[b]	24.79[ab]	2,100.4[ab]
No-fertilizer (NF)	166.13	5.78[b]	234.03[c]	24.08[b]	1,711.0[b]
Variety × Fertilizer					
LP × CF	173.44	8.96	337.47	21.25	2,543.1
LP × OF	184.66	8.06	314.80	20.84	2,137.8
LP × NF	176.22	5.50	300.40	20.03	1,617.9
HD × CF	187.77	9.50	283.07	29.29	3,369.7
HD × OF	144.48	8.06	233.80	28.74	2,052.1
HD × NF	187.78	6.06	234.27	28.13	1,482.1
F – Test					
V	ns	ns	ns	*	ns
F	ns	*	**	**	*
V × F	ns	ns	ns	ns	ns
C.V. (%)	13.93	6.79	8.85	2.56	23.98

Means in the same column followed by the same letter were not significantly different at $P \leq 0.05$ by LSD.
ns, * and ** = non-significant, significant at $P \leq 0.05$ and significant at $P \leq 0.01$, respectively.

and Prasong [18] reported that total phenolic content in colored rice was higher rather than in white rice.

The range of phenolic contents in this study was from 14.79 to 97.89 mg GAE/100 g seeds. When the results were compared with those in other studies, the range found in this study was considered intermediate. Tuaño *et al.* [7] reported that total phenolic compounds ranged from 30.01 to 37.59 mg GAE/100 g wet seeds and Kesarwani *et al*. [8] also reported that the range of phenolic content was from 162.7 to 167.4 mg GAE/100 g fresh seeds. The differences in the ranges of phenolic content in different studies would be due to the differences in rice varieties used and the differences in seed growth stages (mature, immature or dry seeds).

Correlation between grain yield and phenolic content, CGR, leaf area index at 60 DAT, 90 DAT was presented in Figure 2. The results indicated that the correlation between grain yield and LAI 90 ($R^2 = 0.5789$) was highest followed by CGR, phenolic content and LAI 60. A better crop growth rate and high leaf area index at 90 DAT may be used as selection criteria for high grain yield and indicators for crop responses to fertilizer application.

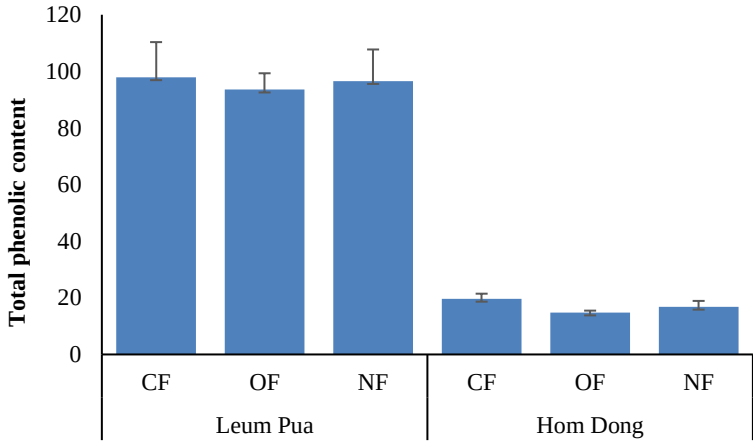

Figure 1. Total phenolic content (mg/GAE100g seeds) in two landrace rice varieties treated with different fertilizer applications, CF = chemical fertilizer, OF =organic fertilizer and NF = no fertilizer.

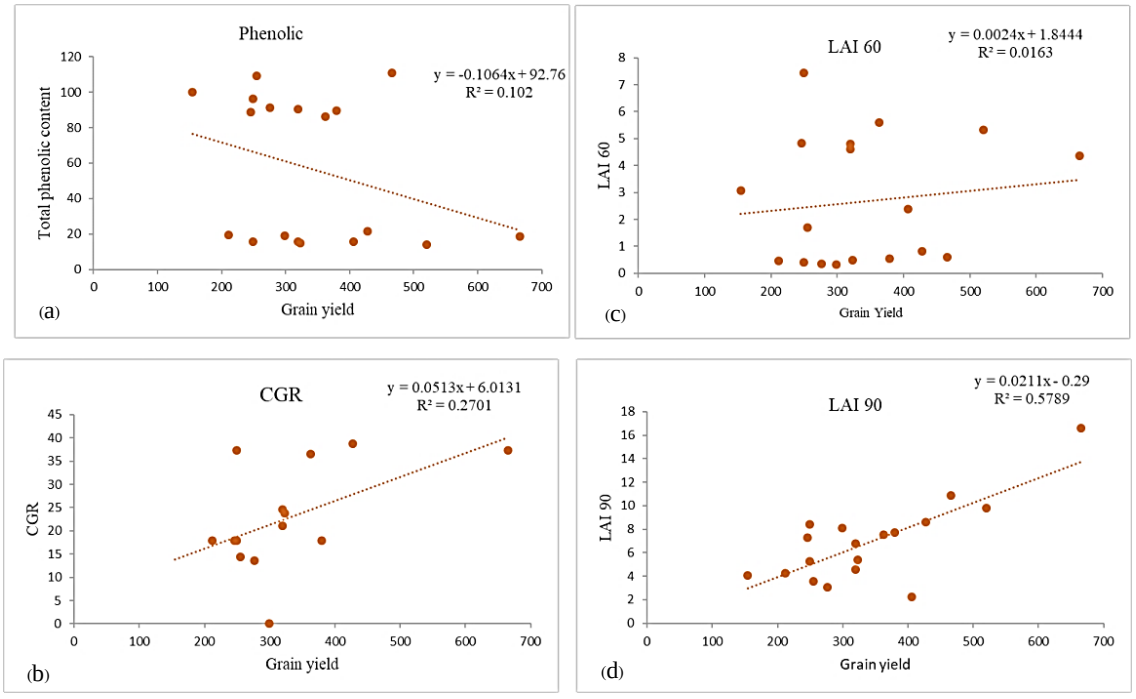

Figure 2. Correlation coefficients between grain yield and total phenolic content (a), grain yield and crop growth rate (b), grain yield and leaf area index at 60 DAT (c) and grain yield and leaf area index at 90 DAT (d) of two rice varieties treated with different fertilizer applications.

4. Conclusions

Organic fertilizer as well as chemical fertilizer increased crop growth rate, leaf area index, yield components and grain yield of two landrace rice varieties. Organic fertilizer gave lower grain yield than chemical fertilizer but not statistically significant. The increase in grain yield was due to the increases in tiller number, grain number and grain weight but not due to plant height. Most interactions between rice variety and fertilizer were not significant, indicating the similar responses of rice varieties to fertilizer application. Leam Phu gave higher total phenolic content than Hom Dong but fertilizer application did not significantly affect the total phenolic content. Although this experiment found that organic fertilizer did not affect phenolic compounds but it was not decreased. The effect of organic fertilizer on individual phenolic acids and antioxidant capacity in landrace rice should further be examined.

5. Acknowledgements

The authors are grateful for the financial support from Faculty of Agricultural Technology, King Mongkut's Institute of Technology Ladkrabang, Bangkok, Thailand.

References

[1] Isaac, R.S.R., Nair, A.S., Varghese, E. and Chavali1, M., 2012. Phytochemical, antioxidant and nutrient analysis of medicinal rice (*Oryza Sativa* L.) varieties found in South India. *Advanced Science Letters*, 5, 1-5.

[2] Chen, C.Y.O. and Blumberg, J.B., 2008. Phytochemical composition of nuts. *Asia Pacific Journal of Clinical Nutrition*, 17, 329-332.

[3] Hossain, M. and Singh, V.P., 2000. Fertilizer use in Asian agriculture: implications for sustaining food security and the environment. *Nutrient Cycling in Agroecosystems*, 57, 155-169.

[4] Ghosh, B.C. and Bhat, R., 1998. Environmental hazards of nitrogen loading in wetland rice fields. *Environmental Pollution*, 102, 123-126.

[5] Moreno-Reséndez, A., Parcero-Solano, R., Reyes-Carrillo, J. L., Salas-Pérez, L., Moncayo-Luján, M. R., Ramírez-Aragón, M.G. and Rodríguez-Dimas, N., 2016. Organic manures improved the phenolic content, antioxidant capacity and soluble solids in pepper. *Food and Nutrition Sciences*, 7, 1401-1413.

[6] Sereme, A., Dabire, C., Koala, M., Somda, M.K. and Traore, A.S., 2016. Influence of organic and mineral fertilizers on the antioxidants and total phenolic compounds level in tomato (*solanum lycopersicum*) var. mongal F1. *Journal of Experimental Biology and Agricultural Sciences*, 4, 414-420.

[7] Tuaño, A.P.P., Xu, Z., Castillo, M.B., Mamaril, C.P., Manaois, R.V., Romero, M.V. and Juliano, B.O., 2011. Content of tocols, γ-oryzanol and total phenolics and grain quality of brown rice and milled rice applied with pesticides and organic and inorganic nitrogen fertilizer. *Philippine Agricultural Scientist*, 94, 211-216.

[8] Kesarwani, A., Chiang, P. and Chen, S., 2017. Distribution of phenolic compounds and antioxidative activities of rice kernel and their relationships with agronomic practice. *The Scientific World Journal*, 61, 1-6.

[9] Torres, A. M., Mau-Lastovicka, T. and Rezaaiyan, R., 1987. Total phenolics and high-performance liquid chromatography of phenolic acids of avocado. *Journal of Agricultural and Food Chemistry*, 35, 921-925.
[10] Analytical Software., 2003. *Statistix8: Analytical Software User's Manual*. Tallahassee, Florida. USA.
[11] Gomez, K.A. and Gomez, A.A., 1984. *Statistical Procedures for Agricultural Research*. 2nd ed. New York: John Wiley & Sons.
[12] Reddy, T.Y. and Reddi, G.H.S., 2002. *Mineral Nutrition, Manures and Fertilizers. Principles of Agronomy*. 3rd ed. Ludhiana: Kalyani. pp. 204-256.
[13] Hasanuzzaman, M., Ahamed, K.U., Nahar, K. and Akhter, N., 2010. Plant growth pattern, tiller dynamics and dry matter accumulation of wetland rice (*Oryza sativa* L.) as influenced by application of different manures. *Nature and Science*, 8, 1-10.
[14] Ko, K.M.M., Hirai, Y., Zamora, O.B. and Guzman, L.E., 2017. Agronomic and physiological response of rice (*Oryza sativa* L.) under different water management system, fertilizer types and seedling age. *American Journal of Planr Science*, 8, 3338-3349.
[15] Kumar, G.S., Reddy, S.N. and Ikramullah, M., 1995. Effect of seedling age and nitrogen level on performance of rice (*Oryza sativa* L.) under late planting. *Indian Journal of Agricultural Science*, 65, 354-355.
[16] Sudarsono, W.A., Melati, M. and Aziz, S.A., 2014. Growth and yield of organic rice with cow manure application in the first cropping season. *Agrivita*, 36, 19-26.
[17] Frias-Moreno, M.N., Olivas-Orozco, G.I., Gonzalez-Aguilar, G.A., Benitez-Enriquez, Y.E., Paredes-Alonso, A., Jacobo-Cuellar, J.L., Salas-Salazar, N.A., Ojeda-Barrios, D.L. and Parra-Quezad, R.A., 2019. Yield, quality and phytochemicals of organic and conventional raspberry cultivated in Chihuahua, Mexico. *Notulae Botanicae Horti Agrobotanici*, 47, 522-530.
[18] Muntana, N. and Prasong, S., 2010. Study on total phenolic contents and their antioxidant activities of Thai white, red and black rice bran extracts. *Pakistan Journal of Biological Sciences*, 13, 170-174.

Control of Pathogenic Bacteria in Cooked Duck Blood Curd using Sodium Diacetate and Sodium Chloride

Pussadee Tangwatcharin* and Worralak Teemeesuk

Department of Animal Production Technology and Fisheries, Faculty of Agricultural Technology, King Mongkut's Institute of Technology Ladkrabang, Bangkok, Thailand

Received: 20 August 2019, Revised: 2 September 2019, Accepted: 11 September 2019

Abstract

The effects of sodium diacetate (SD) and sodium chloride (NaCl) on growth inhibition of four bacterial strains: *Escherichia coli*, *Salmonella* Typhimurium, *Pseudomonas fluorescens* and *Staphylococcus aureus* were investigated by determining the minimum inhibitory concentration and bactericidal concentrations (MIC and MBC), fractional inhibitory and bactericidal concentration index (FICI and FBCI) and survival of these pathogenic bacteria in cooked duck blood curd. SD provided greater overall inhibition to all tested bacterial strains in comparison with NaCl. The effect of SD + NaCl in combination was partially synergistic or synergistic against these pathogenic bacterial, exhibiting FICI and FBCI of 0.75 and 0.25 respectively for *E. coli*, 0.62 and 0.62 respectively for *S.* Typhimurium, 1.00 and 0.62 respectively for *P. fluorescens* and 0.50 and 0.37 respectively for *S. aureus*. For cooked duck blood curd, 0.15% (w/v) SD + 1.25% (w/v) NaCl in combination reduced *E. coli*, *Salmonella* spp., *Pseudomonas* spp. and *S. aureus* ($p < 0.05$) in the range of 0.63 - 1.10 log cycles and controlled the growth of all four bacteria more than the control sample ($P < 0.05$) did. Furthermore, the 0.15% (w/v) SD + 1.25%(w/v) NaCl combination controlled the growth of these bacteria in cooked duck blood curd for 6 days of storage, except in the case of *E. coli*, for which growth was controlled for 4 days of storage. All experimental results were compared to the control sample before storage ($p > 0.05$). The results indicate that SD in combination with NaCl can be incorporated into cooked duck blood curd to effectively reduce and control growth of pathogenic bacteria at 10°C of storage.

Keywords: organic acid salt, pathogenic bacteria, cooked duck blood curd, cold storage
DOI 10.14456/cast.2019.26

1. Introduction

Cooked duck blood curd is one of the favorite blood foods in Thailand. This traditional product is produced from a combination of raw duck blood and water and is clotted by heat. It is distributed as a freshly cooked product soaked in low concentration of salt with a shelf life of approximate two days. In recent times, preservation by chilling has been used to extend the product's shelf life and thus expand existing markets [1]. However, safety issues to do with the presence and growth of pathogenic bacteria in this product are of ongoing concern.

*Corresponding author: Tel.: 011-662-329-8000 Ext. 6047 Fax: 011-662-329-8519
E-mail: putang3009@hotmail.com

Problems associated with the safe preservation of this by-product of slaughter houses have grown to be more complex as today's products require more safety and greater assurance of protection from pathogenic microorganisms. Many chemical antimicrobials have been used to inhibit pathogen growth on meat and meat product surfaces. Sodium diacetate (SD) was shown to be effective in limiting the growth of *Escherichia coli*, *Salmonella* Typhimurium, *Pseudomonas fluorescens* and *S. aureus* [2, 3]. However, in developed countries, the maximum level of sodium diacetate allowed for use in meat products is 0.25% of final product [4, 5]. Sodium chloride (NaCl) was reported to affect the morphology of *E. coli* and *S. aureus*. It was also reported to have a milder effect on cell damage, particularly on *S. aureus* [6]. At low salinity, it causes an immediate influx of small solutes thus relieving physical stress. On the other hand, at high salinity, it causes water efflux which is balanced by an augmentation of compatible solutes, for example glutamate, proline, glycine betaine, trehalose and ectoine [7]. Therefore, the objective of the present study was to compare the antibacterial activity of SD, NaCl and SD+NaCl against *E. coli*, *Salmonella* Typhimurium, *P. fluorescens* and *S. aureus* in cooked duck blood curd.

2. Materials and Methods

2.1 Strains of bacteria

E. coli DMST 4212, *S.* Typhimurium DMST 22842, *P. fluorescens* DMST 20076 and *S. aureus* DMST 4745 were obtained from the culture collection at the Department of Medical Sciences, Ministry of Public Health, Thailand. These bacteria were cultivated on Mueller Hinton agar (MHA, Merck, Germany). Inocula were prepared by transferring 2-3 colonies from MHA to 10 ml of 0.85%(w/v) NaCl (Sigma-Aldrich Pte. Ltd., Singapore) and diluted in 0.85%(w/v) NaCl to 10^8 cfu/ml (McFarland standard of 0.5). These suspensions were further diluted with 0.85%(w/v) NaCl as required. The initial concentration of approximately 5×10^5 cfu/ml was adopted for the minimal inhibitory concentration (MIC), minimal bactericidal concentration (MBC) and synergy methods and approximately 1×10^6 cfu/ml for cooked duck blood curd model.

2.2 MIC and MBC determinations

For each bacterium, MIC was estimated by a broth microdilution method. Distilled water was used for dissolving all the antimicrobials. Subsequent two-fold serial dilutions were performed in medium. The final concentrations of the antimicrobial in wells ranged from 0-2.5% (w/v) for SD (Chemipan Corporation Co. Ltd., Bangkok, Thailand) and 0-20% (w/v) for NaCl. The MIC was reported as the lowest concentration that limited the broth turbidity to below 0.05 at absorbance of 600 nm using a UVM 340 Microplate Reader (Biochrom Ltd., Cambridge, UK). MBC was estimated by comparing the survival numbers of bacteria with their initial numbers. The MBC was then reported as the lowest concentration that killed not less than 99.9% of the initial number of bacteria [8].

2.3 Synergistic effects

To determine whether SD acted synergistically with NaCl, a checkerboard titration was used for analysis of the fractional inhibitory concentration index (FICI) and fractional bactericidal concentration index (FBCI) in Mueller Hinton broth (Merck, Germany). The MIC, MBC, FICI and FBCI analyses were repeated three times and their means were calculated. Synergy was demonstrated when FICI and FBCI < 0.5; partial synergy/additive effect was obvious when the

FICI and FBCI ranged from > 0.5 to 1.0; there was no interaction when the FICI and FBCI was > 1 to < 2, and antagonism was exhibited when the FICI and FBCI was > 2 [9].

2.4 Cooked duck blood curd model

Cooked duck blood curd samples (*Cherry valley* crossbred ducks at 47 d) were collected in three batches at different days from a cooked duck blood curd line at an industrial slaughterhouse in Chachoengsao province, Thailand. 500 g samples were taken, kept in polystyrene boxes containing ice, and transported to the Department of Animal Production Technology and Fisheries, Faculty of Agricultural Technology, King Mongkut's Institute of Technology Ladkrabang for analysis within 3 hrs of sampling.

The samples were used to estimate the effects of the antimicrobials on *E. coli*, *S.* Typhimurium, *P. fluorescens* and *S. aureus*. Each sample was inoculated with all 4 bacteria suspensions as follows: the cooked duck blood curd was soaked in 300 ml of the bacterial inoculum (approximately 10^6 cfu/ml) for 20 min and dried in laminar air flow for 20 min before the addition of the antimicrobials. The initial count of each pathogenic bacterium was approximately 10^4 cfu/g. The sample was randomly separated into two treatments and soaked in 300 ml of the antimicrobial as follows: (1) control –water and (2) 0.15% (w/v) SD +1.25%(w/v) NaCl in combination. Each treatment was packed in a polyethylene plastic bag. Air-circulated refrigeration was used for storing samples at 10ºC for 8 days. The stored samples under refrigeration were sampled for microbiological determination at 0, 2, 4, 6 and 8 days.

2.5 Microbiological analysis

The samples were submitted to count for *E. coli* [10], *Samonella* spp. [11], *Pseudomonas* spp. [12] and *S. aureus* [13] according to standard procedures. *E. coli*, *Samonella* spp., *Pseudomonas* spp. and *S. aureus* were enumerated on violet red bile agar (Merck, Germany) , xylose lysine deoxycholate (Merck, Germany), *Pseudomonas* CFC agar (Merck, Germany) and Baird Parker agar (Merck, Germany) contained 5% (v/v) of egg-yolk tellurite emulsion 20% (Merck, Germany), respectively. The plates were incubated at 35 ± 2ºC for 24-48 h, except for *Pseudomonas* spp., which was incubated at 25 ± 2ºC for 24-48 h. Then, colonies were counted. IMViC test for *E. coli*, triplate sugar iron agar test, lysine iron agar test for *Salmonella* spp., oxidase, aerobicity and ability to ferment glucose for *Pseudomonas* spp. and coagulase test for *S. aureus* by standard methods [14] were determined. The results were calculated to log cfu/g.

2.6 Statistical analysis

Data showing bacterial loading in the cooked duck blood curd model were showed as means and standard deviations. The general linear model procedure was used for estimating significant differences ($p < 0.05$) of all statistical computations. Least squares means were computed and separated ($p<0.05$) with the PDIFF option of GLM. All statistical analyses were executed by SAS v. 9.0 [15].

3. Results and Discussion

3.1 MIC and MBC determinations

The MICs of SD and NaCl for antibacterial action against *E. coli* DMST 4212, *S.* Typhimurium DMST 22842, *P. fluorescens* DMST 20076 and *S. aureus* DMST 4745 were determined to be 0.31, 0.15, 0.15 and 0.31% (w/v) respectively for SD, and 5.00, 10.00, 5.00 and 20.00% (w/v) respectively for NaCl. However, the MBCs of SD were two-fold for all bacteria, except for *E. coli* (eight-fold), which were higher than the analogous MIC. The MBCs of NaCl against all bacteria were 10.00% (w/v), except in the case of *S. aureus* (20%(w/v) (Table 1). An earlier study found that the MIC and MBC of SD against *S. aureus* were 0.78 and 6.25% (w/v) [9]. *Salmonella* Typhimurium was able to grow in the presence of up to 7-8% NaCl at 37ºC [16]. Normally, *Salmonella* and *E. coli* (bacteria belonging to the Enterobacteriaceae family) do not tolerate high salt levels [17]. However, it has been reported that *S. aureus* can tolerate high concentrations of NaCl in liquid medium, with no damage or shrinkage of cellular structure being observed. Under similar conditions, cell injury of *E. coli* appeared [6].

Table 1. Minimum inhibitory concentration (MIC) and minimum bactericidal concentration (MBC) of sodium diacetate (SD) and sodium chloride (NaCl) to inhibit growth of some pathogenic bacteria.

Strains	Antimicrobials	MIC % (w/v)	MBC % (w/v)
Escherichia coli	SD	0.31	1.25
	NaCl	5.00	10.00
Salmonella Typhimurium	SD	0.15	0.31
	NaCl	10.00	10.00
Pseudomonas fluorescens	SD	0.15	0.31
	NaCl	5.00	10.00
Staphylococcus aureus	SD	0.31	0.62
	NaCl	20.00	20.00

3.2 Synergistic effects

The FICIs for the combined action of SD with NaCl on *E. coli* DMST 4212, *S.* Typhimurium DMST 22842, *P. fluorescens* DMST 20076 and *S. aureus* DMST 4745 are shown in Table 2. FICI and FBCI indicated that utilization of SD in combination with NaCl resulted in improved inhibition of all pathogenic bacteria.The enhancing effect of the combination was also evidenced by the bactericidal responses produced at sub-MBC levels for each bacterium. FICI of the combined action of SD +NaCl was 0.75 and 1.00 (0.07%(w/v) + 2.50%(w/v)) for *E. coli* and *P. fluorescens* respectively and 0.62 (0.07% (w/v) +1.25% (w/v)) for *S.* Typhimurium, suggesting partial synergy of the analyzed antimicrobials and 0.50 (0.07%(w/v) +5.00%(w/v)) for *S. aureus*, suggesting synergy of the analyzed antimicrobials. Similarly, FBCI of the combined action of SD + NaCl was 0.25 (0.15%(w/v) +1.25%(w/v)) for *E. coli* and 0.37 (0.15%(w/v) +2.50%(w/v)) for *S. aureus*, again suggesting synergy and 0.62 (0.15%(w/v) +1.25%(w/v)) for *S.* Typhimurium and *P. fluorescens*. The calculation and analysis of FICI and FBCI indicated that the utilization of SD with NaCl resulted in the synergistic inhibition of pathogenic bacteria, potentially resulting from SD. SD is a weak organic acid salt and effectively inhibits most tested bacteria.

Table 2. Fractional inhibitory concentration index (FICI) and fractional bactericidal concentration index (FBCI) of the combined action of sodium diacetate (SD) with sodium chloride (NaCl) to some pathogenic bacteria.

Strains	Indices	Concentrations of SD + NaCl in combination %(w/v)	Values	Interpretation
Escherichia coli	FICI	0.07+2.50	0.75	partial synergy
	FBCI	0.15+1.25	0.25	synergy
Salmonella Typhimurium	FICI	0.07+1.25	0.62	partial synergy
	FBCI	0.15+1.25	0.62	partial synergy
Pseudomonas fluorescens	FICI	0.07+2.50	1.00	partial synergy
	FBCI	0.15+1.25	0.62	partial synergy
Staphylococcus aureus	FICI	0.07+5.00	0.50	synergy
	FBCI	0.15+2.50	0.37	synergy

3.3 Cooked duck blood curd model

The results revealed that the use of 0.15% (w/v) SD + 1.25% (w/v)) NaCl in combination reduced the numbers of *E. coli*, *Salmonella* spp., *Pseudomonas* spp. and *S. aureus* on cooked duck blood curd stored at 10ºC (Figure 1). The four bacteria of the sample soaked in SD in combination with NaCl decreased by 0.63 log cfu/g for *E. coli*, 0.75 log cfu/g for *Salmonella* spp., 1.10 log cfu/g for *Pseudomonas* spp. and 0.82 log cfu/g for *S. aureus*, compared to control sample before storage. Then, growth of the four bacteria was retarded throughout the 6 days of storage at 10ºC, except for *E. coli*, which was retarded for 4 days of storage when compared to the control sample before storage ($p > 0.05$). At the end of the 8-day storage time, the four bacteria in the samples soaked in water (control) were 2.61 log cfu/g for *E. coli*, 2.26 log cfu/g for *Salmonella* spp, 1.59 log cfu/g for *Pseudomonas* spp. and 2.17 log cfu/g for *S. aureus* which were higher than the numbers of the four bacteria in samples soaked in SD in combinations with NaCl ($p < 0.05$). This result could probably explain the role of SD in combination with NaCl as antimicrobial agents. Salts of organic acid have been shown to have antimicrobial effects by causing hyper-acidification via proton donation at the plasma membrane interface of the microorganism and intracellular cytosolic acidification, an excess of which can disrupt the H+ -ATPase enzyme, which is required for ATP synthesis [18]. Lag phase extension and growth rate reduction for *L. mononcytogenes* were also observed in ground ham to which had been added 0.25% SD [19]. *S.* Typhimurium was able to grow in the presence of up to 4%NaCl at 12ºC [16].

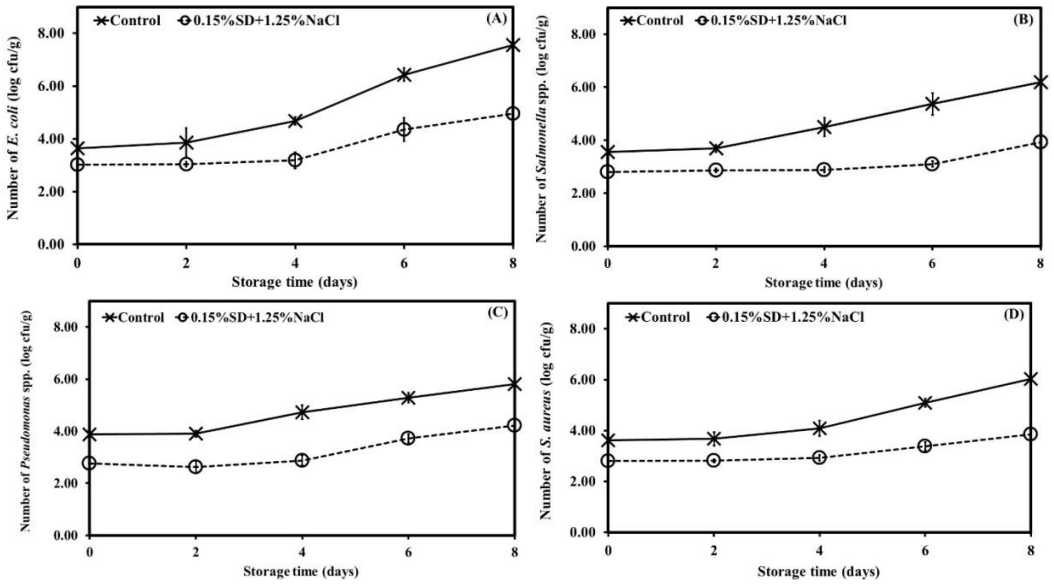

Figure 1. Effect of sodium diacetate (SD) in combination with sodium chloride (NaCl) on *Escherichia coli* (A), *Salmonella* spp. (B), *Pseudomonas* spp. (C) and *Staphylococcus aureus* (D) on cooked duck blood curd stored at 10°C for 8 days.

4. Conclusions

Using SD in combination with NaCl at concentrations lower than the MIC values of each antimicrobial agent is capable of decreasing the number of pathogenic bacteria in cooked duck blood curd, thereby enhancing microbiological safety of cooked duck blood curd. Furthermore, the addition of SD in combination with NaCl is recommended in order to control the growth of pathogenic bacteria effectively.

5. Acknowledgements

The authors are grateful to Ducking Co., Ltd. for the financial support and samples used in this work.

References

[1] Wang, P., Han, M.-Y., Dong, Q.-L., Xu, X.-L., Zhou, G.-H. and Lu, S.-L., 2010. Principal component analysis for textural properties of selected blood curd. *Journal of Texture Studies*, 41(6), 757-773.

[2] Shelef, L.A. and Addala, L., 1994. Inhibition of *Listeria monocytogenes* and other bacteria by sodium diacetate. *Journal of Food Safety*, 14(2), 103-115.

[3] Nanasombat, S. and Chooprang, K., 2009. Control of pathogenic bacteria in raw pork using organic acid salts in combination with freezing and thawing. *Kasetsart Journal (Natural Science)*, 43(2), 576-583.

[4] Health Canada, 2016. *List of Permitted Preservatives (Lists of Permitted Food Additives)*. [online] Available at: http://www.hc-sc.gc.ca/fn-an/securit/addit/list/11-preserv-conserv-eng.php
[5] Food and Drug Administration, 2016. *Sodium diacetate: 21CFR184.1754. CFR - Code of Federal Regulations Title 21*. [online] Available at: https://www.accessdata.fda.gov/scripts/cdrh/cfdocs/cfcfr/CFRSearch.cfm?fr=184.1754
[6] Hajmeer, M., Ceylan, E., Marsden, J.L. and Fung, D.Y. 2006. Impact of sodium chloride on *E. coli* O157:H7 and *S. aureus* analysed using transmission electron microscopy. *Food Microbiology*, 23(5), 446-452.
[7] Krämer, R., 2010. Bacterial stimulus perception and signal transduction: Response to osmotic stress. *The Chemical Record*, 10(4), 217-229.
[8] CLSI, 2002. *Reference method for dilution antimicrobial susceptibility tests for bacteria that grow aerobically*. *Approved Standard M7-A4*. Wayne, Pa: Clinical Laboratory Standards Institute.
[9] Tangwatcharin, P. and Prapaporn, K., 2012. Activity of virgin coconut oil, lauric acid or monolaurin in combination with lactic acid against *Staphylococcus aureus*. *Southeast Asian Journal of Tropical Medicine and Public Health*, 43(4), 969-985.
[10] Bacteriological Analytical Manual (BAM), 2002. *Escherichia coli*. *U.S. Food and Drug Administration.* [Online] Available at: https://www.fda.gov/Food/FoodScienceResearch/LaboratoryMethods/ucm064948.htm
[11] ISO 6579, 2002. *Microbiology of Food and Animal Feeding Stuffs-Horizontal Method for the Detection*. 4th ed. Geneva: International Organization for Standardization.
[12] Rajmohan, S., Dodd, C. E. R. and Waites, W.M., 2002. Enzymes from isolates of *Pseudomonas fluorescens* involved in food spoilage. *Journal of Applied Microbiology*, 93(1), 205-213.
[13] Bacteriological Analytical Manual (BAM), 2001. *Staphylococcus aureus U.S. Food and Drug Administration.* [online] Available at: http://www.fda.gov/Food/FoodScienceResearch/LaboratoryMethods/ucm071429.htm
[14] Collins, C.H., Lyne, P.M. and Grange, J.M., 1991. *Collins and Lyne's Microbiological Methods*. 6th ed. Oxford: Butterworth.
[15] SAS Institute Inc., 2002. *SAS Version 9.0*. Cary, NC: SAS Institute.
[16] Thayer, D.W., Muller, W.S., Buchanan, R.L. and Phillips, J.G., 1987. Effect of NaCl, pH, temperature, and atmosphere on growth of *Salmonella* typhimurium in glucose-mineral salts medium. *Applied and Environmental Microbiology*, 53(6), 1311-1315.
[17] Zambonelli, C., Papa, F., Romano, P., Suzzi, G. and Grazia, L., 1992. *Microbiologia dei Salumi*. Bologna: Calderini Edagricole.
[18] Silva, E.N.G., Almeida, R.C.C., Figueiredo A.C.L. and Miranda, F.A., 2012. Effects of salts of organic acids on the survival of *Listeria monocytogenes* in soft cheeses. *International Journal of Food Science and Technology*, 47(9), 1819-1825.
[19] Hwang, C.A. and Tamplin, M.L., 2007. Modeling the lag phase and growth rate of *Listeria monocytogenes* in ground ham containing sodium lactate and sodium diacetate at various storage temperatures. *Journal of Food Science*, 72(7), M246-M253.

Instructions for Authors

Current Applied Science and Technology journal contains research reports, articles concerning development work, reviews of the literature and research activities. The objectives are to publish and promote research contributions and innovative work in fields associated with applied science and technology. An electronic journal is provided on the website (https://www.tci-thaijo.org/index.php/cast/index). The editors reserve the right to require revision of the submitted manuscript as a condition for final acceptance.

The institute and the editorial board claim no responsibility for the contents or views expressed by the authors of individual articles. Copying is allowed provided that acknowledgement is made. All articles submitted for publication will be assessed by a group of distinguished.

Ethics:

The journal is committed to maintaining the high level of integrity in the content published and has a Conflict of Interest policy in place. The journal uses plagiarism detection software to screen the submissions. If plagiarism is found, the COPE guidelines on plagiarism will be followed. For more details, please see https://www.tci-thaijo.org/index.php/cast/navigationMenu/view/Publication_Ethics.

Page Charge: Free

Submission of Manuscripts:

Manuscripts must be written in English and submitted online. Manuscripts are to be reviewed (double blinded) by at least 3 referees specializing in relevant fields. Revised manuscripts have to be sent online.

All manuscripts should be submitted to: https://www.tci-thaijo.org/index.php/cast/index

Contact:

Editor of Current Applied Science and Technology
King Mongkut's Institute of Technology Ladkrabang
1 Soi Chalongkrung 1, Ladkrabang District,
Bangkok 10520, Thailand
Tel: 662-329-8136
Fax: 662-329-8221
Email: cast@kmitl.ac.th

Manuscript Preparation Guide:

General: Manuscripts must be typewritten using *Microsoft Word for Windows*, single-spaced with margin set-up (in page set up menu) as follows (see also the document template):

Top Margin	1.5"	Bottom Margin	1.5"
Left Margin	1.5"	Right Margin	1.5"

Good quality printouts using A4 paper size are required. Format should be a single column. Times New Roman font type is required. Font sizes for various text functions are as follows:

Text functions	**Size ***	**Typeface**
Title	14 (CT)	Bold
Author and co-authors	11 (CT)	Normal
Address for correspondence	11 (CT)	Normal
Abstract and main text	10 (LJ)	Normal
Section heading and number including "Abstract", "Acknowledgement", "References"	12 (CT)	Bold
Subsection heading and number	11 (LJ)	Bold

* CT = Center Text, LJ = Left Justified.

The corresponding author should be noted (included a Fax number and E-mail address) and indicated with an asterisk. Full postal addresses must be given for all co-authors, keyed to names (if required) by superscripted Arabic numbers.

Paper Length: Should not normally exceed 10 pages including figures and tables
Spelling: American English
Abstract: Should not exceed 250 words
Keywords: Should not exceed 8 keywords
Text: Authors are requested to use the following order when typing:-

All research reports (Full Length or Short Reports): Title, Authors, Affiliations, Abstract, Keywords, Introduction (in reserch papers this must be confined to relevant matters, and must not be a general review of cognate literature), Materials and Methods, Results and Discussion, Conclusions, Acknowledgements, References.

Reviews and Discussion Papers will be considered in any format appropriate to the purposes of the authors, although adherence to the general guidelines described above is encouraged.

Line Art Figures: Figures can be drawn using several packages such as Win Draw®, Auto CAD®, Corel Draw®, VISIO® etc.

Photographs: Actual size photographs are acceptable. However, they can also be put into a text stream using a good-resolution scanner. All photographs must be clear when printed in monochrome.

Graphs: Several packages available today can produce attractive and professional graph presentation. Some also provide curve-fitting function, which can be useful. However, two-dimensional bar charts are preferred. All graphs must be clear in monochrome printing.
Equations and complex expressions: Math CAD®, Math Writer® and Equation Editor® (included in Microsoft Word®) are acceptable for presentation of this type of material.

Citations: Citations in the text should be denoted by numbers between square brackets (i.e. [1, 2], [1-3], [1, 3-8]…) *in the order of first appearance in the text.*

References: References should be numbered to correspond with the text citations. References must be arranged as follows:

Books

Authors, Initials., Year. *Title of Book.* Edition. (only include this if not the first edition) Place: Publisher.

Example:

[1] Barker, R., Kirk, J. and Munday, R.J., 1988. *Narrative Analysis*. 3rd ed. Bloomington: Indiana University Press.

Chapters of edited books

Chapter authors' surname(s), initials., Year of book. Title of chapter. In**:** Book editor(s) initials. surnames, ed. or eds. *Title of Book*. Place of publication: Publisher. Chapter number or first and last page numbers.

Example:

[2] Samson, C., 1970. Problems of information studies in history. In: S. Stone, ed. *Humanities Information Research*. Sheffield: CRUS, pp. 44-68.

E-books

Author, Year, *Title of Book*. [e-book] Place of publication: Publisher. Available through: include e-book source/database, web address or URL.

Example:

[3] Carlsen, J. and Charters, S., eds. 2007. *Global Wine Tourism*.[e-book] Wallingford: CABI Pub. Available through: Anglia Ruskin University Library website <www.libweb.anglia.ac.uk>.

Journal articles

Author, Initials., Year. Title of article. *Full Title of Journal*, Volume number (Issue number), Page numbers.

Example:

[4] Ross, A.B., Junyapoon, S., Jones, J.M., Williams, A. and Bartle, K.D., 2005. A study of different soots using pyrolysis–GC–MS and comparison with solvent extractable material. *Journal of Analytical and Applied Pyrolysis*, 74(1-2), 494-501.

Proceedings

Author, Initials., Year. Title of article. *Full Title of Proceedings*, Place of Conference, Date, page

Example:

[5] Thanaboripat, D., Ruangrattanametee, V. and Srikitkademwat, K., 2010. Control of growth and aflatoxin production of aflatoxin producing fungi in corn by salts. *Proceeding of the 8th International Symposium on Biocontrol and Biotechnology*, Pattaya, Thailand, October 4-6, 2010, 283-289.

Patent

Inventor name, Initial(s)., Assignee., Year. *Title*. Place. Patent number (status, if an application).

Example:

[6] Leonard, Y., Super Sports Limited., 2008. *Tin Can Manufacture and Method of Sealing*. Canada. Pat. 12,789, 675.

Dissertation
Author, Year of publication. *Title of Dissertation*. Level. Official name of University.
Example:
[7] Richmond, J., 2005. *Customer Expectations in the World of Electronic Banking: a Case Study of the Bank of Britain.* Ph.D. Anglia Ruskin University.

Websites
Authorship or Source, Year. *Title of Document*. [online] Available at: include web site address/URL (Uniform Resource Locator).
Example:
[8] NHS Evidence, 2003. *National Library of Guidelines*. [online] Available at: http://www.library.nhs.uk/guidelines

Acknowledgements: These should be as brief as possible.

Proofs:

Proofs will be sent to the corresponding author and *must* be returned as soon as possible. Corrections should be restricted to typesetting errors.

Copyright:

The author(s) transfer(s) the copyright of the article to Current Applied Science and Technology effective if and when the article is accepted for publication.

Page Numbering:

All pages must be sequentially numbered, preferably by using the automatic page numbering function on your computer.

Copyright Material:

It is the authors' responsibility to obtain written permission from the copyright holder (usually the book or journal publisher) to use copyright material, and to send a copy of this consent with the manuscript. This consent is not normally denied but it is an international legal requirement that it be obtained.

Note:

Please note that authors are urged to check their proofs carefully before returning, since the inclusion of late corrections cannot be guaranteed.

Author(s) are responsible for ensuring that the submitted manuscript fully meets the requirements specified in the above Instructions. Manuscripts which fail to do so will be returned unedited to the Author(s) for correction in accordance with the above requirements, before they can be submitted to the processes of Referee evaluation.

1.5 ”

TEMPLATE

Enter title here (14 PT type size, Title Case, Bold, Centered)

Author Information entered here:
Name (in full)

Affiliation
City
Country
(11 pt type size, upper and lower case, centered under the title)

How to Use This Document Template

Insert the information in your document in place of the text here. For the body of your document, use Times New Roman 10 pt. Font, upper and lower case, double-spaced. Allow an extra half space above a line containing superscripts and/or below a line containing subscripts. The whole text should be left-justified. The headings should be 12 pt size, uppercase, bold and centered.

1.5” **Abstract (12pt)** 1.5”

Maximum 250 words here. (10 pt)

.....
.....
.....
.....
.....

Keywords: (10 pt)

Maximum of 8 words

*Corresponding author: Tel.: ……..... Fax: …….
E-mail: ……

1. Introduction (12 pt)

Clearly explain the nature of the problem, previous work, purpose, and contribution of the paper (10 pt).

.....
.....
.....
.....
.....

2. Materials and Methods (12 pt)

.....
.....
.....
.....

3. Results and Discussion (12 pt)

.....
.....…

4. Conclusions (12 pt)

Clearly indicate advantages, limitations and possible applications (10 pt).

.....
.....

5. Acknowledgements (12 pt)

A brief acknowledgement section may be included here (10 pt).

.....
.....

References (12 pt)

References must be numbered in the order cited in the manuscript and indicated in the text by a number in square brackets (e.g. [1, 2]) (10 pt).

Example of References must be arranged as follows:

[1] Barker, R. Kirk, J. and Munday, R.J., 1988. *Narrative Analysis.* 3rd ed. Bloomington: Indiana University Press.

[2] Samson, C., 1970. Problems of information studies in history. In: S. Stone, ed. *Humanities Information Research*. Sheffield: CRUS, pp. 44-68.

[3] Carlsen, J. and Charters, S., 2007. *Global Wine Tourism*. [e-book] Wallingford: CABI Pub. Available through: Anglia Ruskin University Library website <www.libweb.anglia.ac.uk>.

[4] Ross, A.B., Junyapoon, S., Jones, J.M., Williams, A. and Bartle, K.D., 2005. A study of different soots using pyrolysis–GC–MS and comparison with solvent extractable material. *Journal of Analytical and Applied Pyrolysis*, 74(1-2), 494-501.

[5] Thanaboripat, D., Ruangrattanametee, V. and Srikitkademwat, K., 2010. Control of growth and aflatoxin production of aflatoxin producing fungi in corn by salts. *Proceeding of the 8th International Symposium on Biocontrol and Biotechnology*, Pattaya, Thailand, October 4-6, 2010, 283-289.

[6] Leonard, Y., Super Sports Limited., 2008. *Tin Can Manufacture and Method of Sealing*. Canada. Pat. 12,789, 675.

[7] Richmond, J., 2005. *Customer Expectations in the World of Electronic Banking: a Case Study of the Bank of Britain.* Ph.D. Anglia Ruskin University.

[8] NHS Evidence, 2003. *National Library of Guidelines*. [online] Available at: http://www.library.nhs.uk/guidelines

Note:

Tables and Graphs: Minimum of 10 pt type size, all captions should be upper and lower case, centered. Each table and figure must be on a separate page (or pages if required), ***and must be embedded in the text.***

Illustrations and Photographs: Halftones, minimum of 10 pt type size, bold, captions should be in upper and lower case, centered. Images must be computer-designed with clearly visibility.

KING MONGKUT'S INSTITUTE OF TECHNOLOGY LADKRABANG
1 Soi Chalongkrung 1, Ladkrabang District Bangkok 10520, Thailand
Tel: 662-329-8136 Fax: 662-329-8221
E-mail: cast@kmitl.ac.th
Website: https://www.tci-thaijo.org/index.php/cast/index

Contact

Editor of Current Applied Science and Technology
King Mongkut's Institute of Technology Ladkrabang
1 Soi Chalongkrung 1, Ladkrabang District
Bangkok 10520, Thailand
Tel: 662-329-8136 Fax: 662-329-8221
E-mail: cast@kmitl.ac.th
Website: https://www.tci-thaijo.org/index.php/cast/index